Radionuclide-Chelating Agent Complexes in Low-Level Radioactive Decontamination Waste; Stability, Adsorbtion and Transport Potential

Pacific Northwest National Laboratory

U.S. Nuclear Regulatory Commission
Office of Nuclear Regulatory Research
Washington, DC 20555-0001

Radionuclide-Chelating Agent Complexes in Low-Level Radioactive Decontamination Waste; Stability, Adsorbtion and Transport Potential

Prepared by
R.J. Serne, K.J. Cantrell, C.W. Lindenmeier, A.T. Owen,
I.V. Kutnyakov, R.D. Orr, and A.R. Felmy

Pacific Northwest National Laboratory
P.O. Box 999
Richland, WA 99352

Abstract

Leach data for cement solidified spent resins from reactor decontamination suggests that maximum concentrations of organic ligands range from 2×10^{-3} to 10^{-4} M for picolinic acid and 3×10^{-4} to 10^{-5} M for EDTA. Cement leachates may release higher concentrations of organic ligands and lower concentrations of contaminant transition metals than the leachates of spent resins disposed directly in high integrity containers because the free hydroxide produced by cement leaching acts as a regenerating solution for the anion exchange resins, thus releasing the organic ligands and anionic complexes.

Speciation calculations were conducted to determine the significance of organic complexing agents in facilitating transport of radionuclides leached from buried waste forms through soil. The results of these speciation calculations can be condensed to the following conclusions. The potential for EDTA to mobilize metals is highest for divalent cations, and moderate for trivalent actinides. Picolinate appears to have significant potential to mobilize only Ni^{2+} and Co^{2+}. It is important to recognize that speciation predictions ignore the influence of soil adsorption and biodegradation reactions that will compete with and destroy, respectively, the radionuclide/ligand complexes and thus potentially release the metals/radionuclides to act as free ions.

In batch and flow-through adsorption studies, picolinate concentrations have to be $>10^{-4}$ M to significantly lower the adsorption of divalent transition metals (Ni and Co). For the metals Sm^{3+}, Th^{4+}, NpO_2^+, UO_2^{2+}, and oxidized Pu, the picolinate concentration must be $>10^{-3}$ M before adsorption decreases. EDTA forms strong complexes with divalent transition metals and can stop adsorption of Ni and Co when EDTA solution concentrations are $\$10^{-5}$ M. EDTA complexes with oxycations such as NpO_2^+, UO_2^{2+}, and oxidized Pu are much weaker. Adsorption tests suggest that EDTA concentrations would have to be $>10^{-3}$ M to have adverse effects on non-transition metal/radionuclide adsorption onto most soils in contact with leachates at common pH's.

Excepting divalent transition metal complexes, most picolinate and ETDA-metal complexes appear to be labile (readily dissociated) during interactions with soils. As complexes migrate from the disposal facility, dilution and interaction with competing cations in the pore fluids and adsorption reactions will result in dissociation of all but the strongest or most kinetically recalcitrant complexes. It appears that the enhanced migration of cationic metals/radionuclides-organic ligand complexes may be limited to a few unique conditions. Conditions that promote enhanced migration include high concentrations of organic ligands, low concentrations of competing cations, alkaline pH, organic ligands with slow biodegradation rates and kinetically inert and very strong ligand-metal stability constants.

At high pH values such as that created by cementitious wastes, mobilization of Ni^{2+} and Co^{2+} by EDTA becomes very significant and adsorption by soils and sediments is essentially zero. Thus we recommend that mixtures of metal/radionuclides and chelating agents (particularly EDTA) should not be co-disposed with high pH materials such as cement. This also indicates that cementitious waste forms are not a suitable disposal option for mixtures of transition metal/radionuclides and strongly binding chelating agents such as EDTA. For weaker binding organic complexants such as picolinate, citrate, and oxalate, co-disposal of decontamination wastes and concrete should be acceptable.

Contents

Figures

vii

viii

Tables

Foreword

This contractor technical report was prepared by Pacific Northwest National Laboratory[1] (PNNL) under their DOE Interagency Work Order (JCN L1155) with the Radiation Protection, Environmental Risk and Waste Management Branch, Division of Systems Analysis and Regulatory Effectiveness, Office of Nuclear Regulatory Research, U.S. Nuclear Regulatory Commission.

The report is the final contractor report documenting PNNL's research results on radionuclide-chelating complexes from studies performed with decontamination waste collected from operating nuclear power stations and disposed in a low-level waste disposal facility.

The PNNL research study was undertaken to support licensing needs for assessing radionuclide migration in soils under conditions where radionuclides combine with chelating agents to form radionuclide-chelate complexes which could enhance radionuclide migration in soil and increase dose as described in the Statement of Considerations to 10 CFR Part 61. This PNNL report provides data and information on chemical species, adsorption and behavior in typical soils for many radionuclide-chelating complexes found in the leachates of decontamination. Speciation distributions for radionuclides and organic complexing agents were calculated with chemical thermodynamic computer codes using the chemical composition of actual leachates. Both batch and flow experiments were used to obtain adsorption coefficients for the radionuclides, organic ligands and complexes. The report also provides the chemical thermodynamic data used in chemical codes to calculate the chemical species, and identifies areas where important thermodynamic data to calculate radionuclide-chelating chemical species are needed. Research results provided by the PNNL report are expected to be used for assessing the migration of radionuclide complexes in site-specific performance assessments as described in "A Performance Assessment Methodology for Low-Level Radioactive Waste Disposal Facilities," NUREG-1573.

This report is not a substitute for NRC regulations, and compliance is not required. The approaches and/or methods described in this NUREG/CR report are provided for information only. Publication of this report does not necessarily constitute NRC approval or agreement with the information contained herein. Use of product or trade names is for identification purposes only and does not constitute endorsement by the NRC or Pacific Northwest National Laboratory.

Cheryl A. Trottier

Cheryl A. Trottier, Chief
Radiation Protection, Environmental Risk and Waste Management Branch
Division of Systems Analysis and Regulatory Effectiveness
Office of Nuclear Regulatory Research

---

(1) Pacific Northwest National Laboratory is operated for the U.S. Department of Energy by Battelle Memorial Institute under contract DE-AC06-76RL01830.

Acknowledgments

1.0 Introduction

Organic complexes of radionuclides have been implicated in several instances as enhancing the mobility of radionuclides such as ^{60}Co, ^{238}Pu, ^{241}Am, and ^{90}Sr from shallow-land burial grounds at Oak Ridge, Tennessee (Means et al. 1978; Means and Alexander 1981) and at Maxey Flats, Kentucky (Polzer et al. 1982; O'Donnell 1983; Dayal et al. 1986). Organic chelates, such as EDTA and picolinic acid, have also been shown to leach from solidified decontamination wastes from nuclear power stations (McIsaac and Mandler 1989). Thus, chelating agents present in decontamination wastes could enhance the migration of radionuclides away from sites where such wastes are disposed.

Because of the possibility of enhanced migration federal regulations (10 CFR Part 61 "Licensing Requirements for Land Disposal of Radioactive Wastes") within subpart D require waste generators and disposal site owners to take consideration and document handling and disposal details for waste that includes chelating agents. Within 10 CFR 61 two sections in particular explicitly give guidance, Section 61.2 defines what types of chemicals are considered to be "chelating agents" and Section 21.12 discusses the types of information that licensees must provide in requests to dispose of such wastes.

Chemical decontamination is an effective means of removing the build-up of activated metals and other radioactive components that can occur in the cooling systems of nuclear power plants. This build-up of radioactive elements is primarily associated with corrosion products, such as Fe/Ni chromites, chromic oxides, Ni ferrites, and ferric oxides, which are deposited as films in the cooling systems. Removal of such oxide films can significantly reduce the occupational radiation exposure received by personnel while performing maintenance tasks and improve the thermal hydraulic performance of the cooling system.

Three principal chemical decontamination processes are currently used: the low-oxidation-state metal ions (LOMI) process (Shaw and Wood 1985; Swan et al. 1987; Smee et al. 1986), the CAN-DEREM process (Speranzini et al. 1990); and the CITROX process. Two other processes are less commonly used: the DOW NS-1 process (McIsaac and Mandler 1989) and the CAN-DECON process (Speranzini et al. 1990). Some decontamination processes are typically used in conjunction with pre-oxidation steps. These steps involve alternate applications of reducing/complexing agents to dissolve the Fe-oxide coatings and to complex the released radionuclides, and of strong oxidizing agents (such as alkaline permanganate) to oxidize Cr present in the Fe/Ni chromites and to loosen or break up these deposits. The added reducing or complexing agents and oxidizing solutions are then removed by either cation- or anion-exchange resins. These resins constitute the principal waste from the decontamination process and were commonly mixed with cement for stabilization (in the 1980's) and then disposed. Current disposal practices emphasize placing the solidified wastes or dewatered resins directly in high-integrity containers prior to burial in licensed shallow land disposal facilities.

The principal organic chelating/complexing agents present in the decontamination solutions, listed with their associated process, are as follows: 1) citric acid-oxalic acid (CITROX), 2) formic acid-picolinic acid (LOMI), 3) citric acid-ethylenediaminetetraacetic acid (EDTA) (CAN-DEREM), and 4) citric and oxalic acids and diethylenetriaminepentaacetic acid (DTPA) and EDTA (DOW NS-1). This study is principally

concerned with the radionuclides and chelating agents that can be leached from the disposed wastes and the potential for these chelates to enhance or retard migration of the leached radionuclides through surrounding soils and sediments.

The radionuclides and metal ions of primary concern include neutron activation products (isotopes of Co, Cr, Fe, Mn, and Ni), fission products (Cs, Sb, and Sr), actinide elements (U, Am, Cm, Np, and Pu), and major components of groundwaters and soils (e.g., Al, Ca, Mg). The major cations present in the groundwaters are important because they can displace the hazardous radionuclides from the organic chelates.

To address the effects of the chelates on the leaching and migration of radionuclides from disposal facilities requires knowledge of 1) the quantities of chelates and metals that potentially could be leached; 2) the ability of the chelates to bind the released metals in aqueous solution; 3) the ability of surrounding soils or sediments to adsorb the chelates or radionuclide-chelate complexes; and 4) the identification of processes, such as biodegradation, that can break down or degrade the released chelates.

A previously published review was conducted to evaluate current state of knowledge of the effects of chelates on the leaching and migration of radionuclides from buried nuclear wastes (Serne et al. 1996). The review includes four sections: decontamination concerns and treatment and disposal of spent resins, aqueous complexation of radionuclides, adsorption of chelates and radionuclide-chelate complexes, and biodegradation of chelates and radionuclide chelate complexes. All of these factors are important in determining the potential for the chelating agents to affect the leaching of buried waste and the migration of radionuclides in soils and sediments. The section on the aqueous complexation of radionuclides includes a review of the data available for performing thermodynamic equilibrium calculations and a review of analytical methods for identifying radionuclide-organic complexation. In addition, two sections were included that discuss chemical models/codes that use the thermodynamic and adsorption data to predict radionuclide fate and review literature where organic chelating agents have been suspected of causing enhanced migration, respectively.

Following the cited review, speciation calculations were conducted to determine the potential significance of organic chelating/complexing agents in facilitating transport of radionuclides from the waste forms and through soil and aquifer materials. The results and discussion of the speciation calculations are included in this report (Section 4). The speciation calculations were performed using thermodynamic equilibrium calculations to determine the contribution of the organic chelating/complexing agents to the speciation scheme of the important radionuclides and stable metals in the leachates from cement solidified waste and dewatered spent ion exchange resins. Actual leachate data from tests conducted at the Idaho National Engineering and Environmental Laboratory (INEEL) were used to determine the concentrations used in the model calculations. Initially the leachate solutions from cementitious waste forms have a high pH, which results from reactions with portland cement. The chemical evolution of these leachates can be expected to follow two pathways. If the leachates are contained within the waste site with an impermeable barrier, the high pH solutions could be neutralized by carbonic acid from the diffusion of CO_2 from the atmosphere or soil gas. Impermeable barriers are prone to failure and as a result may eventually leak. If the leachates flow through the soil column, it is expected that the pH will decrease due to the natural buffering capacity of the soil. To simulate these pH neutralization processes, the speciation calculations were conducted as a function of pH. Similar thermodynamic calculations for unsolidified dewatered resins were performed on the only data set available (CAN-DEREM spent resins leached in simulated groundwater). We make no claims that the results of these speciation calculations based on the few data sets available cover the whole range of possible leachate concentrations that might exist now or

in the future at licensed shallow land burial facilities. However, the calculations are representative of the highest concentration of organic ligands found to date in laboratory leaching studies.

After the speciation calculations were completed, laboratory adsorption experiments were conducted. Both batch and column experiments were performed. The results and discussion of this work is presented in Section 5. Section 6 presents the conclusions of this project and recommendations and Section 7 lists the references cited. Two appendices are included, the first contains the thermodynamic data used to perform the speciation calculations discussed in Section 4 and the second contains the K_d values for the organic ligands and metals as a function of pH for the batch adsorption tests shown in Section 5.

2.0 Background

A variety of chemical decontamination processes are used to remove the build-up of radionuclides and corrosion products from the cooling systems of nuclear power plants. All of these decontamination processes use one or more chelating agents that can include; ethylenediaminetetraacetic acid (EDTA), picolinic acid, oxalic acid, citric acid, and less frequently, diethylenetriaminepentaacetic acid (DTPA), to complex the released radionuclides. The complexed radionuclides and any excess uncomplexed chelates are then removed onto cation-, anion-, and mixed bed ion exchange resins. The U.S. Nuclear Regulatory Commission (NRC), as defined in 10 CFR 61, is responsible for regulating the disposal of such wastes, including providing regulatory criteria for the co-disposal of organic chelating agents that have the potential to enhance the migration of radionuclides away from disposal sites.

One of the principal pathways for radionuclides migrating away from a disposal site is contact with infiltrating recharge water. The presence of chelating agents in the buried wastes could enhance the subsequent migration of radionuclides in groundwaters if 1) sufficient quantities of chelating agents can leach from the buried wastes, 2) the leached chelating agents form strong radionuclide-chelate complexes, 3) the chelating agents or the radionuclide-chelate complexes do not adsorb to soils or sediments, and 4) the leached chelating agents or radionuclide-chelate complexes do not undergo degradation processes, such as biodegradation, that destroy the chelating agents.

Earlier a literature review was published (Serne et al. 1996) that focused on the following areas: 1) the nature and composition of reactor decontamination solutions; 2) the leaching chemistry of solidified decontamination wastes; 3) the aqueous complexation of radionuclides, including the thermodynamic data available for calculating the stability of radionuclide-chelate complexes and analytical methods for identifying specific radionuclide-chelate complexes; 4) the adsorption of chelating agents and metal-chelate complexes in soils or specific soil components (i.e., oxides and clay minerals); and 5) the biode-gradation of the chelates and radionuclide-chelate complexes present in decontamination solutions. A summary of the major findings of this review is presented below.

From the review of the leaching and decontamination chemistry studies, it appears that the principal decontamination processes used in the mid-1990's were the following: 1) the low-oxidation-state metal ions (LOMI) process (used in about 65 percent of power plant decontaminations performed in the mid 1990's), which uses picolinic and formic acid; 2) the CAN-DEREM process, which uses EDTA and citric acid; and 3) the CITROX process, which uses citric and oxalic acids. Based upon the few studies of decontamination wastes identified in the literature, it appears that organic chelating agents can leach moderately from solidified cements and can increase radionuclide and transition-metal leach rates by factors of 10 to 100. The resulting leach rates still appear to be low, possibly because of the importance of pH-dependent precipitation reactions. In addition, some of these waste forms appear to be physically unstable in low-ionic-strength solutions. Only one set of leach studies of unsolidified (dewatered) spent resins is available in work recently performed at INEEL on three spent resins obtained from a CAN-DEREM process used at Indian Point nuclear reactor. The three resins were leached using static experiments where simulated groundwater was mixed with dewatered spent ion exchange resins at a mass ratio of ~10:1 groundwater to resin. The leachates were separated from the resin aliquots after ~37 and ~90 days of contact. Detailed radionuclide measurements were performed on all leachates and complete cation and anion measurements were performed on selected leachates. Organic ligand measurements in the leachate were performed using ion chromatography. EDTA was found in the leachate from only one resin type. The preliminary results for the chemical composition of the leachate from the one resin that

contained EDTA were recently shared with us such that some speciation calculations could be performed to allow comparison with the cement solidified waste form leachates. The calculations are shown in Section 4. More details on the leach tests will be published by INEEL (Doug Akers, INEEL, personal communication Oct.-Nov. 2001).

The review of the thermodynamic data available for aqueous complexation reactions of chelates with metals and radionuclides focused on tabulating the data for metal-chelate complexes of EDTA, DTPA, picolinic acid, oxalic acid, and citric acid with selected radionuclides (i.e., neutron activation products, fission products, and actinides). A critical evaluation of these data was not performed because several such reviews have been published. Few data more recent than the latest critical review (i.e., Martell and Smith 1989) were found. Therefore, the majority of the data were compiled from the published critical reviews. As expected, this tabulation revealed that a large amount of data is available for transition-metal complexes with all of the ligands of interest in this study, although fewer data are available for DTPA and picolinic acid than for the other chelates. Unfortunately, far fewer data are available for the actinide-chelate complexes that could be present in the decontamination wastes. Based upon these data, it appears that the most important (thermodynamically stable) complexes involve EDTA and picolinate. Oxalate and citrate do not appear to be present in sufficiently high concentrations or to be sufficiently strong chelating agents to form important metal-chelate complexes.

Successful detection of radionuclide-chelate complexes in leachate solutions is very challenging at the low concentrations of chelates and metals found in the reviewed studies. All the published studies only include data on cement solidified spent resins while current practice is to dispose of the spent resins directly in high integrity containers. It is not possible to predict from the published studies what the expected concentrations/radioactivity of the chelating agents, stable metals and radionuclides would be in leachates from the dewatered resins themselves. Although appropriate analytical procedures are still being developed, some promising techniques are becoming available such as liquid chromatography/mass spectrometry (LC/MS). Such direct analytical determinations, once passed the development stage, could complement the thermodynamic calculations in identifying the specific radionuclide-chelate complexes of concern. At the present time these sophisticated analytical procedures are neither routine or economical.

Available research on the adsorption of EDTA, oxalate and citrate and their metal complexes to soils and specific soil components, such as hydrous oxides were reviewed in the previous project (Serne et al. 1996) and more recently in Davis et al. (2000). The following summary was mainly extracted from Serne et al. (1996). Less work has been done on DTPA, and only a few studies have been conducted with picolinic acid see Serne et al. 1996). The adsorption of these chelates and their metal complexes, especially on oxides, can be highly pH-dependent and all of the chelates can undergo what is termed "ligand-like" adsorption (i.e., adsorption of the chelates is strongest at low pH, decreases rapidly in the neutral pH region, and can be negligible at high pH [>8]). In general, relatively high concentrations of oxalate and citrate are required to complex and mobilize metal ions in soils or soil components.

These adsorption/desorption reactions for oxalate and citrate complexes do not appear to have any significant kinetic hindrance, and there is little or no evidence for the adsorption of oxalate-metal or citrate-metal complexes. Owing to the stronger stability of EDTA-metal aqueous complexes at higher pH values, EDTA can reduce metal adsorption onto soils or soil components. However, there is very good evidence for the adsorption of EDTA-metal complexes, particularly on Fe and Al oxides. This metal-chelate adsorption can retard, rather than enhance, the migration of radionuclides in soils and sediments. In addition, certain metal-EDTA complexes, most notably Co-EDTA, appear to be kinetically inert and do not react rapidly with other competing ions in solution. These factors make it especially difficult to

predict quantitatively the effects of EDTA on radionuclide transport in soils or sediments. Similar effects appear to be possible for the adsorption of DTPA, or possibly DTPA-metal complexes, although the data are much more limited. In the case of picolinate, very few studies have been conducted, and it is difficult to reach general conclusions. However, based on the few studies that have been done, it appears that adsorption of picolinate-metal complexes does not occur because both the amine and carboxylate functional groups of the picolinate ion prefer to bond to the adsorbent surface leaving no binding site on the ligand to adsorb metals, and that the formation of kinetically inert picolinate-metal complexes is unlikely. That is, when adsorption does occur, the picolinate molecule uses both of its binding sites to bond with the solid surface in preference to remaining bonded to the metal in the aqueous complex. However, further research in this area is warranted.

A variety of factors can influence the biodegradation of chelating agents and metal (radionuclide)-chelate complexes: 1) the presence of microorganisms capable of degrading the chelates; 2) the adsorption of the chelates to soils or sediments; 3) the aqueous speciation or complexation of the chelates; and 4) specific groundwater conditions, such as the pH and the organic carbon content of the water. In general, it appears that because citrate and oxalate are naturally present in some environmental systems, micro-organisms capable of degrading these acids should be generally present. Picolinate is not normally present in the environment, but natural structural pyridine analogs do exist, suggesting that picolinate-degradative pathways should also exist. There is no natural structural analog for EDTA in environmental systems, and this fact may account for EDTA's general recalcitrance to biodegradation in many environmental systems.

The need for an accurate and adequately complete water analysis as input data is one of the most important factors needed to obtain accurate thermodynamic modeling predictions. Inadequate solution characterization resulting from incomplete analysis of all significant constituents and a lack documentation of the sampling and analytical uncertainties are common problems. As with most computer modeling predictions, the common adage "garbage in equals garbage out," also applies to the application of chemical equilibrium models to aqueous speciation and mass transfer calculations. In the rare cases when the user has a complete and accurate water analysis other limitations include 1) an inadequate conceptual model that ignores the existence of certain aqueous species, sorbed species, and/or solids containing elements and/or ligands of interest (such as complexation of metals by dissolved natural organic compounds); 2) the lack of thermodynamic data for known aqueous species, sorbed species, and/or solids of interest; 3) the lack of internal consistency between parameters within a single thermodynamic database as well as between databases used by different models, and 4) inadequate theoretical understanding and formulation of certain processes, such as absence of models and/or data for sorption, kinetic rates, and solid solution; calculations in high-ionic strength solutions; and disequilibrium between redox couples.

Because thermodynamic databases are a critical component to model accurately aqueous speciation and solubility in soil/water systems, the more knowledgeable the user is with a model's database in terms of the completeness and accuracy of its data, the more likely the results will be correct. Unfortunately, most users cannot be experts with respect to the measurement and derivation of thermodynamic data nor can they afford to do a critical review of thermodynamic data for all aqueous species and solids containing elements of interest to their modeling applications. In these cases, the user should thoroughly document the database used when reporting results of aqueous speciation and solubility modeling calculations.

At present, the geochemical codes MINTEQ and HYDRAQL appear to have the most robust adsorption algorithms and most complete databases for organic ligand-radionuclide complexes. These codes were used in thermodynamic speciation modeling endeavors associated with this project.

Field data that show significant concentrations of radionuclides migrating with an apparent anomalously enhanced rate away from disposal units are scarce. No such studies are available for commercial low-level disposal facilities. At two defense waste facilities (Chalk River, Ontario and Oak Ridge, Tennessee) enhanced ^{60}Co migration has been observed beyond 50 meters from the burial trenches. In the former instance the cobalt appears to be associated with natural dissolved organics from neighboring swamps. In the latter case the cobalt appears to be bound to EDTA, likely present in the original waste stream.

The work presented in this document includes speciation calculations of radionuclide chelate interactions as a function of pH and laboratory adsorption results conducted using batch and column techniques.

3.0 Methods and Materials

3.1 Speciation Calculation Methods and Assumptions

Speciation calculations were conducted to determine the potential significance of organic chelating/ complexing agents in facilitating transport of radionuclides leached from cement solidified decontamination waste and through soil and aquifer materials. One set of calculations were also performed for leachate contacting a spent resin from the CAN-DEREM process with simulated groundwater based on the chemical composition recently obtained under contract with INEEL.

Potential impacts for organic complexes were assessed using thermodynamic equilibrium calculations to determine the contribution of the organic chelating/complexing agents to the speciation scheme of the important radionuclides and stable metals in the leachates. Initially the leachate solutions from cementitious waste forms have a high pH, which results from reactions with portland cement. The chemical evolution of these leachates can be expected to follow two pathways. If the leachates, are contained within the waste site with a water impermeable barrier, the high pH solutions could be neutralized by carbonic acid from the diffusion of CO_2 from the atmosphere or soil gas. After the barriers degrade, waste leachates percolate into the soil column. For this scenario, the pH will decrease due to the natural buffering capacity of the soil. To simulate these processes, speciation calculations were conducted as a function of pH. In these calculations it was assumed that the three principal soil components affecting pH and the subsequent speciation of important radionuclides and chelating agents are calcite, amorphous ferric hydroxide and gibbsite. That is, the soil system was simplified to consist of these three solids. The soil gas was maintained as a closed system; that is the partial pressure of carbon dioxide was allowed to vary with pH while maintaining equilibrium with calcite. It is well known that cement environments are not in equilibrium with air (Criscenti et al. 1996). In the calculations dissolution/precipitation of these three solids was included; however, adsorption reaction to these three solids was not included.

The chemical equilibrium code HYDRAQL (Papelis et al. 1988) was used to perform the speciation calculations for the cement leachates and MIMEQL+ (Schecher and McAvoy 1998) was used to perform the calculations on the leachate from the dewatered CAN-DEREM resin. Most of the stability constants for the organic chelating/complexing agents used as decontaminating agents were not included in either codes database. Therefore, the thermodynamic database file for each code was modified to include the organically chelated/complexed species needed to perform the calculations. Most organic-radionuclide/ metal stability constant values incorporated into the database were estimated from the compilation listed in Appendix A (Serne et al. 1996). Krupka and Serne (1998) was used as the source of Pu(IV) stability constants for inorganic complexes. Unfortunately, no stability constants for key organic ligands and the more oxidized forms of Pu [Pu(V) and Pu(VI)] are available. Thermodynamic data added to the two codes databases were adjusted to zero ionic strength using the Davies equation. The thermodynamic database used in the calculations from both codes and reported in this document is attached as Appendix A, for completeness.

The chelate, radionuclide, corrosion product and common groundwater ion concentrations selected for the speciation modeling calculations were based on a review of decontamination waste form leachate data (Serne et al. 1996). Most of this data was produced by researchers at the Idaho National Engineering and Environmental Laboratory (INEEL). Laboratory work was conducted with several decontamination waste streams and cementitious, solidified decontamination waste forms from commercial reactors. Leach experiments and physical stability tests were conducted. Details of this work can be found in

McIsaac and Akers (1991), Morcos et al. (1992), Akers et al. (1993a,b; 1994a,b), McIsaac and Mandler (1989), McIsaac et al. (1991,1992) and McIsaac (1993). The most important decontamination processes from a waste disposal perspective are LOMI, CAN-DEREM and CITROX. A total of six cementitious leachates were selected for the modeling analysis which were expected to be representative of any leachates derived from the LOMI, CAN-DEREM and CITROX processes. In general, the concentrations of the chelating agents and metals used in the speciation calculations were selected to be the highest values measured in any of the INEEL leachates for a given waste form. INEEL used the ANSI/ANS 16.1 leach protocol (ANS 1986) for the leach tests on cement solidified resins. ANSI/ANS 16.1 calls for frequent exchanges of the leachate such that equilibrium concentrations are not guaranteed. Thus one leach test of a given specimen typically produced 7 to 10 or more leachate solutions. We attempted to use the highest concentrations observed in the leach tests.

For the one set of leach tests conducted on dewatered spent resins from the CAN-DEREM process static leach tests were performed. Two contact times were chosen ~27 and ~93 days. The test results for the longer time period were used to choose the leachate composition that was speciated versus pH.

Two LOMI leachates from solidified cement wastes were modeled. These are referred to as the James A. FitzPatrick and Peach Bottom waste-form leachates. Leachate data for cement solidified CAN-DEREM process resins are not currently available, however, leachates from two other processes were selected as alternates. The first leachate was derived from the CAN-DECON process which is a precursor of the CAN-DEREM process and is very similar with the exception that it contains oxalic acid. The CAN-DECON leachate is referred to as Millstone. The second leachate was derived from the NS-1 process (which is no longer used). Waste ion-exchange resin derived from the NS-1 process contained similar concentrations of EDTA and citric acid as the CAN-DECON process but also contains DTPA (Table 12, Akers et al. 1994b). This leachate is referred to as the Pilgrim leachate. The two CITROX leachates modeled are Brunswick and Cooper. Total solution concentrations of the chelating agents and metals used to conduct the speciation calculations for the leachates from the cement solidified wastes are listed in Table 3.1.

Table 3.2 lists the chemical composition of Hanford groundwater before and after equilibration with cement. The composition of the simulated Hanford groundwater in Table 3.2 was combined with the products in Table 3.1 to perform the speciation calculations. The comparable leachate composition, including the major common cations and anions from the groundwater for the one data set for dewatered spent resins leached in simulated groundwater are shown in Table 3.3. Dewatered resins are generally disposed in high integrity containers (either high density polyethylene or plastic lined steel containers).

3.2

Table 3.1. Starting Concentrations of Chelating Agents and Metals Used in Equilibrium Modeling of Cementitious Waste Form Leachates (moles/liter)

Facility	FitzPatrick	Peach Bottom	Pilgrim	Millstone	Brunswick	Copper
Decon Process	LOMI	LOMI	NS-1	CAN-DECON	CITROX	CITROX
Picolinate	1.6×10^{-3}	2.9×10^{-4}	0.0	0.0	0.0	0.0
Citrate	0.0	0.0	1.1×10^{-5}	2.6×10^{-5}	2.8×10^{-5}	2.7×10^{-7}
EDTA	0.0	0.0	2.6×10^{-5}	2.7×10^{-4}	0.0	0.0
Oxalate	0.0	0.0	1.7×10^{-4}	1.1×10^{-4}	3.9×10^{-6}	1.2×10^{-4}
DTPA	0.0	0.0	2.5×10^{-6}	0.0	0.0	0.0
Co	1.0×10^{-10}	3.1×10^{-7}	1.0×10^{-10}	7.3×10^{-7}	7.3×10^{-6}	4.8×10^{-6}
Ni	1.6×10^{-6}	9.2×10^{-7}	2.9×10^{-5}	1.1×10^{-6}	5.3×10^{-6}	1.0×10^{-4}
Zn	1.0×10^{-10}	7.6×10^{-7}	1.0×10^{-10}	1.0×10^{-10}	1.0×10^{-10}	1.0×10^{-10}

Table 3.2. Major Ion Concentrations (total) in Synthetic Hanford Groundwater, Before, and After Equilibration with Portlandite

Constituent	Before	After
Ca	2.63×10^{-2}	2.63×10^{-2}
K	3.76×10^{-3}	3.76×10^{-3}
Mg	8.20×10^{-3}	1.30×10^{-7}
Na	2.04×10^{-2}	2.04×10^{-2}
CO_3	2.72×10^{-2}	7.00×10^{-6}
Cl	1.81×10^{-2}	1.81×10^{-2}
NO_3	3.20×10^{-5}	3.20×10^{-5}
SO_4	1.68×10^{-2}	1.68×10^{-2}
pH	8.9	12.3

Various solutions were used in experiments at INEEL to determine the leachability of the FitzPatrick and Brunswick waste forms including synthetic Hanford and Barnwell groundwaters, seawater and deionized water. The speciation calculations for these two wastes were performed only for leachates which used Hanford groundwater. The other waste forms (Peach Bottom, Millstone, Pilgrim and Cooper) were leached only in deionized water. Because the cement dominates the leachate composition there is little difference in the leachate composition from the deionized water, Hanford, or Barnwell groundwaters. Thus we believe the speciation calculations of the INEEL leachates from cement solidified wastes would apply for any typical groundwater contacting solidified cementitious spent decontamination resins. Seawater was not considered further because disposal sites planned in the United States will not be influenced by seawater. In general a conservative approach was taken (calculations were conducted to determine the highest possible impact of the chelating agents for each leachate solution). This was accomplished by conducting the speciation calculations using concentrations of stable metals and chelating/complexing agents which approximated the highest values measured in leachates from each waste form. The radionuclide concentrations measured in the leachates are at trace concentrations (a concentration of 1×10^{-10} M was assumed for modeling purposes). Because the major ion concentrations of the cement solidified waste form leachates were not measured in the INEEL work, they were assumed to be that of synthetic Hanford groundwater (Table 5, McIsaac et al. 1991) in equilibrium with portlandite. Major ion concentrations (total) in Hanford groundwater and synthetic Hanford groundwater in equilibrium with portlandite (calculated with HYRDAQL) are shown in Table 3.2. Equilibration of Hanford groundwater with portlandite results in the removal of nearly all the carbonate and most of the magnesium. This is due to precipitation of calcite and brucite, respectively. The calcium lost from precipitation of calcite is replaced by dissolution of portlandite.

Subsequent speciation calculations for the cement solidified waste leachates were conducted as a function of pH from 4 to 12 in increments of 0.4 pH units. In each of these calculations the solution was assumed to be in contact with 0.01 mole/L each of calcite ($CaCO_3[s]$), amorphous iron hydroxide ($Fe[OH]_3[am]$), and gibbsite ($Al[OH]_3[s]$). These solids were allowed to dissolve or precipitate as necessary to maintain equilibrium. They represent major constituents in most sediments that rapidly react with solutions that percolate through sediments. Adsorption was not included in the calculations.

Recently a leaching experiment on non-solidified decontamination waste material (spent ion-exchange resin) from the CAN-DEREM process was conducted at INEEL. The measured composition of one of these leachate solution is shown in Table 3.3. Measurements include pH, major cations and anions and chelating agents. For the leachate from the dewatered CAN-DEREM process resin the measured pH was 7.49 but for completeness we varied the pH from 6 to 10 for comparison purposes. We again kept the leachate in contact with the same finite masses of calcite, amorphous iron oxide and gibbsite to represent the reactions with soil. Once again adsorption was not included in the calculations.

Table 3.3. Major Ion Concentrations in Non-Solidified Decontamination Waste Leachates			
pH 7.49			
Cation	Concentration (moles/liter)	Anion	Concentration (moles/liter)
Ca^{2+}	3.00×10^{-4}	Cl^-	4.73×10^{-3}
Cr^{3+}	1.10×10^{-4}	SO_4^{2-}	5.78×10^{-4}
K^+	7.00×10^{-4}	HCO_3^-	0
Mg^{2+}	1.90×10^{-4}		
Mn^{2+}	2.46×10^{-4}	EDTA	2.4×10^{-4}
Ni^{2+}	1.28×10^{-4}		
Na^+	5.20×10^{-3}		
Co^{2+}	$<4.0 \times 10^{-7}$		
Fe^{3+}	$<1.0 \times 10^{-5}$		
Cu^{2+}	$<1.0 \times 10^{-6}$		
Zn^{2+}	$<6.0 \times 10^{-6}$		
Al^{3+}	$<1.0 \times 10^{-5}$		

Significant differences are apparent between these results and those of the cement solidified wastes (Table 3.1). The major differences occur in the concentrations of transition metals leached from the non-solidifed waste. High concentrations of Ni^{2+}, Cr^{3+}, and Mn^{2+} were measured in the non-solidified waste leachate. For the cement solidified waste leachates, Ni^{2+} concentrations were generally low and Cr^{3+}, and Mn^{2+} were below the detection limit likely because of precipitation reactions at the high pH in cement leachates. In the non-solidified waste leachates EDTA was the only chelating agent detected in this leachate solution. The measured concentration was similar to that of the cement solidified CAN-DECON waste leachate.

To estimate the effect of changes in pH and contact with natural soil components on the speciation of the metals and radionuclides in the waste leachate, additional speciation calculations were conducted on the leachate from the dewatered spent resin waste. These calculations were conducted by maintaining equilibrium with 0.01 mole/L each of calcite, amorphous iron hydroxide, and gibbsite. The pH was adjusted between 6 and 10. The solubility of Cr^{3+} was assumed to be controlled by $Cr(OH)_3(am)$.

3.2 Experimental Methods for Batch Adsorption

A series of batch adsorption experiments were conducted with Ni^{2+}, Sm^{3+}, Th^{4+}, NpO_2^+, UO_2^{2+}, and PuO_2^{2+}. These metals and radionuclides were selected to be representative of metals and radionuclides in leachates with oxidation states that ranged from +2 to +6. This range in oxidation states covers the total range of possibilities for metals that form moderate to strong complexes with organic ligands. Two chelating agents were included in the study; picolinate and EDTA. The speciation calculations shown in Section 4 indicated that these were the two most important chelating agents. Three well-characterized natural soils and a Fe-coated sand were available from another project so to maximize the amount of adsorption testing that could be done for the available budget they were used as representative adsorbents. Several of the chosen adsorbents are also similar to soils at existing or currently inactive commercial low-level waste disposal sites. Characterization data from the other project for these soils are reported in Table 3.4. The <2 mm size fraction from each of the soils was used in all experiments. The first soil (identified as MNC-70) is classified as clayey, kaolinitic, thermic Typic Hapludult. The MNC-70 soil has a slightly acidic pH, low organic carbon, no carbonate, a moderately low cation exchange capacity and moderately high iron (ferric) content. This soil is representative of well-weathered soils from the humid Southeastern United States. The second soil (identified as LK-1) is classified as a fine, montmorillonitic, thermic, Vertic Argiudoll. The LK-1 soil has a near neutral pH, moderate organic carbon, slight trace of carbonate and a relatively high cation exchange capacity consisting of mostly alkaline-earth cations and a moderate iron oxide content. This soil is representative of soils from a temperate climate such as the Midwestern United States. The third soil (identified as Milford-1) is from the Ultisol order collected at a depth of 2 meters from a glacio-fluvial gravel sediment pit exposing the lower Columbia formation located in Delaware.

The Fe-coated sand is a synthetic soil created by using a natural quartz sand which was acid washed to remove metals and then coating the sand with ferric oxyhydroxide. The iron oxyhydroxide gel was first synthesized by hydrolysis of a 0.24 mol/L solution of ferric chloride solution (Zachara et al. 1987). This was accomplished by adjusting the solution pH to approximately 7.5 with CO_2-free sodium hydroxide. The gel was equilibrated approximately 24 hours. After this the gel was mixed with the sand and allowed to age for approximately 4 days. The pH of the solution was maintained at 6.5 to 7.0, and washed daily with 0.1 mmol/L NaCl solution. The coated material was then filtered in a large Buchner funnel and dried in a forced air oven at 35°C. This synthetic soil is similar to the sand, with enriched hydrous oxides contents, near the commercial burial ground at the Hanford reservation.

Prior to performing each adsorption experiment, the soils were pre-equilibrated in a 0.003 Molar $Ca(ClO_4)_2$ solution at pH values between 4 and 9 at pH intervals of approximately 0.5 pH units. The calcium perchlorate is a simple non-interacting electrolyte used to simulate a simple groundwater that will not add complications to the study of organic-radionuclide complex interactions with representative soils. In most experiments, approximately 0.5 gm of soil was added to 30 ml of solution; however, for the nickel adsorption experiments using the LK-1 soil, a ratio of approximately 2 gm of soil was added to

Table 3.4. Chemical and Particle Size Characteristics of the Soils							
		Carbon (%)			Particle Distribution (%)		
Soil Type	pH in H_2O	Total C	Organic C	Inorg. C	Clay	Silt	Sand
MNC-70	5.33	0.07	0.07	0.00	28	48	24
LK-1	6.94	0.39	0.28	0.11	46	44	10
Milford-1	4.91	0.035	0.035	0.00	<1	<1	100
Fe-Coated	N/A	0.00	0.00	0.00	<1	<1	100
Exchangeable Cations (meq/100 g)							
	Al	Ba	Ca	Mg	K	Na	La
MNC-70	0.27	0.07	0.17	0.94	0.12	0.2	0.54
LK-1	0.00	0.05	16	7.17	0.28	1.68	<0.05
Milliford-1	Total 4.91						
Fe-Coated	N/A						
Fe Content (wt. %)							
	Fe(II)			Fe(III)		Fe (total)	
MNC-70	0.31			4.77		5.08	
LK-1	0.2			3.38		3.58	
Milford-1	--			--		0.30	
Fe-Coated	--			--		1.23	

30 ml of solution to obtain a better measure of adsorption from the change in concentrations between the influent and effluent solutions. For tests where there is low adsorption it is difficult to get good data if there is not measurable removal of the adsorbate after contact with the soil. One obvious positive step is to add more soil until the difference in the concentrations of the adsorbate between the beginning and end of the test is readily measurable. The pH was adjusted over a period of several days to a few weeks by addition of acid ($HClO_4$) or base (CO_2 free NaOH) until the pH drift was less than 0.5 pH units over a 24 hour period. The pH adjustments and equilibrations were conducted in an inert atmosphere chamber (N_2 glovebox) to maintain CO_2-free conditions. Once the slurry pH had stabilized, the solution was removed and fresh 0.003 M calcium perchlorate solution at the desired pH was added to the tubes while still in the chamber. A small aliquot of concentrated radiolabeled stock solution was then added to the tubes.

For EDTA-metal complex adsorption experiments, stock solutions containing the equal molar concentration (1.5×10^{-3} M) of EDTA and metal (UO_2^{2+} or Ni^{2+}) were added together. EDTA in these stock solutions was spiked with ^{14}C-labeled EDTA. The stock solutions containing nickel were spiked with

[63]Ni. After all reagents and tracers were added to the stock solutions, they were adjusted to a pH of 7.0. The final concentration of both EDTA and metal in the experiments (slurries of soil and simplified groundwater, $Ca[ClO_4]_2$) was 10^{-5} M. Following the addition of the EDTA-metal complex solutions, the vials were gently agitated for 16 hr at which time the tests were stopped. Each vial was then centrifuged at 2,500 rpm for 20 minutes, the pH measured, and an aliquot of the supernate removed and filtered with a 0.2 μm syringe filter. The filtered supernate was used for liquid scintillation counting and/or uranium analysis. The adsorption experiments were run in duplicate and blanks (solution only) were run for each pH. Liquid scintillation counting was conducted with a Wallac OY Inc. model 1415 liquid scintillation counter (Turku, Finland). Uranium was determined by laser-phosphorimetry (Chemchek Instruments Inc., Richland, Washington).

In addition to the EDTA-metal adsorption experiments, adsorption experiments were also conducted with picolinate-metal complexes. For these experiments, the following metals were used: Ni^{2+}, Sm^{3+} [analog for trivalent actinides], Th^{4+} [analog for quadrivalent actinides], NpO_2^+, UO_2^{2+}, and PuO_2^{2+}. These experiments were generally conducted in the same manner as the previous experiments with UO_2^{2+} and Ni^{2+} and EDTA. In some cases, different chelate to metal ratios were used. Only iron oxide coated sand and Milford soil were used as adsorbents in the picolinate-metal adsorption experiments. ^{14}C-labeled picolinate was added as a tracer to determine picolinate adsorption. For the picolinate-Sm^{3+} adsorption experiments, a beta emitting tracer was used ($^{151}Sm^{3+}$) to determine Sm^{3+} adsorption. For PuO_2^{2+} an alpha emitting tracer was used ($^{239}PuO_2^{2+}$). ^{239}Pu was measured using liquid scintillation counting. For the NpO_2^+ and Th^{4+} experiments gamma emitting tracers were used ($^{237}NpO_2^+$ and $^{228}Th^{4+}$). In the Th^{4+} experiments, $^{232}Th^{4+}$ was added to maintain the required mass concentration. Gamma spectroscopy was conducted with a high performance (60% efficient) germanium detector (Oxford, Inc.).

In one of the nickel-picolinate adsorption experiments, nickel was measured independently with Inductively Coupled Plasma - Optical Emission Spectrometer (ICP-OES) (Perkin Elmer 3300 Dual View). This was done to compare the results with the tracer techniques and verify their accuracy.

For the Pu experiments, the source of the Pu spiking solution was ^{239}Pu in HNO_3 with an indeterminate oxidation state (an unknown mixture of +3, +4, +5, +6). We transformed this mixed spike into the most oxidized state (+6 oxidation state) because the most common disposal environments are oxidizing and Pu in its higher oxidation states is expected to be more mobile. We transformed the mixed Pu spike to the +6 state by taking an aliquot of our standard solution and heating it to dryness. The ^{239}Pu was redissolved in 8M HNO_3 and reduced to a +4 state using H_2O_2. This solution again was heated to dryness and redissolved in 8M HNO_3. $NaBiO_3$ was then added and the solution vial was sealed and heated. The solution was periodically checked by UV-vis spectrometry until the oxidation reaction was complete. Again the solution was heated to dryness and brought back up in 0.1M $HClO_4$. This step was repeated twice to ensure complete removal of excess HNO_3. The +6 oxidation state was verified by UV-vis spectrometry. The oxidation state of the standard was checked periodically.

For the picolinate/^{239}Pu adsorption experiments, an aliquot of the +6 oxidation state ^{239}Pu standard was then combined with a ^{14}C labeled picolinate spiking solution to achieve an equal molar concentration of 1.0×10^{-4} M. The pH of the spiking solution was then adjusted to 7.0 and allowed to equilibrate for 24 hours. Prior to addition of the spike to the adsorption vials, the Pu oxidation state was verified as being +6.

Because of the high activity of the ^{239}Pu, a decision was made to run the adsorption tests with a final equal molar ^{239}Pu/picolinate concentration of 1.0×10^{-6} M. These same concentrations of chelate and radionuclide were also used in the ^{237}Np experiments (all other previous tests were run at an equal molar concentration of 1.0×10^{-5} M). In these experiments, the beta spectra for the ^{14}C was swamped out by ^{241}Pu impurity in our stock ^{239}Pu solution; resulting in poor data quality for the picolinate concentrations. An additional adsorption experiment was conducted at a molar ratio of 1000:1 picolinate to Pu to allow for better resolution of the ^{14}C labeled picolinate concentrations and to determine the effects of a large excess of picolinate on adsorption. The 1000:1 series has 10^{-5} M picolinate and 10^{-8} M ^{239}Pu concentrations.

3.3 Experimental Methods for Column Adsorption

Following the batch adsorption experiments, six column adsorption experiments were conducted to establish whether changing the soil to solution ratio dramatically and introducing hydrologic transport would affect the adsorption properties of the organic-nuclide complexes. In the disposal environment the soil to leachate ratio will be much greater than in the batch tests and flow will occur that can change the fluid composition from that observed in the batch tests where reaction products can not be transported away.

The six columns with dimensions of approximately 2.6 cm diameter by 18.4 cm length (see Table 3.5) were packed with air-dry sediments using a vibrating wand to homogeneously shake sediment as it was poured slowly into the column in a continuous fashion. Known sediment weights were used to attain a desired bulk density [1.5 to 1.7 g/cm^3] on final packing. The packing was visually inspected to verify that a relatively homogeneous bedding structure was obtained. From the known column dimensions (column volume), weight of sediment, and measured particle density for each sediment, the porosity of each column could be calculated. The values are shown in Table 3.5. As a check on the porosity, the columns were reweighed after they were filled with the background electrolyte. Assuming the density of the dilute background electrolyte is 1.00 g/cm^3, the volume of water added is a measure of the porosity. As shown in Table 3.5 [table columns 7 and 11], the measured and calculated porosity are the same for each packed column, essentially corroborating all the measurements/calculations. Flow was established in an up flow direction in each column to attempt to maintain saturated conditions. Prior to the start of each adsorption-desorption experiment, the columns were equilibrated with the background electrolyte [0.003 Molar

							Length of	Volume of			
		Wt. of	Wt. of		Wt. of	Volume	Soil	Soil	Bulk		
		Empty	Column and	Wt. of	Column, Soil	of Pores,	Column,	Column	Density,		Particle
Column #	Soil	Column, g	Soil, g	Soil, g	and H$_2$0, g	g	cm	cm^3, ml	g/cm^3	Porosity	Density, g/cm^3
1	Milliford	136.99	302.37	165.38	328.80	26.43	18.40	98.67	1.68	0.27	2.29
2	Milliford	138.13	302.96	164.83	329.50	26.54	18.35	98.40	1.68	0.27	2.29
3	Milliford	136.48	302.89	166.41	330.28	27.39	18.40	98.67	1.69	0.28	2.33
4	Milliford	137.34	302.98	165.64	330.14	27.16	18.40	98.67	1.68	0.28	2.32
5	Fe coated	136.83	282.58	145.75	318.50	35.92	18.40	98.67	1.48	0.36	2.32
6	Fe coated	136.83	283.39	146.56	320.40	37.01	18.50	99.20	1.48	0.37	2.36

Table 3.5. Physical Properties of Experimental Columns

Ca(ClO$_4$)$_2$; pH ~7] for ~8-16 hrs (1 to 2 pore volumes) to "pre-equilibrate" the sediment with the solution. In the Milford soil tests for columns 3 and 4, the sediment was first equilibrated with dilute NaOH to simulate cement leachate interactions.

The flow rate in each column was controlled by a constant flow rate hospital grade peristalic pump to be approximately 3.4 mL/min for the Milford soil columns and 4.5 mL/min for the iron coated sand columns. These volumetric flow rates equate to 3 pore volumes per day (or 8 hour residence time). A pore volume is the volume of fluid needed to fill the void space (porosity) in the column. After this "pre-conditioning," the same simple background electrolyte solution containing known concentrations of the metal/ radionuclide and organic ligand spiked with appropriate metal and ^{14}C tracers were injected into the columns for up to 10-15 days at the same flow rate. The pH of the influent solution was adjusted to pH 7.5 ± 0.5 before contacting the sediments. Breakthrough curves for the tracers were generated from measurements of aliquots of effluent taken every few hours during the injection period. In some cases, injection of the metal/radionuclide and tracers laden simple electrolyte was discontinued and further flushing was continued with the background electrolyte to study the desorption of the tracers. It was discovered after the first few column tests with the Milford soil that Milford soil has a net weak acidic nature (porewater pH is ~4.9). It was found that the column effluents from the first two columns was approximately 5, at which there is appreciable adsorption of the metal-ligand complexes and the free ligand. The major goal for the column tests was to explore environments in which the batch tests had shown little adsorption of the ligand and metal-ligand complex. We were concerned that the relatively strong adsorption in the first two Milford soil columns had been exacerbated by the acidic pH. Therefore the latter two Milford tests on columns 3 and 4 were preflushed with several pore volumes of weak sodium hydroxide solution prior to equilibrating with the background electrolyte. As a result, neutralization capacity of the natural acidity in the Milford soil was overshot to simulate reaction with cement leachate such that once the metal-ligand-radiotracer solutions were injected, the effluent pH for the last two Milford columns remained close to 9.8 during the entire test. Based on the batch tests at pH

3.10

9.8 metal-organic complexes and the free ligand should show insignificant adsorption. Thus it was felt that the last two Milford soil column tests would represent "worst case" enhanced transport for complexes in a cement leachate dominated column. The column experiments specifics are described in Table 3.6.

Table 3.6. Column Experiment Details			
Soil	**Ligand (M)**	**Metal**	**Comments**
FeOX-sand	Picolinate (10^{-4})	Ni (10^{-6})	Tracer for 29 PV, flush for 15 more; pH ~6.7 for 20 PV then increased to 7.4
Miliford	Picolinate (10^{-4})	Ni (10^{-6})	Tracer for 30 PV then flush for 12 more PV; pH dropped by soil to ~5 throughout test except for a few spikes up to pH ~7 near 25 and 30 PV
Miliford	Picolinate (10^{-5})	Ni (10^{-6})	Tracer for 30 PV then stop column: soil dropped the effluent pH to ~5 throughout the test
Miliford	Picolinate (10^{-4})	Pu (10^{-7})	Soil flushed with weak NaOH to get rid of acid buffering capacity; tracer for 49 PV then flush for 31 more PV; effluent pH stayed near 9.8 for whole test
FeOX-sand	EDTA (10^{-5})	Ni (10^{-5})	Tracer for 49 PV then flush for 20 more PV; pH remained near 7.5 throughout test
Miliford	EDTA (10^{-5})	Ni (10^{-5})	Soil flushed with weak NaOH to get rid of acid buffering capacity; tracer for 47 PV then flush for 31 more PV; effluent pH stayed near 9.8 for whole test

Three nickel-picolinate column experiments were performed. One nickel-picolinate column adsorption experiment was completed with the iron oxide coated sand using Ni at 1 x 10^{-6} M and picolinate at 1 x 10^{-4} M. Two nickel-picolinate column adsorption experiments were conducted with Milford soil and Ni concentrations at 1 x 10^{-6} M and picolinate concentrations at 1 x 10^{-4} M and 1 x 10^{-5} M, respectively. One Pu-picolinate experiment was performed with Milford soil at a Pu concentration of 1 x 10^{-7} M and a picolinate concentration of 1 x 10^{-4} M. Two Ni-EDTA column adsorption experiments were conducted, one with iron oxide coated sand and one with Milford soil. In both cases, the Ni and EDTA concentrations were 1 x 10^{-5} M. As in the batch experiments, radioactive tracers were used to track the adsorption of both the metals and the chelating agents.

After each column experiment was finished, the column was disassembled and the packed sediment was sliced into 2 cm thick layers. This soil material was then extracted with 1.0 M nitric acid so that a mass balance of the tracer could be conducted. A 5-to-1 weight ratio of nitric acid to soil was used for the

extraction step. The extractions were conducted in centrifuge tubes that were placed on a tube rotator overnight. The extractions were conducted twice, each time for 16 to 24 hrs and the quantity of tracer extracted in the two extractions was combined to get the total mass of metal and organic ligand extracted from the sediment. The quantity of tracer transported through the column in the Ca perchlorate solutions was added to the quantity of extractable tracer. This total was compared to the total quantity of tracer injected into the column to determine a mass balance. If the mass balance agreed to within 10%, the data were considered to be reliable and the column test a success.

4.0 Speciation Calculations

4.1 Speciation in Initial Cement Dominated Leachates

Significant complexation of metals/radionuclides by organic chelating/complexing agents is predicted for several of the leachates from cement solidified decontamination wastes (assumes equilibrium with portlandite, Table 4.1). The percent distribution of the picolinate complexes in the LOMI leachates (Peach Bottom and FitzPatrick) are shown in Table 4.1. Picolinate complexes were the dominate species for Co^{2+} and Ni^{2+} in the FitzPatrick leachates. For the rest of the radionuclides and metals complexation by picolinate was unimportant. The balance of the species for Am^{3+}, Co^{2+}, Fe^{3+}, Mn^{2+}, Ni^{2+}, Pu^{3+}, Pu^{4+}, and Zn^{2+} not listed in Table 4.1, were hydrolysis species. For Sr^{2+} the remaining species were free Sr^{2+}, $SrOH^+$, and $SrSO_4^0$. Cs^+ was essentially uncomplexed. The major differences between the FitzPatrick and Peach Bottom leachates were the concentrations of picolinate and nickel. The picolinate and nickel concentrations used in the Peach Bottom leachate calculations were 2.9×10^{-4} M and 9.2×10^{-7} M, respectively, and 1.6×10^{-3} M and 1.6×10^{-6} M in the FitzPatrick leachate. These differences may reflect the fact that the FitzPatrick waste forms crumbled during the leach testing whereas the Peach Bottom samples remained intact.

Table 4.1. Percent Distribution of Picolinate Complexes in LOMI Leachates (Peach Bottom and FitzPatrick) in Equilibrium with Portlandite (pH 12.3)		
Radionuclide or Metal	**Peach Bottom**	**FitzPatrick**
Am^{3+}	0.0	0.0
Cs^+	0.0	0.0
Co^{2+}	0.0	59.7
Fe^{3+}	0.0	0.0
Mn^{2+}	0.0	1.3
Ni^{2+}	1.8	94.3
Pu^{3+}	0.0	0.0
Pu^{4+}	0.0	0.0
Sr^{2+}	0.0	0.0
Zn^{2+}	0.0	0.0

The percent distribution of complexes in the initial Pilgrim leachate (in equilibrium with portlandite) that contains EDTA and DTPA are given in Table 4.2. Complexation of radionuclides/metals with citric acid and oxalic acid was insignificant in the Pilgrim leachates. For Am^{3+}, Pu^{3+}, and Sr^{2+} complexes with DTPA are the dominant species. Cs^+ and Fe^{3+} were essentially uncomplexed by organic ligands. A small to moderate amount of organic (both EDTA and DTPA) complexation occurred for Co^{2+}, Mn^{2+}, and Zn^{2+}. The balance of the species not included in Table 4.2 for Co^{2+}, Fe^{3+}, Mn^{2+}, Ni^{2+}, and Zn^{2+} were hydrolysis complexes. Cs^+ exists in the leachates essentially as the free ion.

Significant complexation by organic ligands also is predicted for some of the radionuclides in the Millstone (CAN-DECON process) leachates. Mn^{2+}, Ni^{2+}, Sr^{2+}, and Zn^{2+} were dominated by EDTA or mixed OH-EDTA complexes (Table 4.3). Complexation by citrate and oxalate was insignificant in the Millstone leachates. For Am^{3+}, Co^{2+}, Fe^{3+}, Pu^{3+}, and Pu^{4+} hydrolysis was strong enough to dominate the speciation scheme for these ions. Cs^+ again remained essentially as the free ion.

Predictions for CITROX leachates for Brunswick and Cooper cement solidified waste forms show that metals/radionuclides should not be complexed to any significant extent by organic chelating agents in the initial leachate solutions. The speciation scheme of all of the radionuclides, studied with the exception of Cs^+ and Sr^{2+} were dominated by hydrolysis. Cs^+ occurred in these leachates as the free ion. Sr^{2+} was mostly free, but about 30% occurred as sulfate complexes.

Table 4.2. Percent Distribution of EDTA and DTPA Complexes in NS-1 Pilgrim Leachates in Equilibrium with Portlandite (pH 12.3)				
Radionuclide or Metal	% M-EDTA	% M(OH)-EDTA	% M-DTPA	Total
Am^{3+}	0.0	0.0	87.3	87.3
Cs^+	0.0	0.0	0.0	0.0
Co^{2+}	0.0	59.7	7.2	10.9
Fe^{3+}	0.0	0.0	0.0	0.0
Mn^{2+}	19.6	0.0	2.7	22.3
Ni^{2+}	0.0	0.0	0.0	0.0
Pu^{3+}	0.0	0.0	87.3	87.3
Pu^{4+}	0.0	0.0	0.0	0.0
Sr^{2+}	32.7	0.0	61.9	94.6
Zn^{2+}	0.0	44.6	0.0	44.6

Table 4.3. Percent Distribution of EDTA Complexes in CAN-DECON Millstone Leachates in Equilibrium with Portlandite (pH 12.3)			
Radionuclide or Metal	% M-EDTA	% M(OH)-EDTA	Total
Am^{3+}	21.4	0.0	21.4
Cs^+	0.0	0.0	0.0
Co^{2+}	30.7	0.0	30.7
Fe^{3+}	0.0	0.0	0.0
Mn^{2+}	72.8	0.0	72.8
Ni^{2+}	32.5	63.3	95.8
Pu^{3+}	21.4	0.0	21.4
Pu^{4+}	0.0	0.0	0.0
Sr^{2+}	98.5	0.0	98.5
Zn^{2+}	0.0	89.5	89.5

4.2 Speciation in pH Adjusted Leachates from Cement Waste Forms

By decreasing the pH and maintaining equilibrium with calcite, amorphous iron hydroxide, and gibbsite at a total finite concentration of 0.01 mole/L each, significant alterations in the equilibrium speciation were found to occur in the leachates. Although this scenario is used to simulate the consequences of interactions between the cement dominated leachate with a typical soil, these calculations are also generally applicable for a situation where the leachate is contained within the waste site and is neutralized with carbonic acid. Influx of carbon dioxide is not likely to reduce the pH below 8 and in nearly all instances, the speciation of the major chelating agents is not affected by Fe^{3+} or Al^{3+} complexation (see later discussion) at these high pH values. Significant complexation of the chelating agents with Ca^{2+} does occur between pH 12 and 8; however, because the concentration of Ca^{2+} in equilibrium with both portlandite and calcite are essentially the same (see Table 3.2), the speciation results discussed below are applicable to both the soil percolation-neutralization scenario and the CO_2 gas diffusion neutralization scenario that were described in Section 3.1.

The following figures portray the speciation calculation results for the various leachates as the pH is lowered from high values (>12) found in the environments dominated by cement. For each figure, the y axis is the percent of the total metal/radionuclide/chelating agent and the x axis is pH. (An) represents trivalent actinides (Pu^{3+}, Am^{3+}, and Cm^{3+}), other metals and radionuclides use their appropriate elemental symbol. The ligands are represented as (OH) for hydroxide (hydrolysis) species, (In) for all other inorganic ligands such as Cl^-, SO_4^{2-}, CO_3^{2-} as well as the free radionuclide/metal, (Pic) for picolinate, (Cit) for citrate, (Ox) for oxalate, (EDTA) for ethylenediaminetetraactetate, and (DTPA) for diethylenetriaminepentaacetate. The subscript (x) signifies that several species are present that were summed to give a total. This was done to keep the figures from becoming excessively cluttered. Most often the subscript is used to indicate the sum of a series of hydrolysis species, such as $AmOH_2^+$,

Am(OH)$_2{}^+$, and Am(OH)$_3{}^0$. In other cases, the speciation modeling calculations predict that more than one organic ligand (chelating agent) may attach to a metal atom to form ML, ML$_2$, ML$_3$, etc., or in some cases a mixed species such as MLOH.

Results of the LOMI Peachbottom equilibrium speciation calculations for a number of radionuclides are illustrated in Figures 4.1 through 4.6. From Figure 4.1, it is apparent that complexation of the trivalent actinides (Am^{3+} and Pu^{3+}) by picolinate in the Peachbottom leachates is relatively minor, peaking near 20% between pH values of 5 and 9. Similar behavior is observed for Mn^{2+} (Figure 4.3). For Co^{2+}, Ni^{2+}, and Zn^{2+} (Figures 4.2, 4.4, 4.6), picolinate complexes dominate the speciation scheme throughout most of the pH range studied. At high pH, >11 for Co^{2+}, >11.5 for Ni^{2+}, and >9.5 for Zn^{2+}, hydrolysis dominates the speciation. Sr^{2+} was not significantly complexed by picolinate. For Pu^{4+} (Figure 4.5) picolinate complexes are not important. Carbonate complexes dominate the speciation scheme of Pu^{4+} up pH 8.3; beyond this pH hydrolysis dominates. Figure 4.7 shows the speciation scheme of picolinic acid in the Peachbottom leachates, as a function of pH. CaPic$^+$ and free picolinate are the major species of picolinic acid from pH 12 down to 5. Below pH 5 protonation of picolinate increases as the pH decreases. A small amount of the Fe(OH)Pic$^+$ species is also observed to occur.
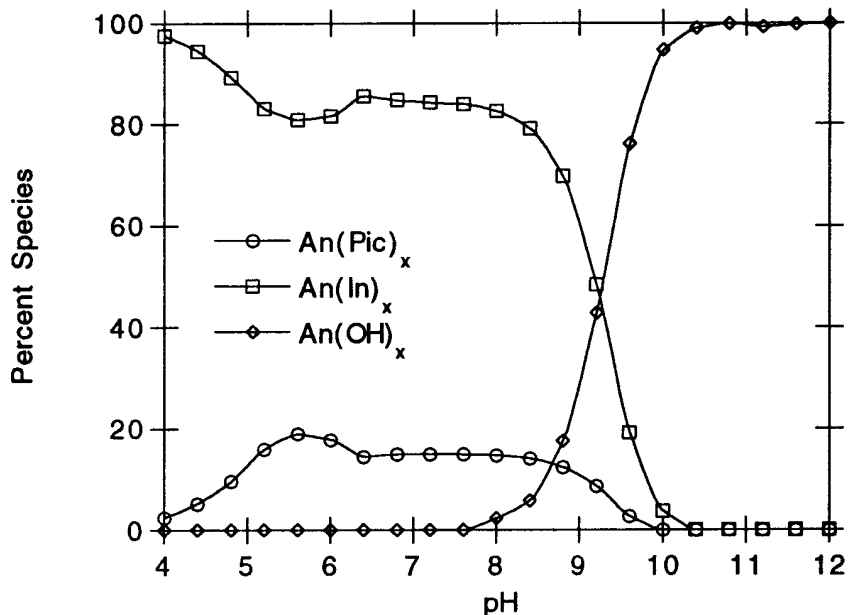
Figure 4.1. Speciation Distribution for Trivalent Actinides in Peach Bottom (LOMI) Leachate

4.4
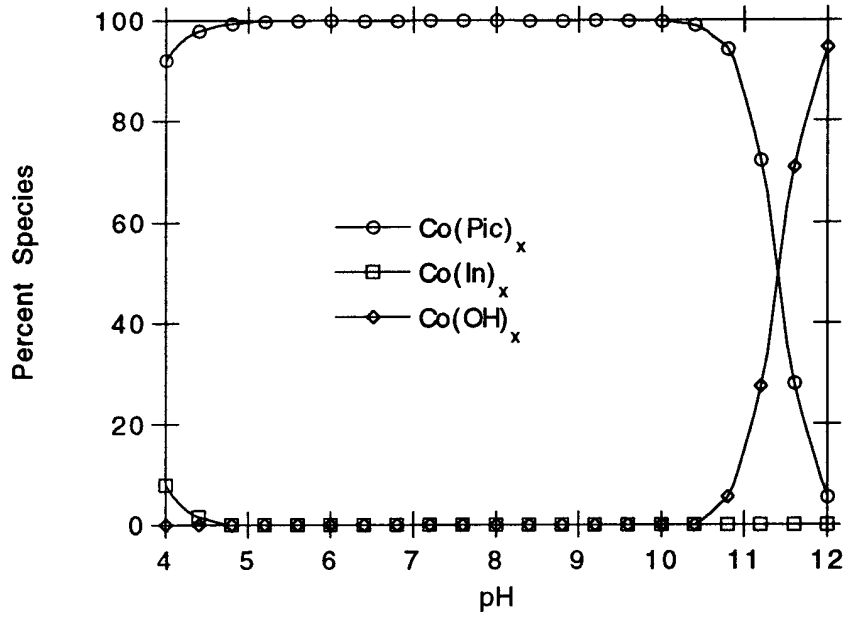
Figure 4.2. Speciation Distribution for Cobalt in Peach Bottom (LOMI) Leachate
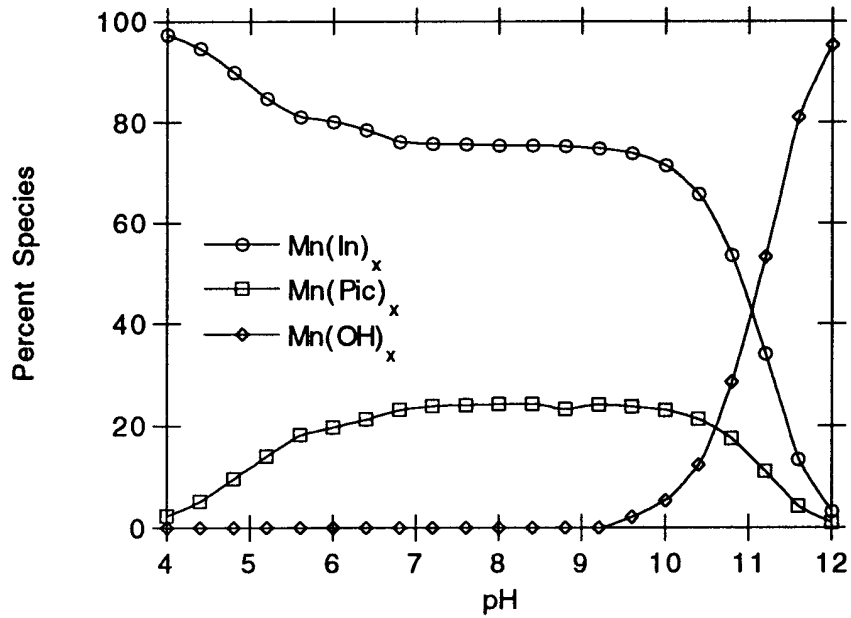
Figure 4.3. Speciation Distribution for Manganese in Peach Bottom (LOMI) Leachate

4.5
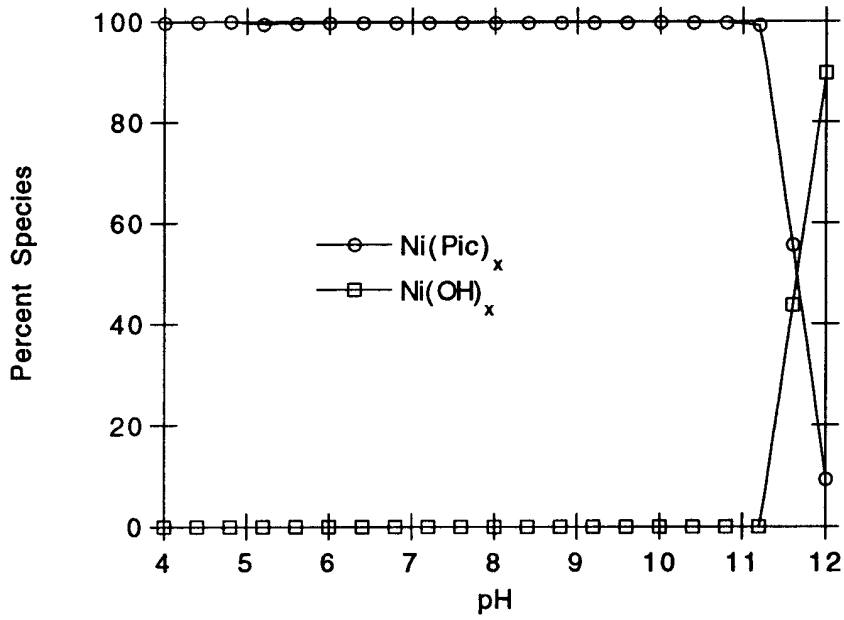
Figure 4.4. Speciation Distribution for Nickel in Peach Bottom (LOMI) Leachate
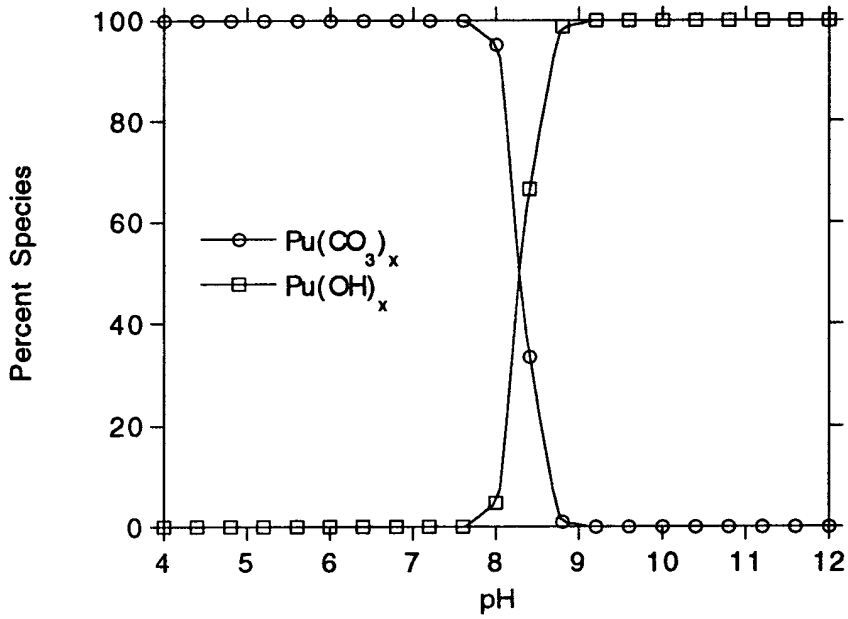
Figure 4.5. Speciation Distribution for Plutonium (IV) in Peach Bottom (LOMI) Leachate

4.6
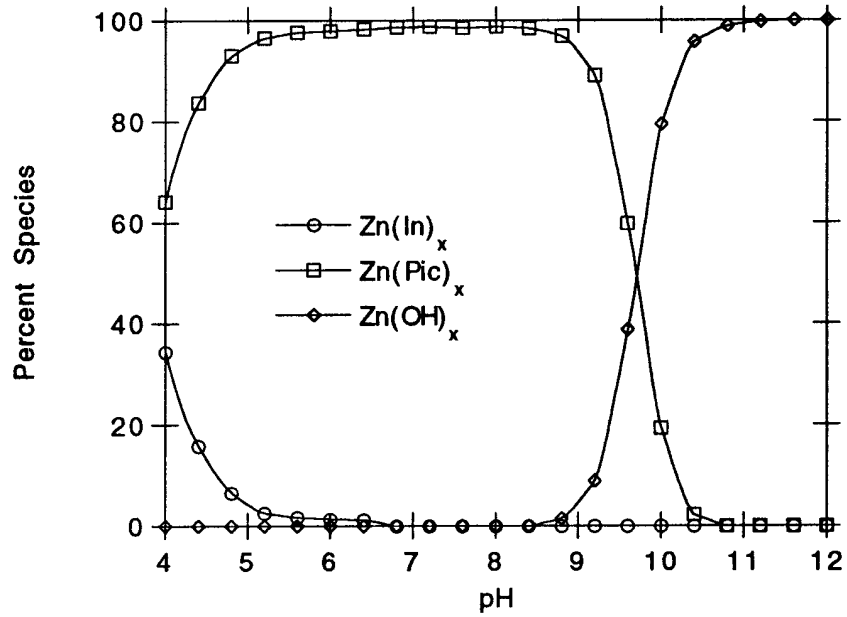
Figure 4.6. Speciation Distribution for Zinc in Peach Bottom (LOMI) Leachate
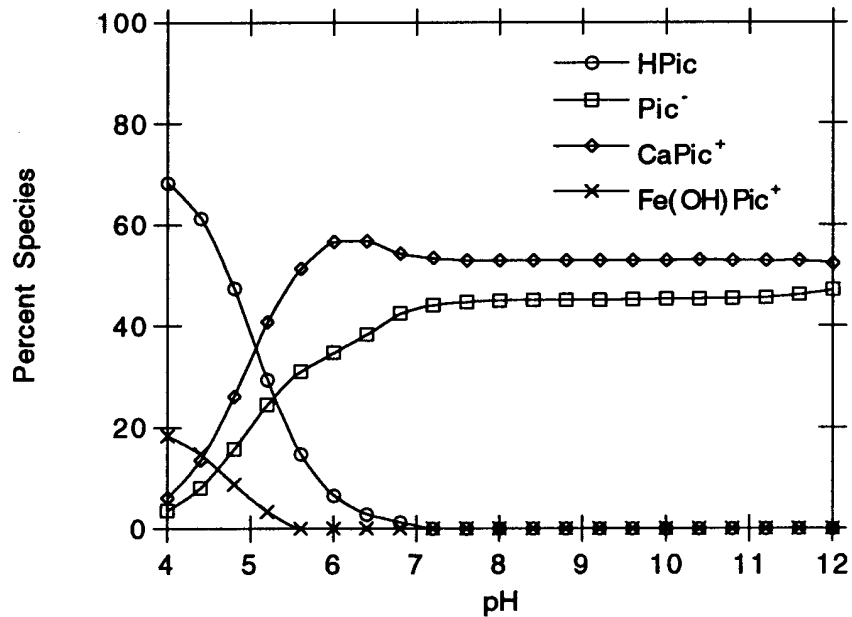
Figure 4.7. Speciation Distribution for Picolinic Acid in Peach Bottom (LOMI) Leachate

In general, the speciation of the radionuclides in the LOMI FitzPatrick leachates are similar to those of Peachbottom leachates. Because of the higher picolinate concentrations in the FitzPatrick leachates the importance of picolinate complexation is even greater than for Peachbottom. In the case of the trivalent actinides (Am^{3+} and Pu^{3+}) picolinate complexation increases to a peak of near 70% between pH values of 5 and 9. Mn^{2+} complexation with picolinate peaked at about 66%. For Co^{2+}, Ni^{2+}, and Zn^{2+}, the dominance of picolinate complexes shifted to higher pH values. For Co^{2+} and Ni^{2+}, picolinate complexes dominated at all pH values. For Zn^{2+}, hydrolysis begins to dominate the speciation above pH 10.5.

In the NS-1 Pilgrim leachate, trivalent actinide (Am^{3+} and Pu^{3+}) speciation (Figure 4.8) is dominated by complexation with chelating agents from pH 12 down to pH 5. Below this pH, inorganic species begin to dominate the trivalent actinide speciation scheme. The DTPA complex is the dominant species from pH 12 to pH 8. Oxalate complexes dominate from pH 8 to about 5. For Co^{2+}, (Figure 4.9) complexes with EDTA and DTPA are the dominant species from pH 11.8 to pH 9. For Mn^{2+} (Figure 4.10), the EDTA complex is dominant from pH 12 down to 10. For Ni^{2+} (Figure 4.11), $NiEDTA^{2-}$ is the most important species in the pH range of 5 to 11. Above pH 11, hydrolysis becomes the dominant species. Below pH 5, free Ni^{2+} and inorganic complexes of Ni^{2+} dominate. Organic complexation of strontium (Figure 4.12) is dominant above pH 10.5. Below pH 10.5 complexation of strontium with EDTA and DTPA falls off rapidly and free Sr^{2+} and inorganic complexes predominate. Pu^{4+} speciation is not affected by organic complexation in the Pilgrim leachates. For zinc (Figure 4.13), EDTA complexes ($ZnEDTA^{2-}$ and $Zn(OH)EDTA^{3-}$) dominate the speciation scheme from pH 12 down to pH 9. Below pH 8, Zn in predominantly in the form of inorganic species and free zinc. The speciation schemes of EDTA and DTPA are illustrated in Figures 4.14 and 4.15. For both EDTA and DTPA, complexes with Ca^{2+} are the dominant species from pH 12 down to nearly pH 11. Nickel chelates dominate the speciation of EDTA from pH 11 to approximately pH 5 and pH 11 to pH 7 for DTPA. Fe^{3+} chelates dominate below these pH values.

Organic complexation in the CAN-DECON Millstone leachate is significantly greater than for the Pilgrim leachate. This is due primarily to the higher EDTA concentrations (Table 3.1). For nearly all of the radionuclides (Am^{3+}, Pu^{3+}, Co^{2+}, Mn^{2+}, Ni^{2+}, Sr^{2+}, Zn^{2+}, Figures 4.16-4.21), EDTA complexes dominate the speciation scheme from pH 12 down to pH 6.5 or below. Only for Pu^{4+} is organic complexation relatively insignificant. From pH 12 down to 5.5 Pu^{4+} is dominated by hydrolysis and carbonate complexation (Figure 4.22). From pH 5.5 to 4.0 citrate complexes dominate the Pu^{4+} speciation scheme. In the Millstone leachates chelates with calcium dominate the EDTA speciation scheme from pH 12 to 7; below this pH, chelates with Fe^{3+} are the dominant species for EDTA as shown in Figure 4.23.

With a few exceptions both CITROX leachates, Cooper and Brunswick, have relatively little organic complexation of the radionuclides. The most significant complexation was determined for the trivalent actinides and nickel in the Cooper leachate. Oxalate complexes comprised nearly 90% of the species distribution for Am^{3+} and Pu^{3+} (Figure 4.24) between pH 5 and 9. Oxalate complexes accounted for approximately 28% of nickel species from pH 5.5 to 9 in the Cooper leachates (Figure 4.25). The speciation scheme of oxalate in the Cooper leachate is illustrated in Figure 4.26. Ca^{2+} chelates are the
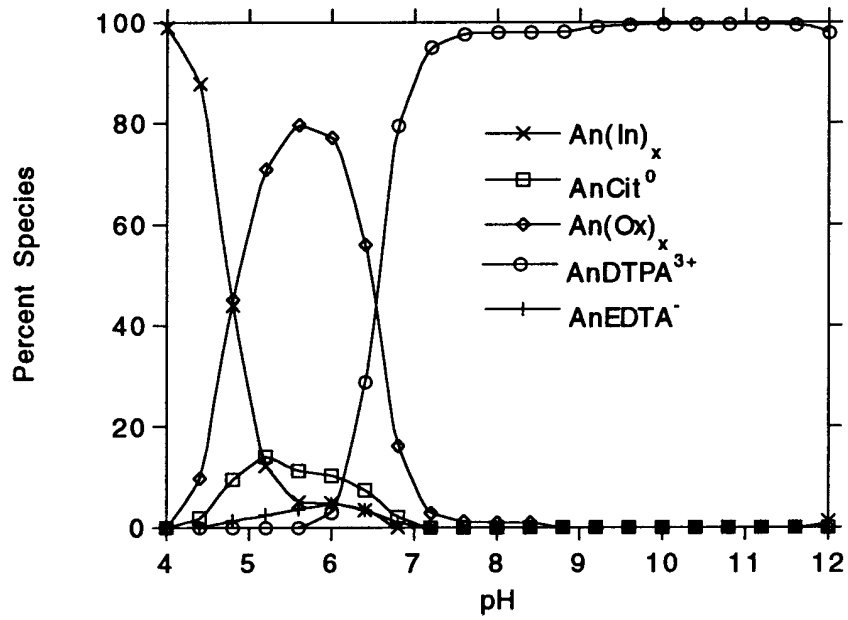
Figure 4.8. Speciation Distribution for Trivalent Actinides in Pilgrim (NS-1) Leachate
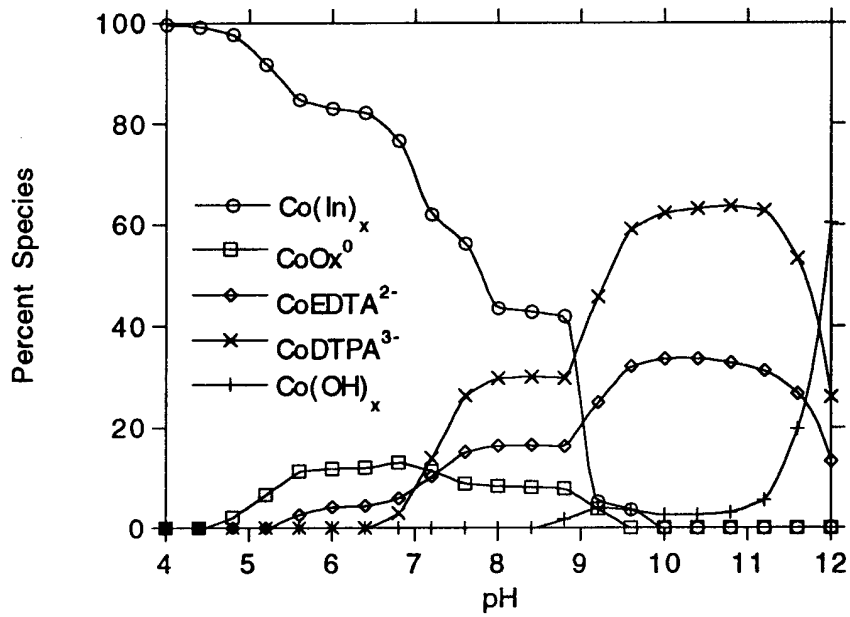
Figure 4.9. Speciation Distribution for Cobalt in Pilgrim (NS-1) Leachate

4.9
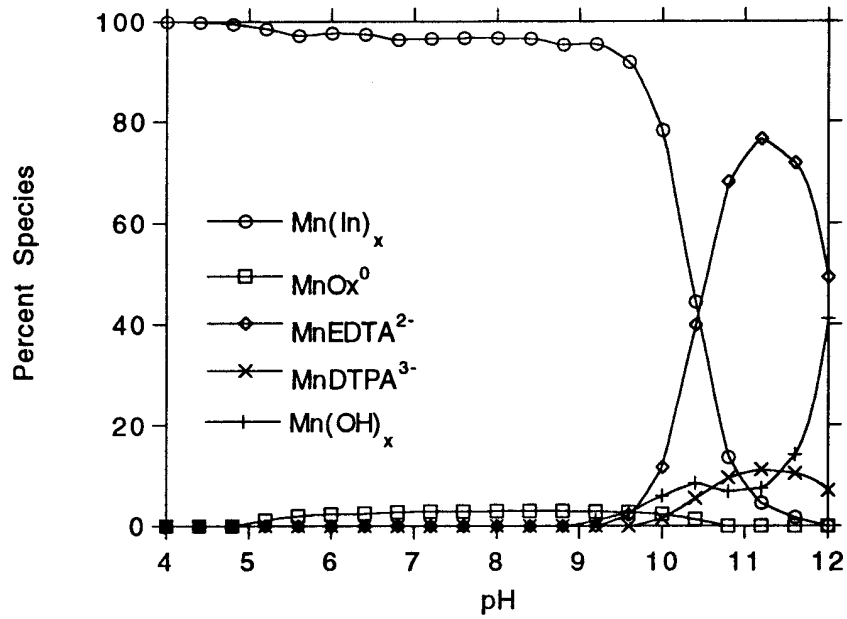
Figure 4.10. Speciation Distribution for Manganese in Pilgrim (NS-1) Leachate
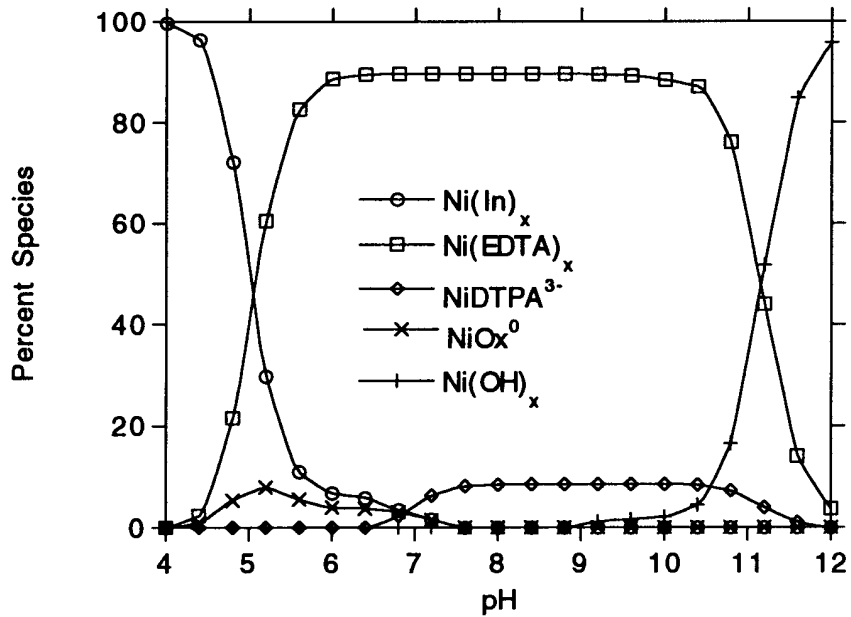
Figure 4.11. Speciation Distribution for Nickel in Pilgrim (NS-1) Leachate
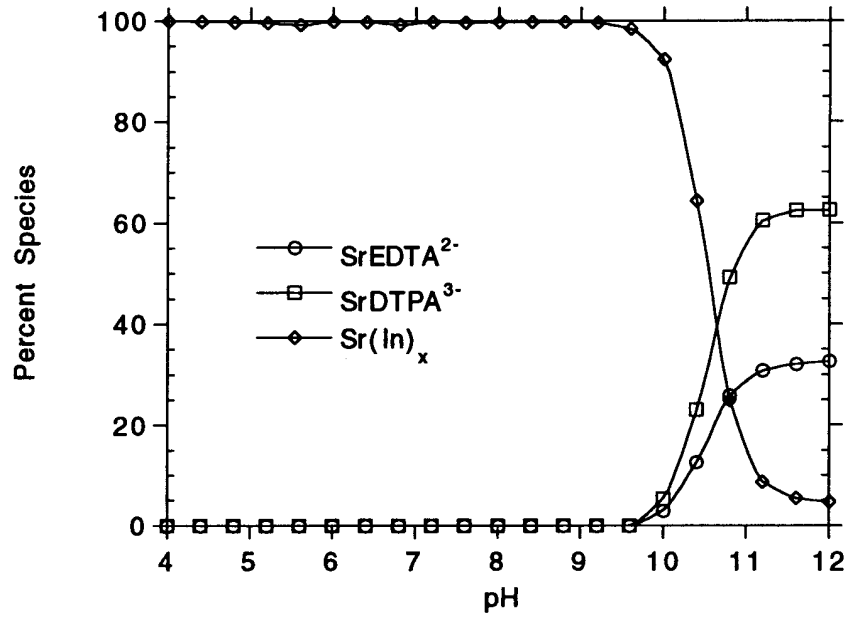
Figure 4.12. Speciation Distribution for Strontium in Pilgrim (NS-1) Leachate
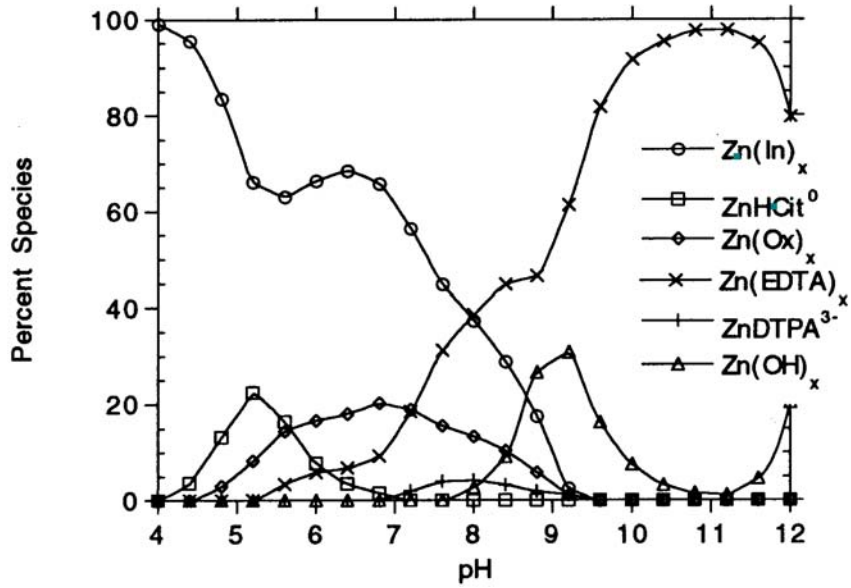
Figure 4.13. Speciation Distribution for Zinc in Pilgrim (NS-1) Leachate
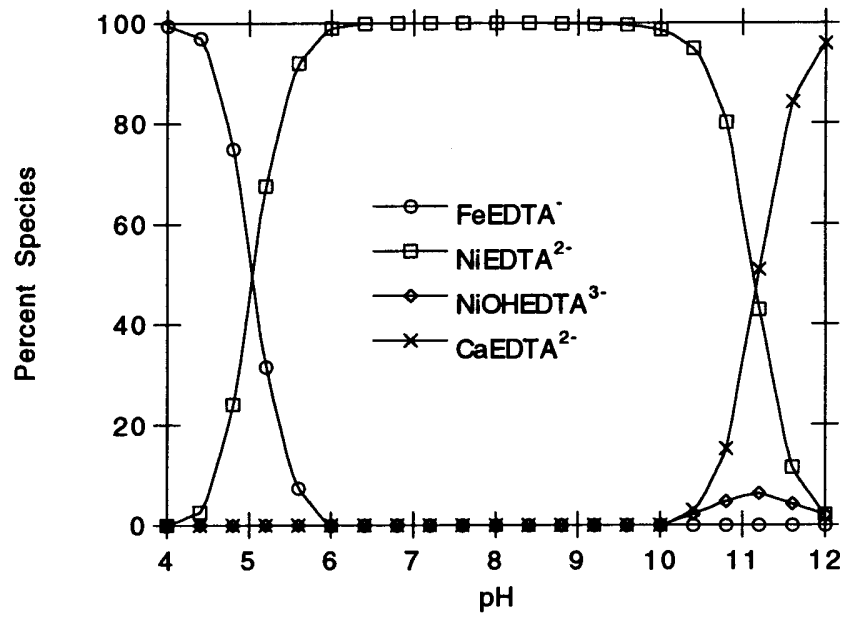
Figure 4.14. Speciation Distribution for EDTA in Pilgrim (NS-1) Leachate
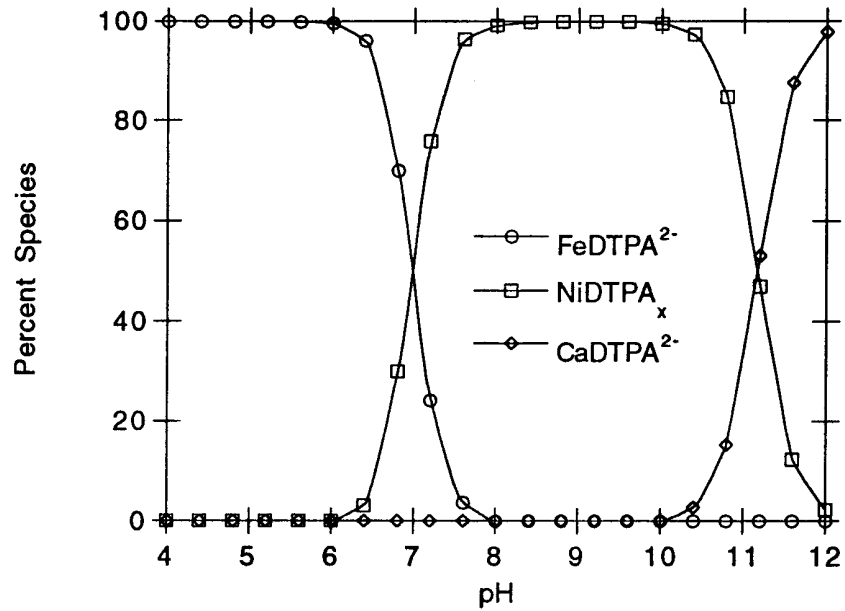
Figure 4.15. Speciation Distribution for DTPA in Pilgrim (NS-1) Leachate
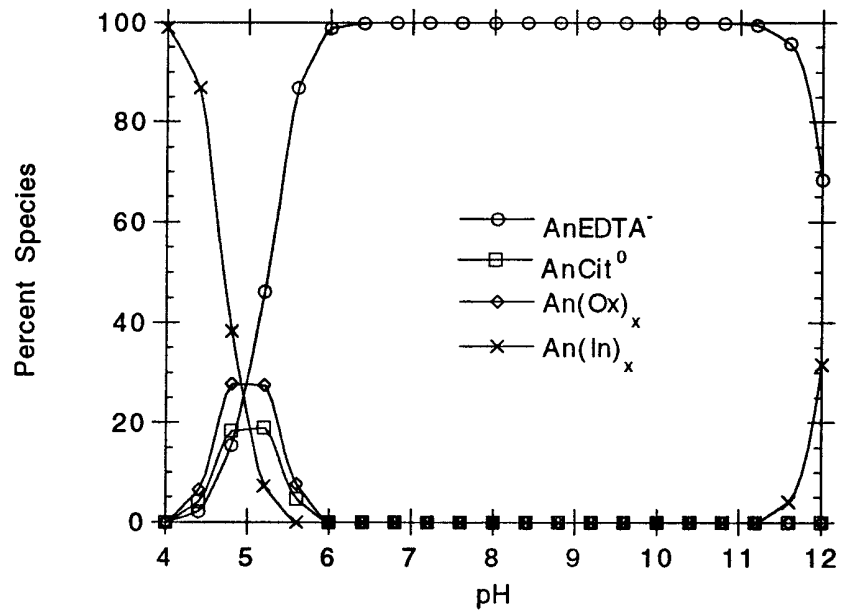
Figure 4.16. Speciation Distribution for Trivalent Actinides in Millstone (CITROX) Leachate
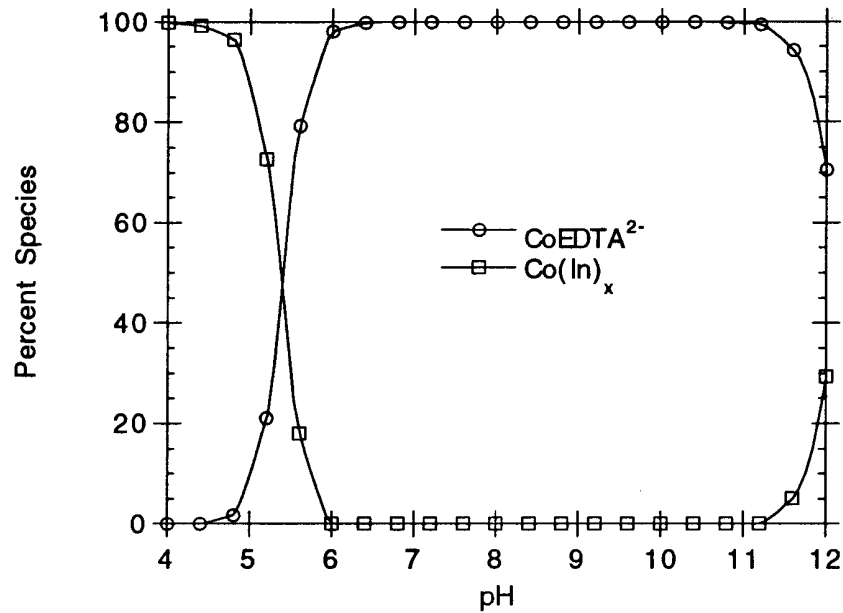
Figure 4.17. Speciation Distribution for Cobalt in Millstone (CAN-DECON) Leachate
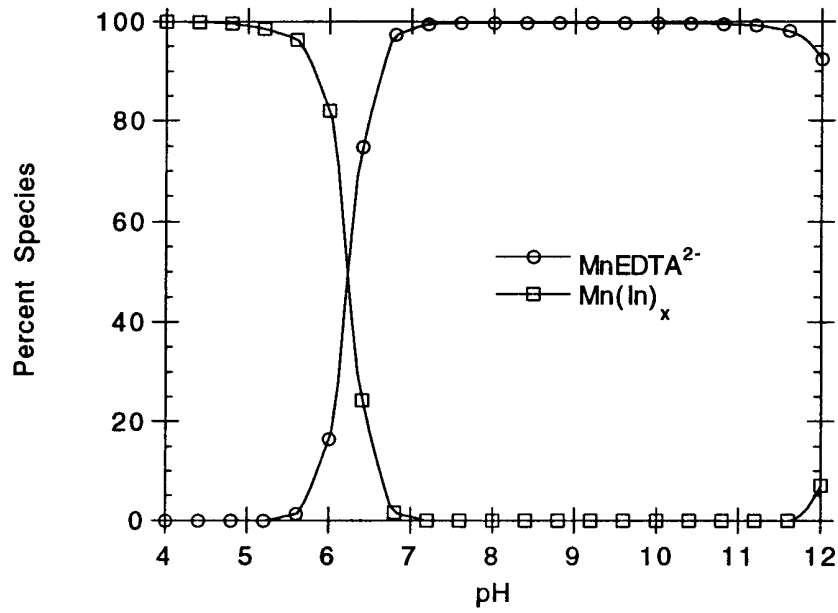
Figure 4.18. Speciation Distribution for Manganese in Millstone (CAN-DECON) Leachate
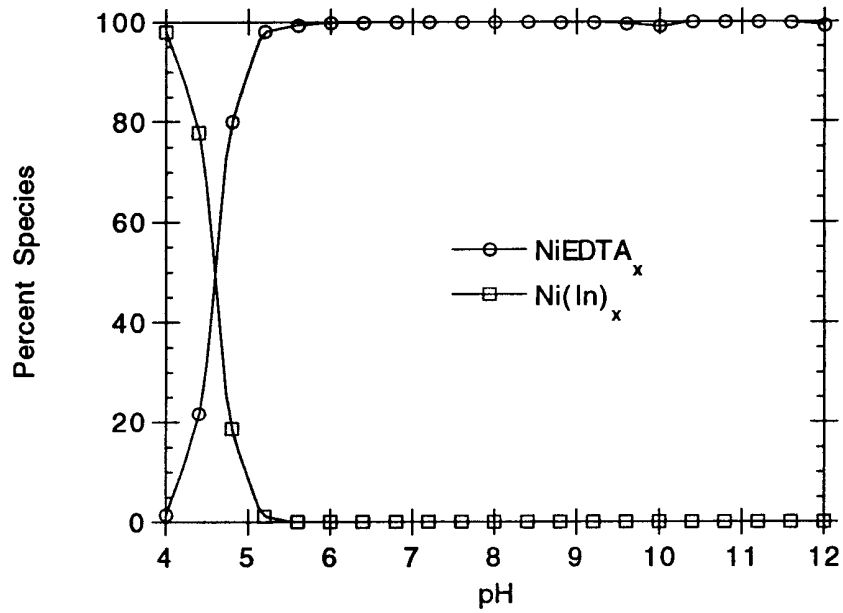
Figure 4.19. Speciation Distribution for Nickel in Millstone (CAN-DECON) Leachate
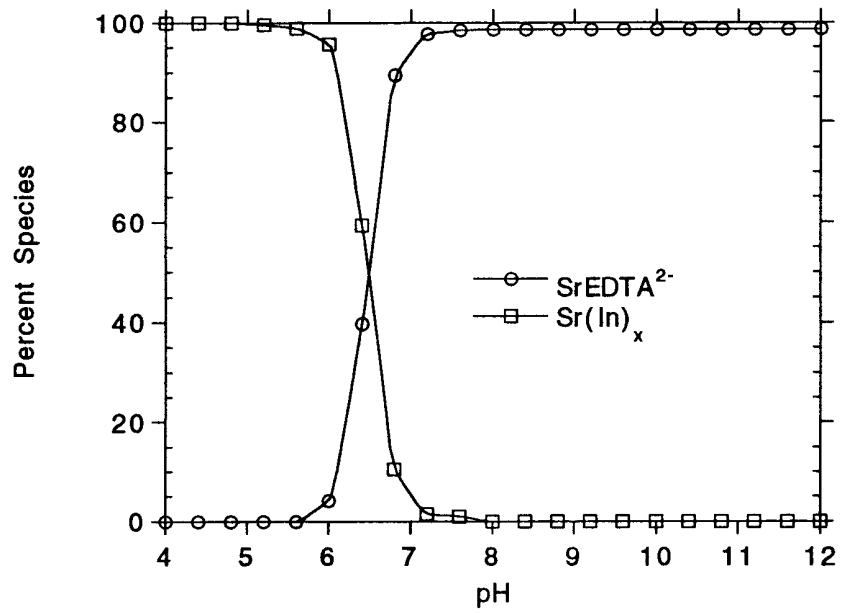
Figure 4.20. Speciation Distribution for Strontium in Millstone (CAN-DECON) Leachate
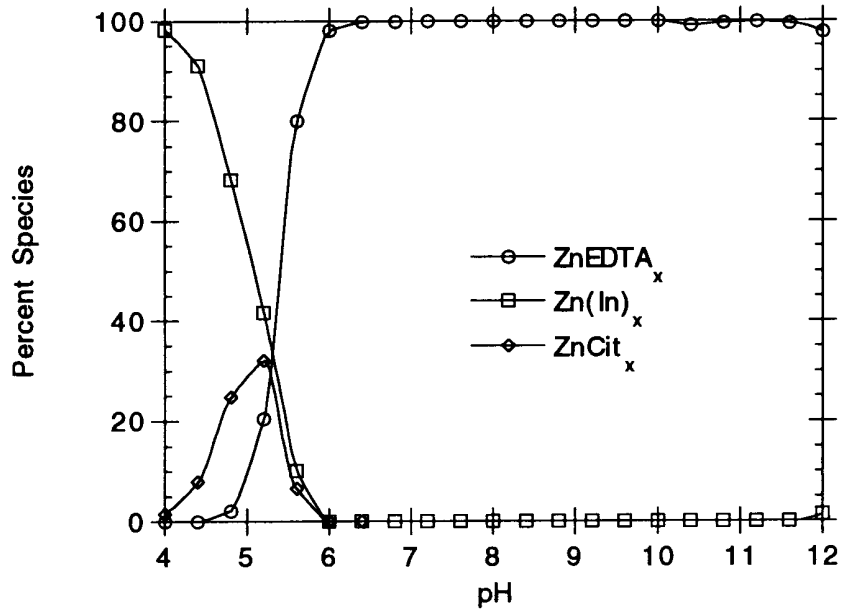
Figure 4.21. Speciation Distribution for Zinc in Millstone (CAN-DECON) Leachate
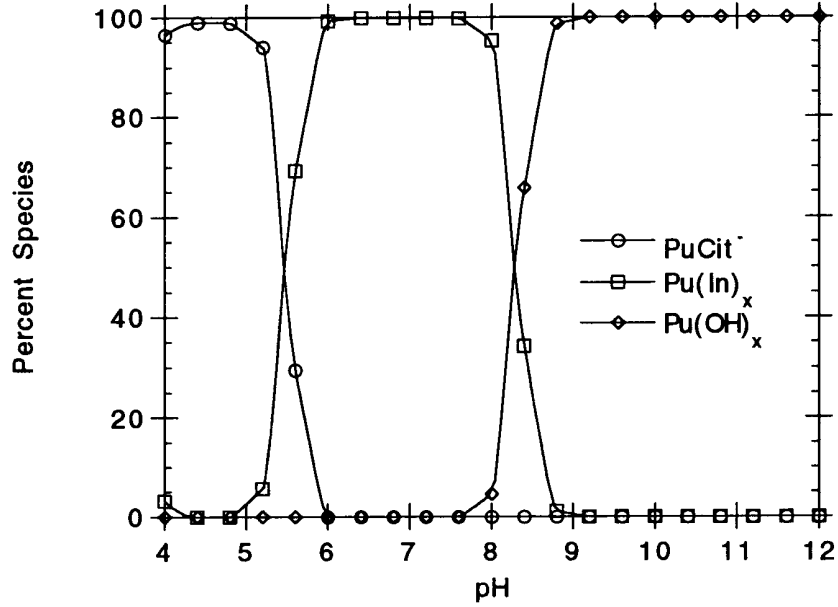
Figure 4.22. Speciation Distribution for Plutonium (IV) in Millstone (CAN-DECON) Leachate
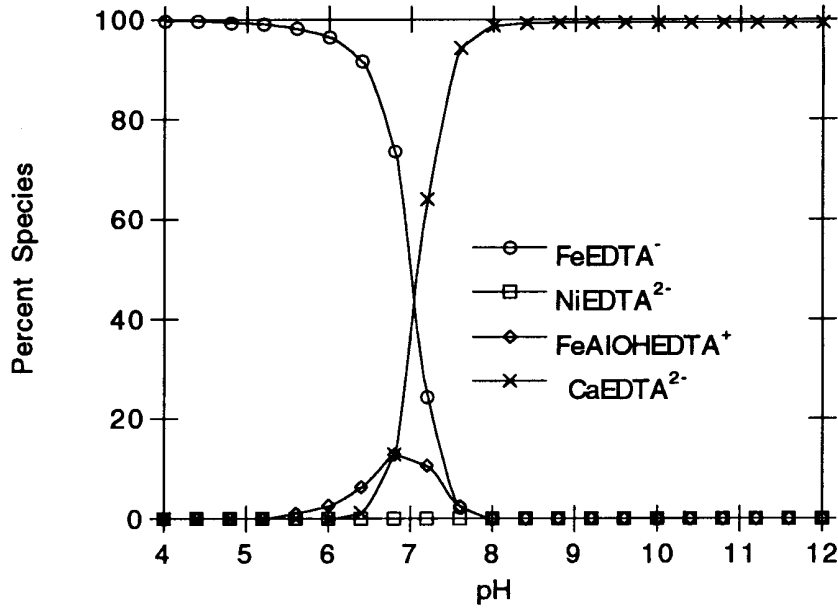
Figure 4.23. Speciation Distribution for EDTA in Millstone (CAN-DECON) Leachate
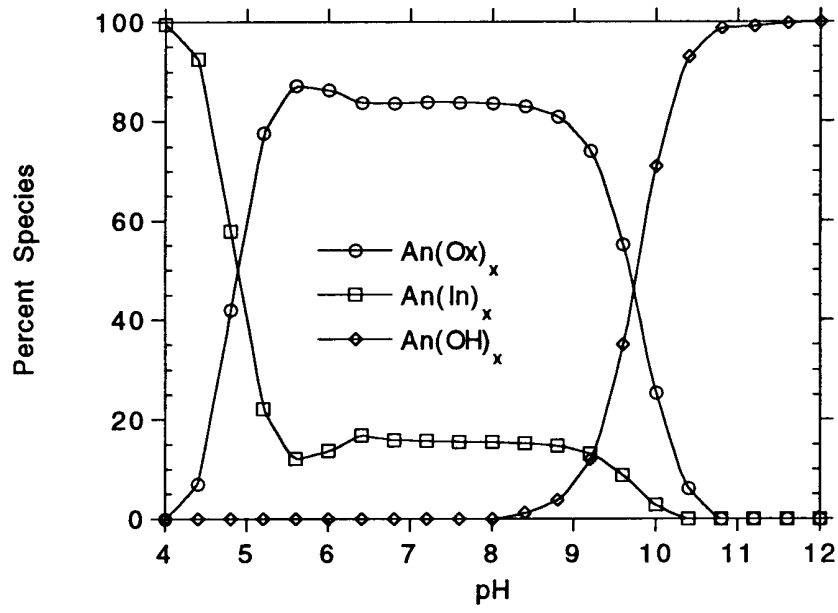
Figure 4.24. Speciation Distribution for Trivalent Actinides in Cooper (CITROX) Leachate
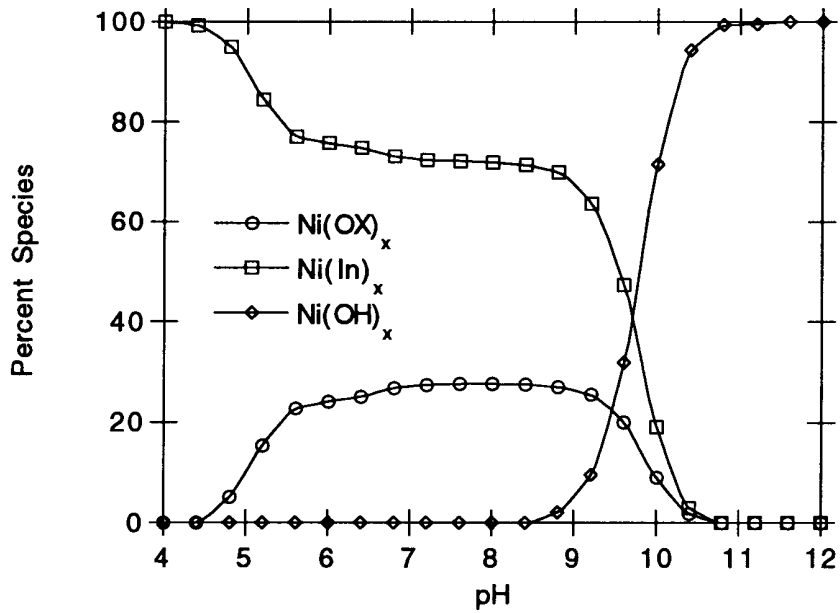
Figure 4.25. Speciation Distribution for Nickel in Cooper (CITROX) Leachate

4.17
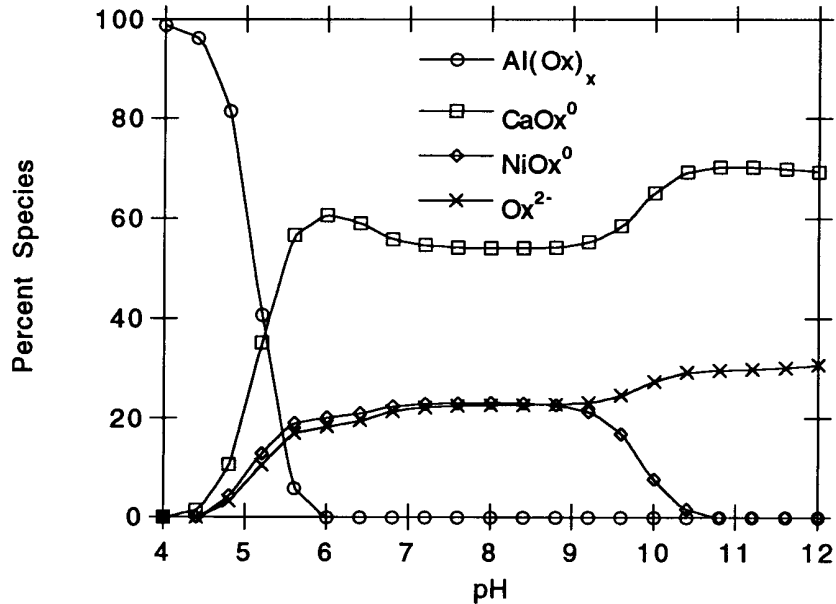
Figure 4.26. Speciation Distribution for Oxalic Acid in Cooper (CITROX) Leachate

dominant species with smaller contributions from $NiOx^0$ and free oxalate from pH 12 to approximately pH 5. $AlOx^+$ is the dominant oxalate species below pH 5.

The Brunswick leachates had significantly lower concentrations of oxalate than the Cooper leachates (despite the fact that both waste forms dissaggregated into small pieces during leaching) and except for the trivalent actinides very little organic complexation occurred in the Brunswick leachates (Figure 4.27). Chelates with oxalate formed nearly 60% of the Am^{3+} and Pu^{3+} species in the Brunswick leachates and citrate complexes were significant from pH 9 to 10.

The results of the equilibrium speciation calculations conducted in this section indicate that for many radionuclides and stable metals, the degree of complex formation with organic chelating/ complexing agents in waste form leachates is significant. In many cases, they are the dominant species. Equilibration with portlandite results in leachates with very high pH values. The resulting high concentrations of OH^- can, in many cases, effectively compete with the organic ligands and increase the tendency of the radionuclides/metals to precipitate. Note that anion exchange resins are frequently regenerated using NaOH solutions. In effect cement leachate may be acting as a regenerant, causing the release of anionic complexes and free anionic ligands from the spent resins. The results indicate that chelating/complexing agents could play a significant role in mobilizing radionuclides co-disposed with these agents in low-level waste sites, especially at pH values below 10.

4.18
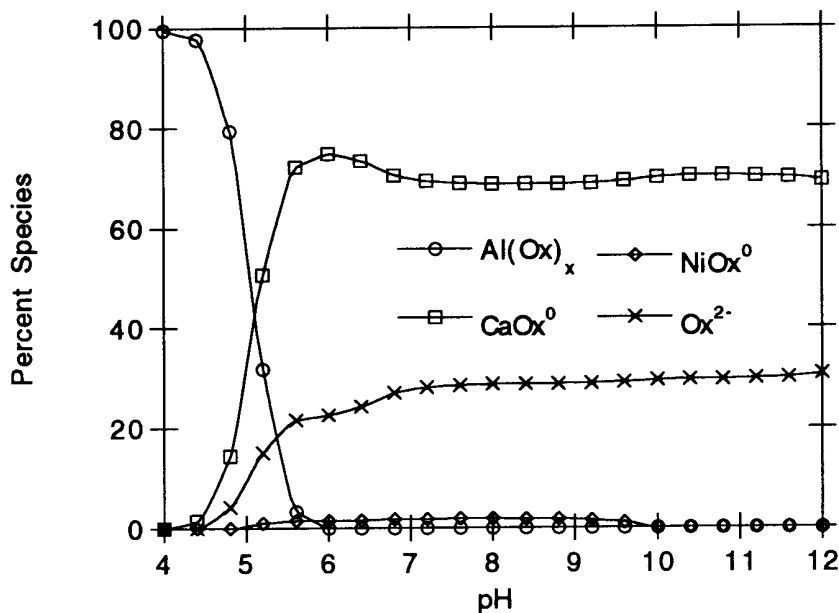
Figure 4.27. Speciation Distribution for Oxalic Acid in Brunswick (CITROX) Leachate

4.3 Speciation of Non-Solidified Decontamination Waste Leachate

Table 4.4 shows the calculated speciation distribution for radionuclides and metals of interest. The distribution is presented in terms of the two major EDTA complexes and the total of the free or inorganic complexes. If the metal was not measured above the detection limit (see Table 3.3), the radionuclide or metal was taken to have a concentration of 1.0×10^{-10} M for purposes of the speciation calculations, as was done for previous speciation calculations for cement leachates. Effectively we assumed Am, Cs, Pu^{3+}, and Pu^{4+} were present in the leachates at 10^{-10} M and all others were present at concentrations shown in Table 3.3.

From the results presented in Table 4.4, it is apparent that EDTA dominates the speciation scheme of Am^{3+}, Co^{2+}, Fe^{3+}, Ni^{2+}, Pu^{3+}, and Cr^{3+}. Note that 1.4×10^{-5} moles/liter (13%) of Cr^{3+} was calculated to precipitate as $Cr(OH)_3(am)$. EDTA accounts for fractional speciation of Mn^{2+} and Zn^{2+} (7% and 23%, respectively). Cs^+, Pu^{4+}, and Sr^{2+} remain uncomplexed by EDTA under these conditions. Based on the results of Table 4.4 it is apparent that an excess of metals relative to EDTA occurs in the leachate solution. As a result, complexation by EDTA will preferentially occur with the metals that have the largest equilibrium stability constants. For example, the three transition metals that occur in the leachate at relatively high concentration (Cr^{3+}, Ni^{2+}, and Mn^{2+}) have EDTA stability constants (log K) of 35.7, 20.3, and 15.8, respectively. Both dissolved Cr^{3+} and Ni^{2+} are essentially completely complexed by EDTA, but only a small percentage of Mn^{2+} is complexed by EDTA. This is because the dissolved Cr^{3+} and Ni^{2+} bind 2.28×10^{-4} moles/liter of EDTA, leaving only 1.6×10^{-5} moles/liter EDTA left to bind with Mn^{2+} and other metals present at very low concentrations ($<10^{-6}$ M).

Table 4.4. Speciation Distribution of Dissolved Radionuclides and Metals Calculated for Non-Solidified Decontamination Waste Leachate			
Radionuclide or Metal	% M-EDTA	% M(OH)-EDTA	% Free or Inorganic Complexes
Am^{3+}	100	0	0
Cs^+	0	0	100
Co^{2+}	93.1	0	6.9
Fe^{3+}	16.1	83.2	0.7
Mn^{2+}	6.6	0	93.4
Ni^{2+}	100	0	0
Pu^{3+}	100	0	0
Pu^{4+}	0	0	100
Sr^{2+}	0	0	100
Zn^{2+}	22.8	0	77.2
Cr^{3+}	37.4	62.6	0

4.4 Speciation of pH Adjusted Non-Solidified Decontamination Waste Leachate

Speciation distribution plots for Cr^{3+}, Am^{3+}, Co^{2+}, Mn^{2+}, Ni^{2+}, Zn^{2+} and EDTA are presented in Figures 4.28 through 4.34. In Figure 4.28, the speciation distribution of Cr^{3+} is shown. At low pH Cr-EDTA- dominates. As the pH increases, $Cr(OH)EDTA^{2-}$ becomes increasingly important and peaks at about 7.5. At pH 7 $Cr(OH)_3(am)$ begins to precipitate. As this precipitation occurs, EDTA is released and becomes available to complex other metals.

Am^{3+} speciation is shown in Figure 4.29 and is dominated by the Am-EDTA- species for the entire pH range. Carbonate complexes make a small contribution to the speciation of scheme of Am^{3+} at pH 7 and 10.

The speciation scheme of Co^{2+} is illustrated in Figure 4.30. At pH 6 Co^{2+} occurs mostly as the free ion while about 42% occurs as the $Co-EDTA^{2-}$ complex. As the pH increases the $Co-EDTA^{2-}$ complex becomes increasingly dominant. At pH values above 6.5 the $Co-EDTA^{2-}$ complex is the dominant species. Above pH 9.5, $COOH^+$ makes a minor contribution to the speciation scheme.
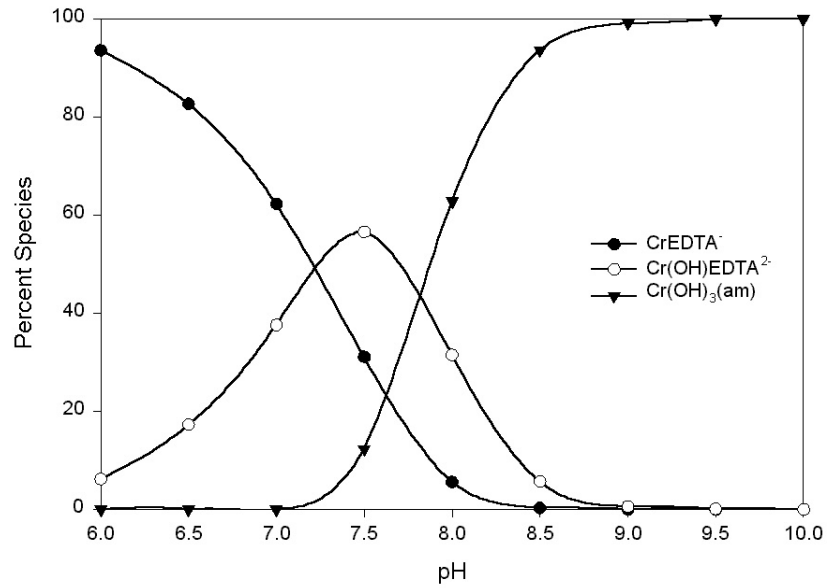
Figure 4.28. Speciation Distribution for Cr³⁺ in Non-Solidified Leachate
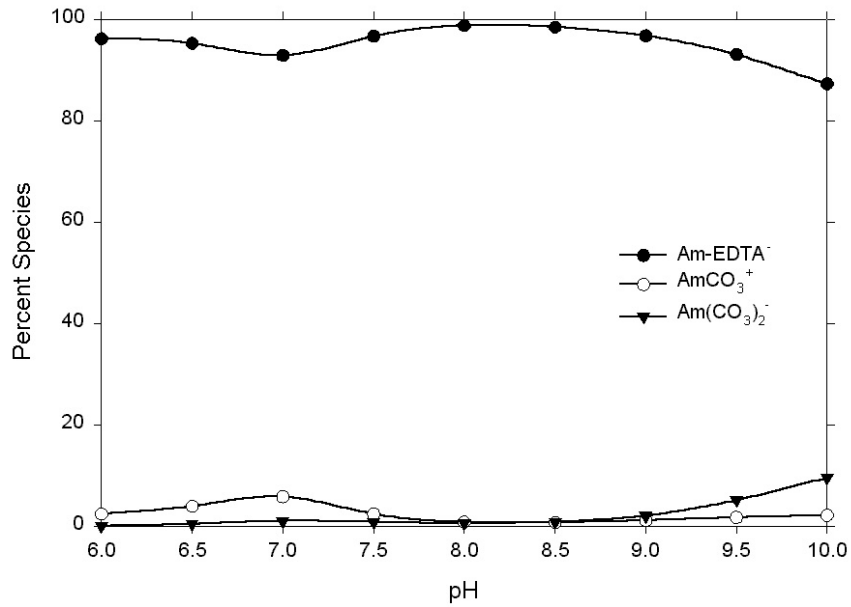
Figure 4.29. Speciation Distribution for Am³⁺ in Non-Solidified Leachate

4.21
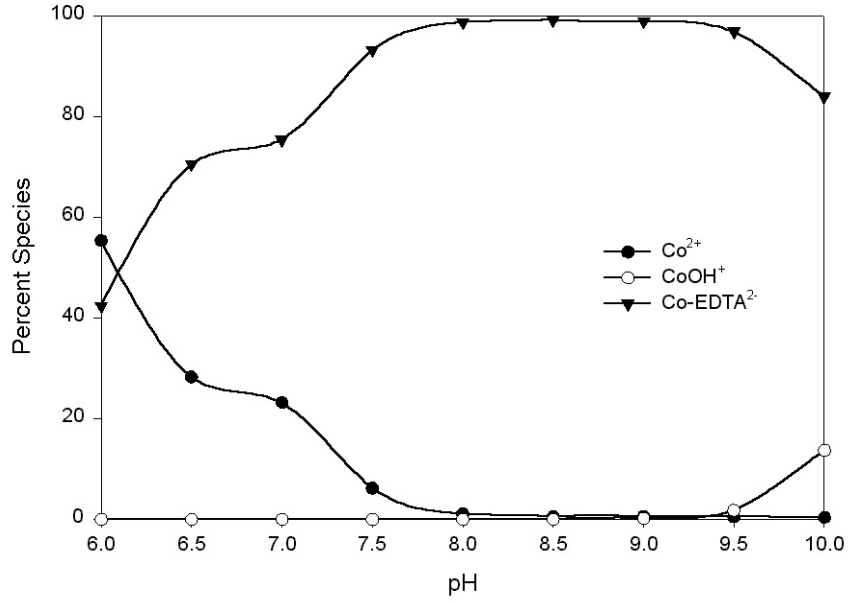
Figure 4.30. Speciation Distribution for Co²⁺ in Non-Solidified Leachate
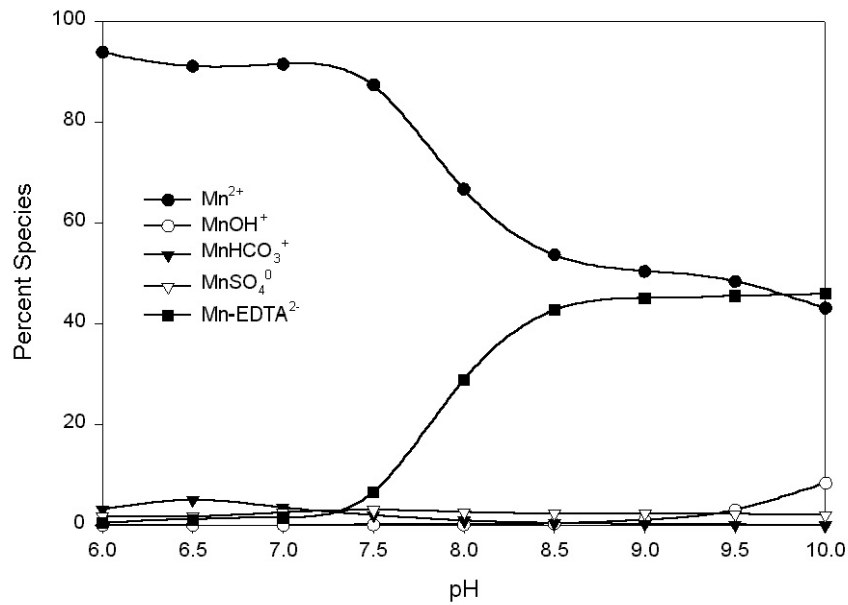
Figure 4.31. Speciation Distribution for Mn²⁺ in Non-Solidified Leachate

4.22
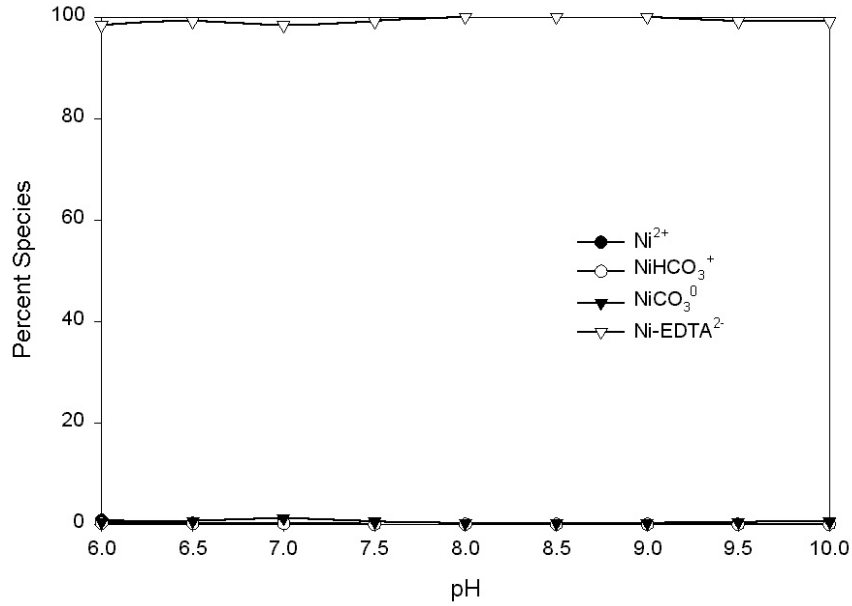
Figure 4.32. Speciation Distribution for Ni²⁺ in Non-Solidified Leachate
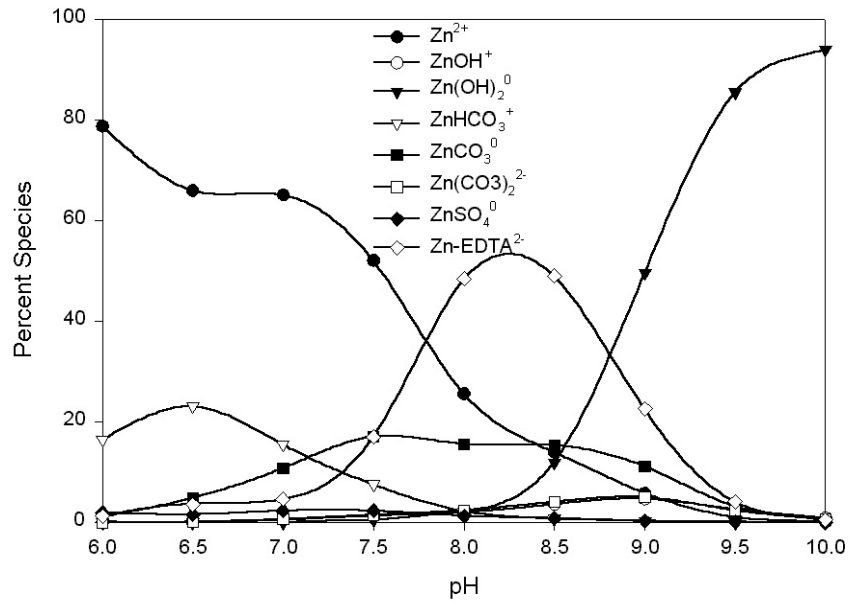
Figure 4.33. Speciation Distribution for Zn²⁺ in Non-Solidified Leachate
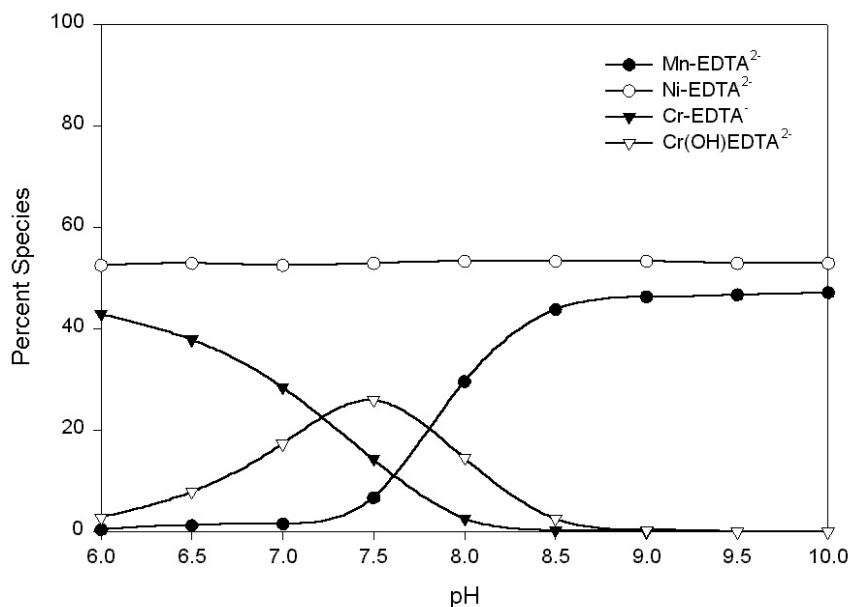
Figure 4.34. Speciation Distribution for EDTA in Non-Solidified Leachate

The distribution of Mn^{2+} species is exhibited in Figure 4.31. At pH values below 7.5 the free Mn^{2+} ion is the dominant species. As the pH increases, complexation by EDTA increases. At pH values above 8.5 about 45% of the Mn^{2+} is complexed by EDTA. This increase in the complexation of Mn^{2+} by EDTA with pH is due to release of EDTA complexed with Cr^{3+} as $Cr(OH)_3(am)$ begins to precipitate. Minor amounts of various inorganic complexes with Mn^{2+} also occur.

Speciation of Ni^{2+} is shown in Figure 4.32 and is dominated by the $Ni\text{-}EDTA^{2-}$ complex at all pH values. Zn^{2+} speciation is presented in Figure 4.33. At the lower pH values Zn^{2+} occurs mostly as the free ion. A significant contribution to the speciation scheme of Zn^{2+} by the $Zn\text{-}EDTA^{2-}$ complex occurs in the pH range of about 7.5 to 9. Above pH 9 $Zn(OH)_2^0$ becomes increasingly dominant. Minor contributions to the speciation scheme also occur below pH 9.5 from various inorganic species.

The speciation distribution of EDTA is shown in Figure 4.34. The $Ni\text{-}EDTA^{2-}$ complex makes up about 53% of the EDTA speciation throughout the pH range of interest. At pH 6 the $Cr\text{-}EDTA^-$ complex makes up about 43% of the EDTA species. As the pH increases to 7.5, the $Cr\text{-}EDTA^-$ complex is partially converted to the $Cr(OH)EDTA^{2-}$ complex. Above this pH $Cr(OH)_3(am)$ begins to precipitate and $Mn\text{-}EDTA^{2-}$ replaces the $Cr\text{-}EDTA^-$ and $Cr(OH)EDTA^{2-}$ complexes.

The speciation of Pu^{3+} (not shown) is the same as that for Am^{3+}. Cs^+ and Sr^{2+} are uncomplexed throughout the pH range of 6 to 10. Fe^{3+} remains precipitated as amorphous iron hydroxide, Al^{3+} remains precipitated as gibbsite, and Pu^{4+} is precipitated as $Pu(OH)_2CO_3(s)$, throughout the pH range of 6 to 10.

5.0 Adsorption Results and Discussion

5.1 Batch Adsorption Experiments

5.1.1 Ni-Picolinate System

Nickel adsorption onto iron oxide coated sand as a function of pH in the absence of any complexing ligand is shown in Figure 5.1. The figure shows the typical cationic adsorption behavior expected for nickel (e.g., Bryce et al. 1994; Coughlin and Stone 1995; Dzombak and Morel 1989). Cationic type behavior on variable charged surfaces such as hydrous ferric oxides (HFO) arises from the amphoteric nature of the hydroxyl groups associated with the surface (e.g., $=FeOH$, $=FeO^-$, $=FeOH_2^+$). As the pH of the solution in contact with the surface decreases, the hydronium ion (H_3O^+, simplified as H^+) concentration increases. This increase in hydronium ion results in protonation of these surface sites and an increase in the net positive charge on the oxide surface. As the pH increases these same sites become increasingly deprotonated resulting in a net negative charge on the surface. As a result of this phenomenon, typical adsorption behavior for free cations exhibits near zero adsorption at low pH, followed by an increase in adsorption with pH to nearly 100% within a relatively narrow pH range. The pH range where this "adsorption edge" occurs depends on the affinity between the metal ion and the surface of interest. For a free anion, the behavior is nearly the opposite, with nearly 100% adsorption occurring at low pH and adsorption dropping off with increasing pH as the number of available positive surface sites decreases.
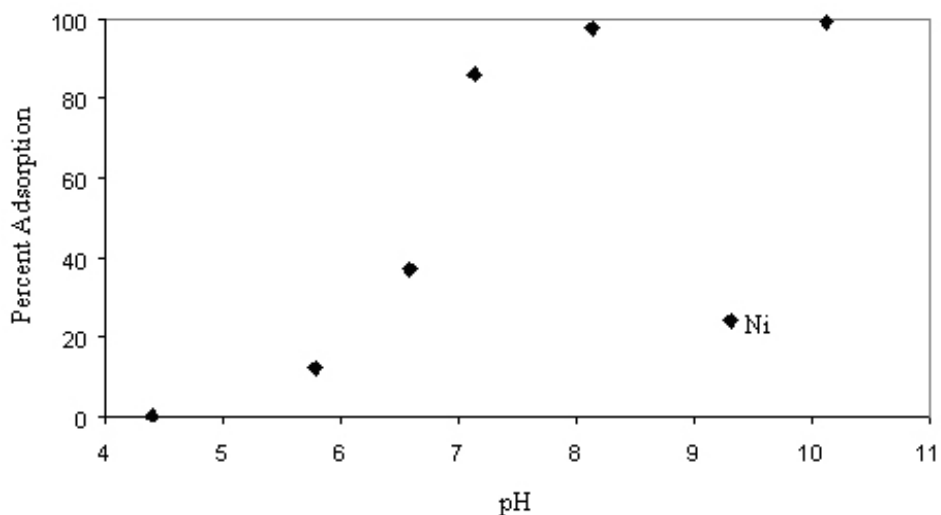
Figure 5.1. Percent Adsorption of Ni^{2+} on 1.2% Iron Oxide Coated Sand as a Function of pH (0.5 g soil/30 ml, 0.003 molar $Ca[ClO_4]_2$ solution, with an initial Ni^{2+} concentration of 10^{-5} M)

Figure 5.2 illustrates the affect of addition of picolinate at a concentration of 10^{-3} M to the adsorption behavior of Ni present at 10^{-5} M. Adsorption of both nickel and picolinate are illustrated. Essentially no nickel adsorption is observed and very little if any picolinate is adsorbed. These results indicate that the quantity of picolinate in solution greatly exceeded the adsorption capacity of the iron oxide coated sand. For example, the maximum adsorption capacity of hydrous ferric oxide for EDTA at pH 4.5 was determined to be 0.0049 mol/mol of Fe (Szescody et al. 1994). For the experiment illustrated in Figure 5.2, this would equate to a maximum adsorption capacity for picolinate of 1.0×10^{-6} moles (assuming two moles of picolinate could adsorb for every mole of EDTA that could be adsorbed). The total quantity of picolinate in the experiment was 3.0×10^{-5} moles [10^{-3} M⊘0.03 liters], indicating that a maximum of about 3% of the picolinate [$10^{-6} \div 3 \times 10^{-5}$] could have been adsorbed. The combination of high stability constants for nickel picolinate complexes and high concentration of picolinate resulted in essentially complete complexation of the nickel, preventing adsorption of free nickel. For the conditions of this experiment the dominant nickel species are NiL_2^0 and NiL_3^-, where L- represents the negatively charged picolinate ion. Because the high concentration of picolinate overwhelmed the adsorption capacity of the iron oxide sand, adsorption of the nickel picolinate complexes was also prevented.

When the concentration of picolinate is reduced by an order of magnitude, typical anionic adsorption behavior was observed (Figure 5.3). In this case, the greatest degree of picolinate adsorption was observed at the lowest pH values. This is consistent with the concentration of positive surface sites increasing with decreasing pH. The concentration of picolinate is still high enough to cause the nickel to remain predominately in the form of nickel picolinate complexes and prevent the adsorption of nickel.

Figure 5.2. Percent Adsorption of Ni^{2+} and Picolinate on 1.2% Iron Oxide Coated Sand as a Function of pH (0.5 g soil/30 ml, 0.003 molar $Ca[ClO_4]_2$ solution, with initial concentrations of Ni^{2+} and picolinate of 10^{-5} M and 10^{-3} M, respectively)

Figure 5.3. Percent Adsorption of Ni^{2+} and Picolinate on 1.2% Iron Oxide Coated Sand as a Function of pH (0.5 g soil/30 ml, 0.003 molar Ca[ClO$_4$]$_2$ solution, with initial concentrations of Ni^{2+} and picolinate of 10^{-5} M and 10^{-4} M, respectively)

When the concentration of picolinate is reduced by another order of magnitude [to 10^{-5} M], the situation changes again (Figure 5.4). In this case, picolinate illustrates the typical anionic adsorption behavior at low pH values, but additional adsorption is observed at higher pH values (unlike a typical anion). The nickel shows cationic adsorption behavior, but the adsorption is suppressed at pH values between 7 and 9, relative to that observed in Figure 5.1. These observations are consistent with a moderate or low degree of complexation of nickel by picolinate and adsorption of nickel and possibly positively charged nickel picolinate complexes [NiPic$^+$]. Also note that the adsorption of picolinate reaches a maximum at about 80% of the total picolinate present. The pK for picolinic acid is 5.4, therefore, as the pH decreases to below 6, increased absorption of picolinate is curtailed due to protonation. As a result, the percentage of adsorption for picolinate never goes above 80%.

Three additional adsorption experiments were conducted with the nickel-picolinate system using Milford soil instead of the iron oxide coated sand. The highest and lowest concentrations of picolinate were used for these experiments (10^{-3} M and 10^{-5} M). The results of these experiments are shown in Figures 5.5 and 5.6. Results illustrated in Figure 5.6, include two separate experiments conducted under identical conditions; the only difference being the method used for the nickel analysis. In the first case, the nickel and the picolinate were measured using the radioactive tracer technique that was used for most of the experiments conducted for this study. In the second case, the nickel was measured using inductively coupled plasma optical emission spectroscopy (ICP). An attempt was made to measure the picolinate concentrations using an organic carbon analyzer, but the concentrations were too low to provide reliable results. The nickel results obtained using the two methods are fairly consistent. The results and conclusions that can be drawn from these experiments are essentially the same as those determined with the iron oxide coated sand discussed previously. That is, at a concentration of 10^{-3} M picolinate in the
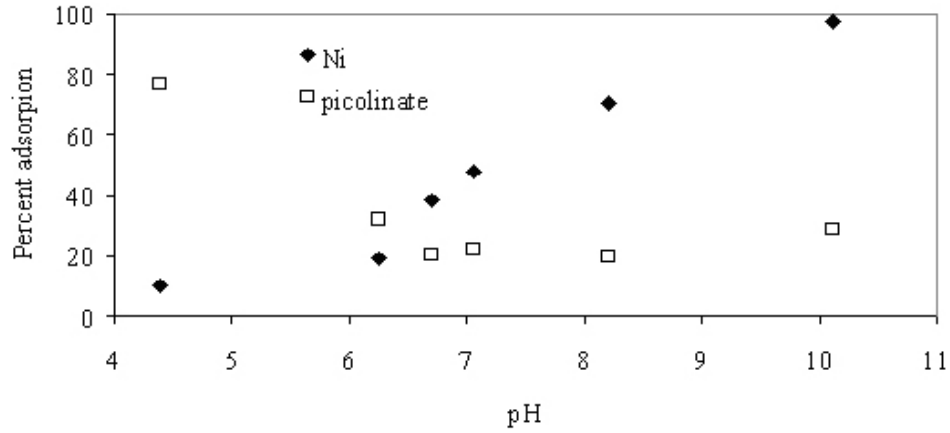
Figure 5.4. Percent Adsorption of Ni^{2+} and Picolinate on 1.2% Iron Oxide Coated Sand as a Function of pH (0.5 g soil/30 ml, 0.003 molar Ca[ClO$_4$]$_2$ solution, with initial concentrations of Ni^{2+} and picolinate of 10^{-5} M and 10^{-5} M, respectively)

Figure 5.5. Percent Adsorption of Ni^{2+} and Picolinate on Milford Soil as a Function of pH (0.5 g soil/30 ml, 0.003 molar Ca[ClO$_4$]$_2$ solution, with initial concentrations of Ni^{2+} and picolinate of 10^{-5} M and 10^{-3} M, respectively)

5.4
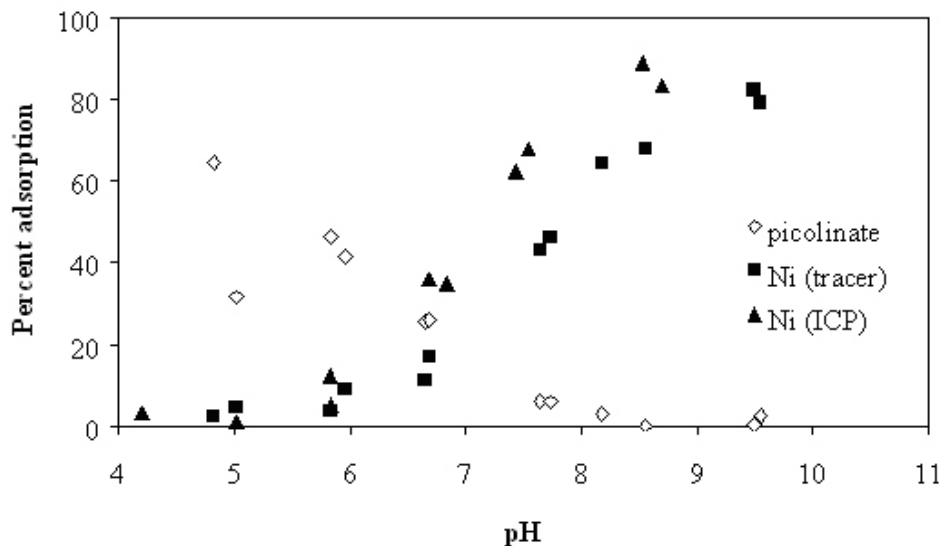
Figure 5.6. Percent Adsorption of Ni^{2+} (as measured by Ni-63 tracer and ICP methods) and Picolinate on Milford Soil as a Function of pH (0.5 g soil/30 ml, 0.003 molar Ca[ClO$_4$]$_2$ solution, with initial concentrations of Ni^{2+} and picolinate of 10^{-5} M and 10^{-5} M, respectively)

presence of 10^{-5} M nickel, picolinate prevents Ni adsorption by forming anionic/neutrally charged complexes. The excess free picolinate anion overwhelms any available positively charged surface sites, resulting in relatively little free ligand adsorption. At 10^{-5} M picolinate, nickel complexation is relatively insignificant and both nickel and picolinate adsorption behavior is analogous to their respective free species.

5.1.2 Ni-EDTA System

The adsorption of nickel and EDTA onto iron oxide coated sand as a function of pH is shown in Figure 5.7. This experiment was conducted with equal initial concentrations of 10^{-5} M for the metal and ligand. Both the nickel and the EDTA exhibit typical anionic adsorption behavior; the adsorption is strongest at low pH and drops off dramatically with increasing pH. It is readily apparent that the nickel is strongly complexed with EDTA and that these anionic complexes are forming surface complexes on the iron oxide coated sand. These observations and the fact that this behavior occurs at a relatively low EDTA concentration of 10^{-5} M, illustrates the fact that EDTA forms much stronger complexes with nickel than does picolinate. Bryce et al. (1994) observed very similar behavior for the Ni-EDTA system.

Nickel and EDTA adsorption results for three different soils (Milford, LK-1, and MNC-7) are illustrated in Figures 5.8, 5.9, and 5.10, respectively. The same experimental conditions used for the iron oxide coated sand experiment discussed above and illustrated in Figure 5.7 were used for these three experiments. In all three cases, the adsorption of nickel is coincident with EDTA, reflecting the formation of
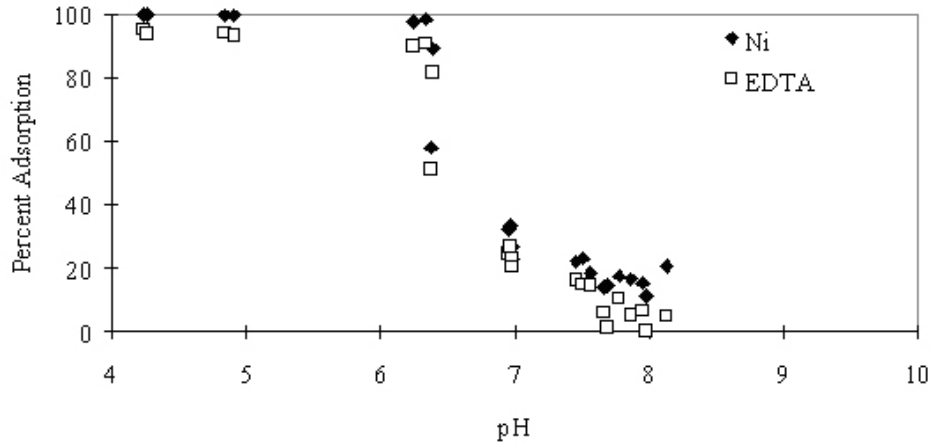
Figure 5.7. Percent Adsorption of Ni^{2+} and EDTA on 1.2% Iron Oxide Coated Sand as a Function of pH (0.5 g soil/30 ml, 0.003 molar Ca[ClO$_4$]$_2$ solution, with initial concentrations of Ni^{2+} and EDTA of 10^{-5} M and 10^{-5} M, respectively)

Figure 5.8. Percent Adsorption of Ni^{2+} and EDTA on Milford Soil as a Function of pH (0.5 g soil/30 ml, 0.003 molar Ca[ClO$_4$]$_2$ solution, with initial concentrations of Ni^{2+} and EDTA of 10^{-5} M and 10^{-5} M, respectively)

Figure 5.9. Percent Adsorption of Ni^{2+} and EDTA on LK-1 Soil as a Function of pH (0.5 g soil/30 ml, 0.003 molar Ca[ClO$_4$]$_2$ solution, with initial concentrations of Ni^{2+} and EDTA of 10^{-5} M and 10^{-5} M, respectively)

Figure 5.10. Percent Adsorption of Ni^{2+} and EDTA on MNC-7 Soil as a Function of pH (0.5 g soil/30 ml, 0.003 molar Ca[ClO$_4$]$_2$ solution, with initial concentrations of Ni^{2+} and EDTA of 10^{-5} M and 10^{-5} M, respectively)

strong anionic nickel-EDTA complexes [likely $NiEDTA^{-2}$]. Of these three soils MNC-7 exhibits the highest degree of adsorption for the complex. MNC-7 has the highest total iron concentration (Table 3.3) and tends to adsorb the nickel-EDTA complexes very similarly to that of the iron oxide coated sand. Both the Milford and the LK-1 soil exhibit diminished adsorption relative to the iron oxide coated sand and the MNC-7 soil. The reasons for low adsorption on the Milford soil are readily apparent. Milford soil has the lowest iron oxide content of the three soils and is essentially all sand with very little clay (Table 3.3). The reasons for the low adsorption of the LK-1 soil are less obvious. The LK-1 soil has a moderately high iron oxide content as well as the highest clay content of the three soils (Table 3.3). One possible explanation for relatively low adsorption of the LK-1 soil is that the iron oxides in this soil are more crystalline in nature. For example, Hsi and Langmuir (1985) demonstrated that adsorption of uranyl species is stronger onto HFO and goethite than on synthetic and natural hematite, a more crystalline form of Fe(III) oxide. This appeared to be directly related to the concentration of adsorption sites of the materials, which is directly related to the surface area of the material. For example, the HFO used by Hsi and Langmuir (1985) had a surface area of 306 m^2/g and a site density of 20 sites/nm^2, whereas their synthetic hematite had a surface area of 3.1 m^2/g and a site density of 19 sites/nm^2. The LK-1 soil also has a relatively low organic carbon content, but significantly higher than the other two soils. Perhaps the natural organic acids (humic substances) in this soil are acting as effective competitors for adsorption sites with the nickel-EDTA complexes.

5.1.3 Sm-Picolinate System

The adsorption of Sm^{3+} an analogue for trivalent actinides, such as Am^{+3}, Cm^{+3} and reduced Pu^{+3}, and picolinate onto iron oxide coated sand as a function of pH is shown in Figure 5.11. This experiment was conducted with equal initial concentrations of 10^{-5} M. Sm^{3+} shows typical cationic type adsorption; low adsorption at low pH with increasing adsorption with increasing pH and nearly complete adsorption at the
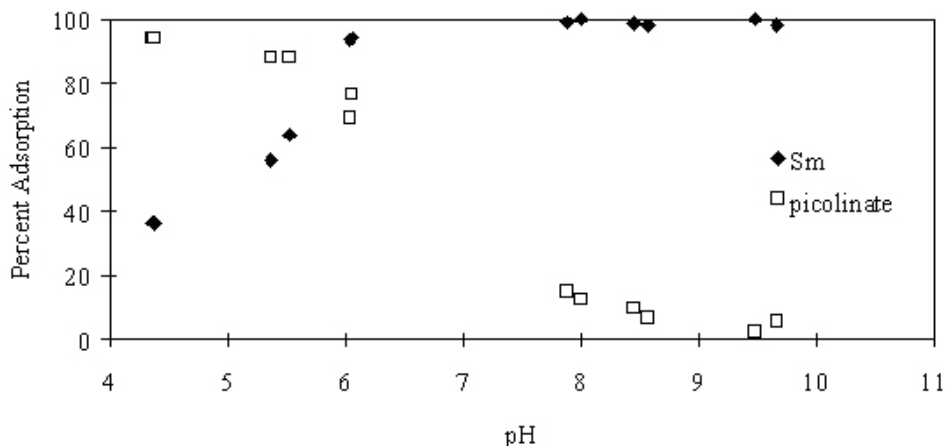
Figure 5.11. Percent Adsorption of Sm^{3+} and Picolinate on 1.2% Iron Oxide Coated Sand as a Function of pH, (0.5 g soil/30 ml, 0.003 molar Ca[ClO$_4$]$_2$ solution, with initial concentrations of Sm^{3+} and picolinate of 10^{-5} M and 10^{-5} M, respectively)

5.8

highest pH values. Picolinate is exhibiting typical anionic adsorption behavior; the adsorption is strongest at low pH and drops off significantly with increasing pH. These results clearly illustrate the lack of significant interaction between picolinate and Sm^{3+}. Both components are acting completely independently and are not affecting the behavior of the other component. Although not shown the adsorption of Sm^{+3} onto soils without any picolinic acid present is similar to the data shown in Figure 5.11.

The results of two additional adsorption experiments with Sm^{3+} and picolinate for Milford soil are shown in Figures 5.12 and 5.13. In both cases, the picolinate concentration is 10^{-5} M. The Sm^{3+} concentration for the experiment shown in Figure 5.12 is 10^{-8} M, and 10^{-5} M for the experiment shown in Figure 5.13. The results for both of these experiments are essentially the same as that shown in Figure 5.11, with the exception that the picolinate adsorption onto the Milford soil is diminished relative to the iron oxide coated sand. This is not surprising after consideration of the low iron oxide content of the Milford soil (Table 3.3) and the fact that iron oxides tend to be some of the most potent adsorbents in natural soils.

5.1.4 Th-Picolinate System

Adsorption results for Th^{4+} and picolinate at initial concentrations of 10^{-5} M onto iron oxide coated sand are illustrated in Figure 5.14. Th^{4+} shows the general adsorption trends typical of cations with the exception that the decrease in adsorption with decreasing pH is much more gradual than for most metal ions. This result is most likely the result of partial precipitation of thorium hydroxide even at low pH values that is interpreted as adsorption even under acidic conditions in these batch tests. The initial Th^{4+} concentration used in this experiment appears to have exceeded its solubility limit for pH values above approximately 4.5 (Felmy et al. 1991).
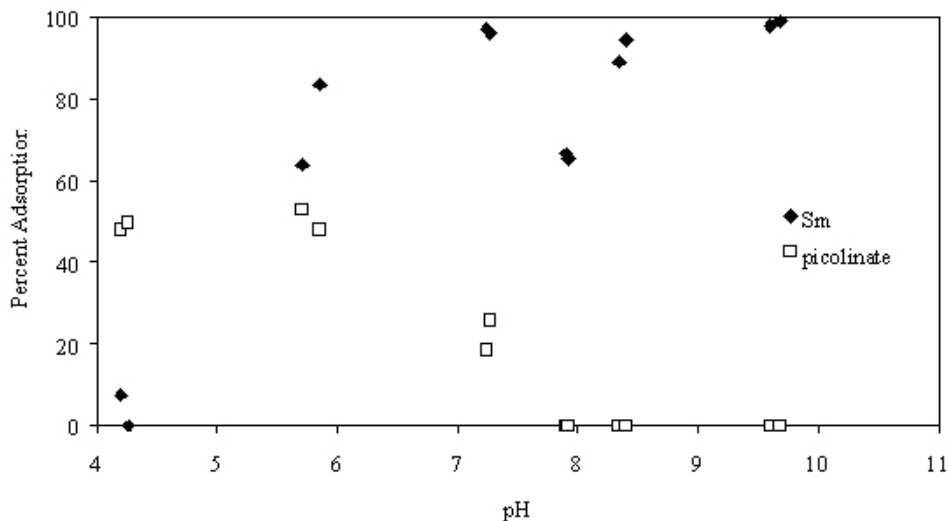
Figure 5.12. Percent Adsorption of Sm^{3+} and Picolinate on Milford Soil as a Function of pH (0.5 g soil/30 ml, 0.003 molar Ca[ClO$_4$]$_2$ solution, with initial concentrations of Sm^{3+} and picolinate of 10^{-8} M and 10^{-5} M, respectively)
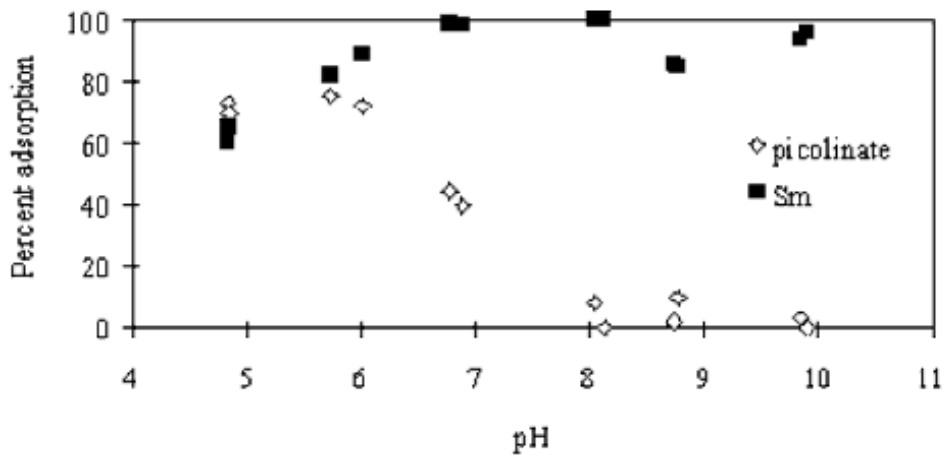
Figure 5.13. Percent Adsorption of Sm^{3+} and Picolinate on Milford Soil as a Function of pH (0.5 g soil/30 ml, 0.003 molar Ca[ClO$_4$]$_2$ solution, with initial concentrations of Sm^{3+} and picolinate of 10^{-5} M and 10^{-5} M, respectively)
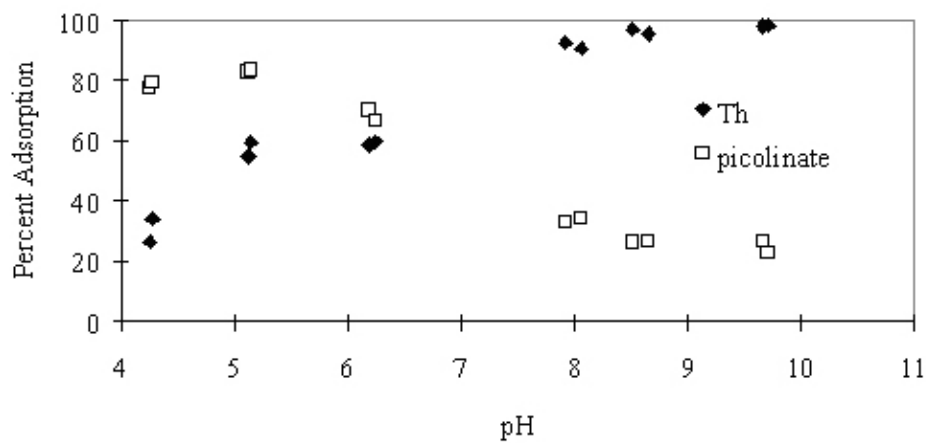
Figure 5.14. Percent Adsorption of Th^{4+} and Picolinate on 1.2% Iron Oxide Coated Sand as a Function of pH (0.5 g soil/30 ml, 0.003 molar Ca[ClO$_4$]$_2$ solution, with initial concentrations of Th^{4+} and picolinate of 10^{-5} M and 10^{-5} M, respectively)

The picolinate also shows the general features of anionic adsorption typically observed; however, significant adsorption of picolinate remains at alkaline pH values. This is contrary to what is typically observed for uncomplexed picolinate and may be the result of co-precipitation of picolinate with thorium hydroxide.

Another Th^{4+} - picolinate adsorption experiment was conducted with Milford soil (Figure 5.15). The results of this experiment are nearly same as that determined for the iron oxide coated sand; both for Th^{4+} and picolinate. We thus conclude that picolinate is not forming strong complexes with Th and by analog with other quadravalent actinides such as Np(IV) or Pu(IV).

5.1.5 Np-Picolinate System

The adsorption of NpO_2^+ with no organic ligand present onto iron oxide coated sand as a function of pH is shown in Figure 5.16. This experiment was conducted at an initial Np concentration of 6.7×10^{-7} M. The NpO_2^+ shows typical cationic type adsorption. Figure 5.17 shows results for another adsorption experiment on iron oxide coated sand conducted at the same initial NpO_2^+ concentration and a picolinate concentration of 10^{-5} M. Here again the adsorption behavior of NpO_2^+ is cationic in character. In addition, the picolinate is exhibiting typical anionic adsorption behavior. Both components are acting completely independently and are not affected by the behavior of the other component, clearly indicating a lack of significant interaction between picolinate and NpO_2^+. It is possible that NpO_2^+ is a reasonable analogue for Pu(V), which would lead to the conclusion that Pu(V) does not form strong complexes with picolinate at picolinate concentrations less than 1×10^{-4} M.
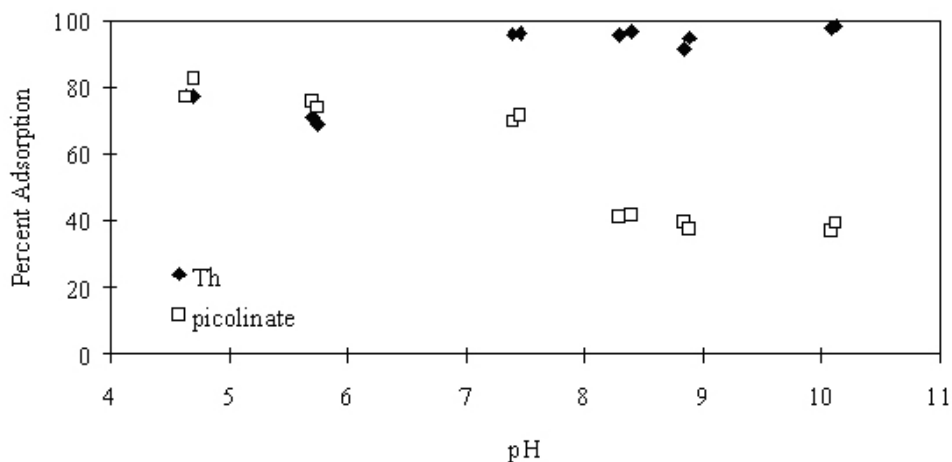
Figure 5.15. Percent Adsorption of Th^{4+} and Picolinate on Milford Soil as a Function of pH (0.5 g soil/30 ml, 0.003 molar $Ca[ClO_4]_2$ solution, with initial concentrations of Th^{4+} and picolinate of 10^{-5} M and 10^{-5} M, respectively)
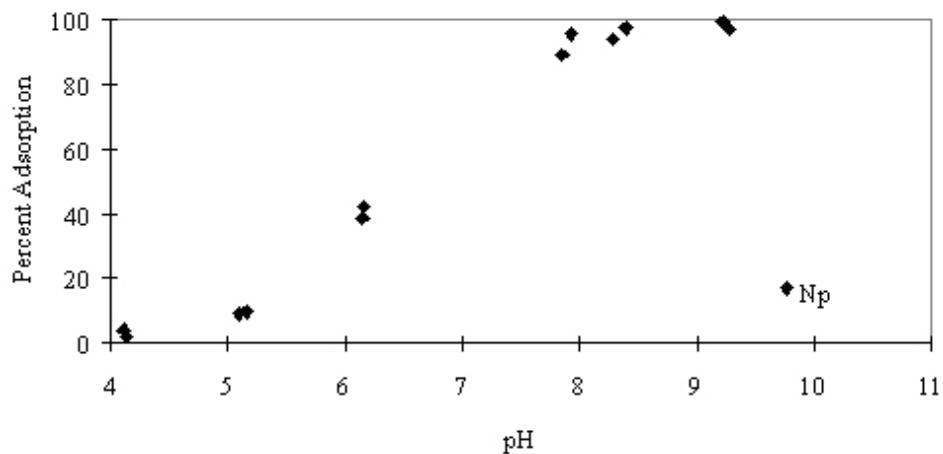
Figure 5.16. Percent Adsorption of NpO_2^+ on 1.2% Iron Oxide Coated Sand as a Function of pH (0.5 g soil/30 ml, 0.003 molar $Ca[ClO_4]_2$ solution, with an initial NpO_2+ concentration of 6.7×10^{-7} M)
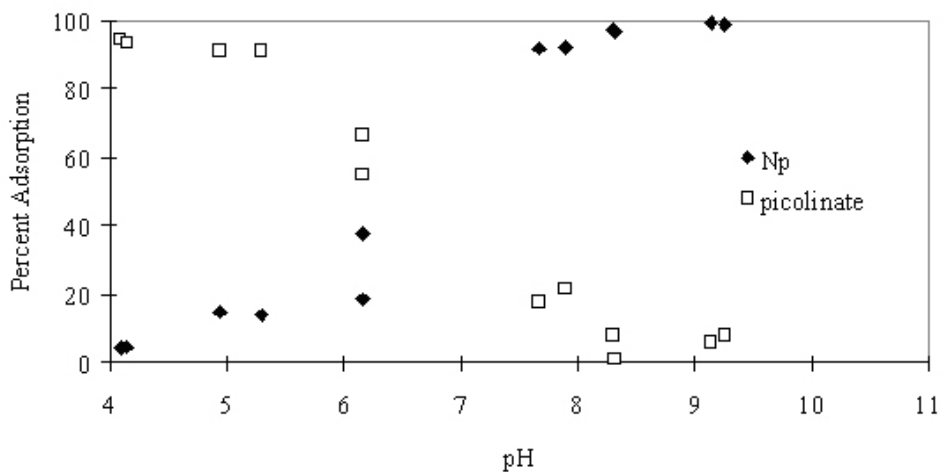
Figure 5.17. Percent Adsorption of NpO_2^+ and Picolinate on 1.2% Iron Oxide Coated Sand as a Function of pH (0.5 g soil/30 ml, 0.003 molar $Ca[ClO_4]_2$ solution, with initial concentrations of NpO_2^+ and picolinate of 6.7×10^{-7} M and 10^{-5} M, respectively)

Two more experiments were conducted with NpO_2^+ using Milford soil as the adsorbent. Figure 5.18 shows the results for adsorption of NpO_2^+ only on Milford soil and Figure 5.19 illustrates results from another experiment with both NpO_2^+ and picolinate on Milford soil. In both cases, the results are practically the same as those observed for the iron oxide coated sand, except that both solutes exhibit slightly lower adsorption, which is again due to the low concentration of strong adsorbents in this soil.

5.1.6 U-Picolinate System

The adsorption of U(VI) added as free UO_2^{2+} in the carbonate-free or carbonate-limited tests and picolinate onto iron oxide coated sand as a function of pH is shown in Figure 5.20. This experiment was conducted with initial concentrations of 10^{-5} M for U(VI) and 10^{-3} M for picolinate. The U(VI) shows typical cationic adsorption behavior observed for various iron oxides in the absence of complexing anions (Hsi and Langmuir 1985). As indicated earlier, the high concentration of picolinate (10^{-3} M) used in this experiment greatly exceeded the quantity of available adsorption sites, resulting in relatively little or no removal due to adsorption. It is apparent from these results that insignificant interaction occurs between picolinate and U(VI) in solution. Both components are acting completely independently and are not affecting the behavior of each other. If our tests would have been at equilbrium with carbon dioxide the adsorption of U(VI) at higher pH values would have dropped because of the formation of strong inorganic complexes between UO_2^{2+} and carbonate. See Davis (2001) for an excellent discourse of U(VI) adsorption in the presence of carbonate solutions.
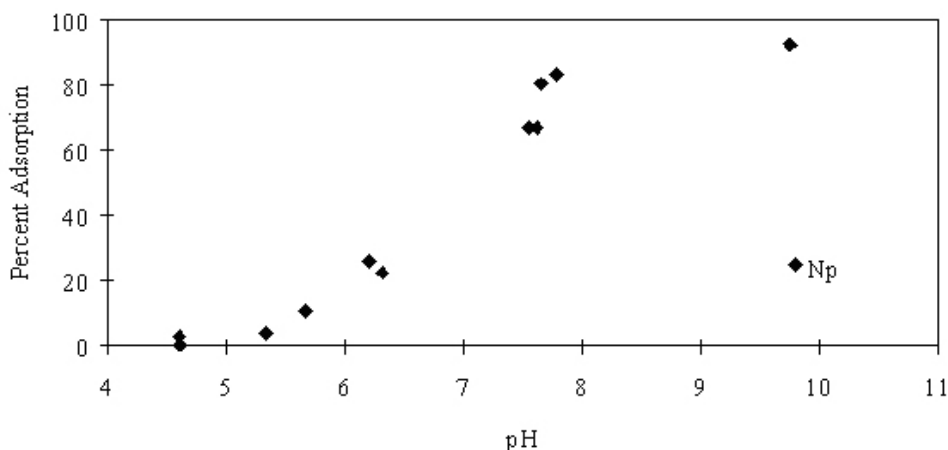
Figure 5.18. Percent Adsorption of NpO_2^+ on Milford Soil as a Function of pH (0.5 g soil/ 30 ml, 0.003 molar Ca[ClO$_4$]$_2$ solution, with an initial NpO_2^+ concentration of 6.7x10^{-7} M)
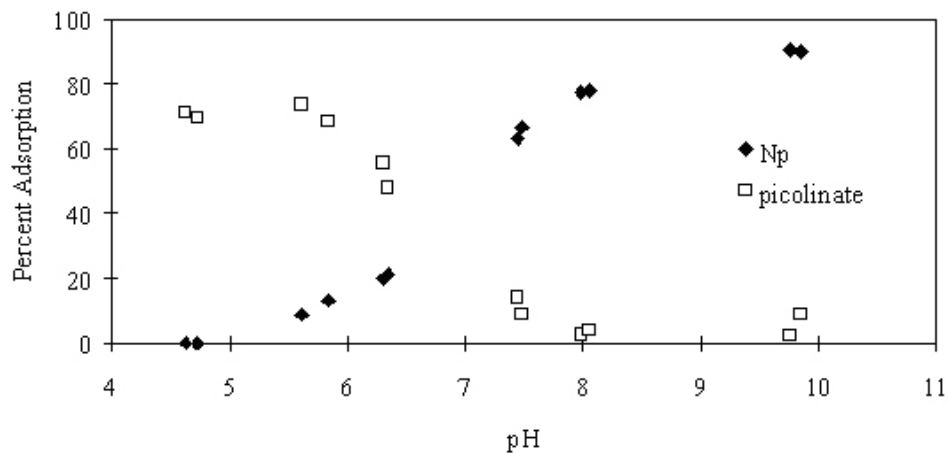
Figure 5.19. Percent Adsorption of NpO_2^+ and Picolinate on Milford Soil as a Function of pH (0.5 g soil/30 ml, 0.003 molar $Ca[ClO_4]_2$ solution, with initial concentrations of NpO_2^+ and picolinate of $6.7x10^{-7}$ M and 10^{-5} M, respectively)
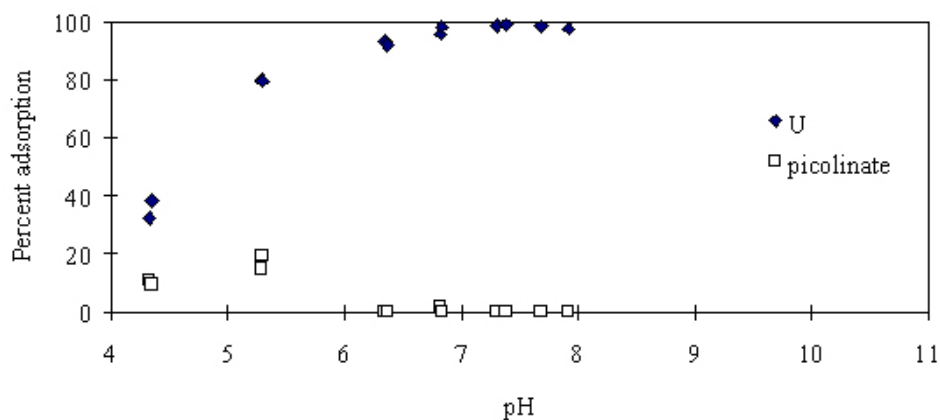
Figure 5.20. Percent Adsorption of UO_2^{2+} and Picolinate on 1.2% Iron Oxide Coated Sand as a Function of pH (0.5 g soil/30 ml, 0.003 molar $Ca[ClO_4]_2$ solution, with initial concentrations of UO_2^{2+} and picolinate of 10^{-5} M and 10^{-3} M, respectively)

5.14

Another adsorption experiment conducted using the same conditions used in the previous experiment are shown in Figure 5.21 for adsorption onto Milford soil. Adsorption of both U(VI) and picolinate is very similar to that of the iron oxide coated sand except that the increase in adsorption of U(VI) with pH is more gradual than that observed for the iron oxide coated sand, consistent with the low concentration of strong adsorbents in the Milford soil. The free picolinate anion shows a very low percentage adsorption because its solution concentration is very high relative to the quantity of available positively charged surface sites on the Milford soil.

5.1.7 U-EDTA System

The adsorption of U(VI), added as UO_2^{2+} in these carbonate-free or carbonate-limited tests, and EDTA onto iron oxide coated sand as a function of pH is shown in Figure 5.22. This experiment was conducted with equal initial concentrations of 10^{-5} M. U(VI) is again showing typical cationic adsorption behavior observed for various iron oxides in the absence of complexing anions. The EDTA is again exhibiting typical anionic adsorption behavior; however, less adsorption is observed at lower pH values than was observed in the nickel experiment (Figure 5.7). Girvin et al. (1993) observed similar behavior during the study of Co^{+2}-EDTA adsorption onto δ-Al_2O_3. Note that adsorption of Ni^{2+} onto iron oxides is nearly
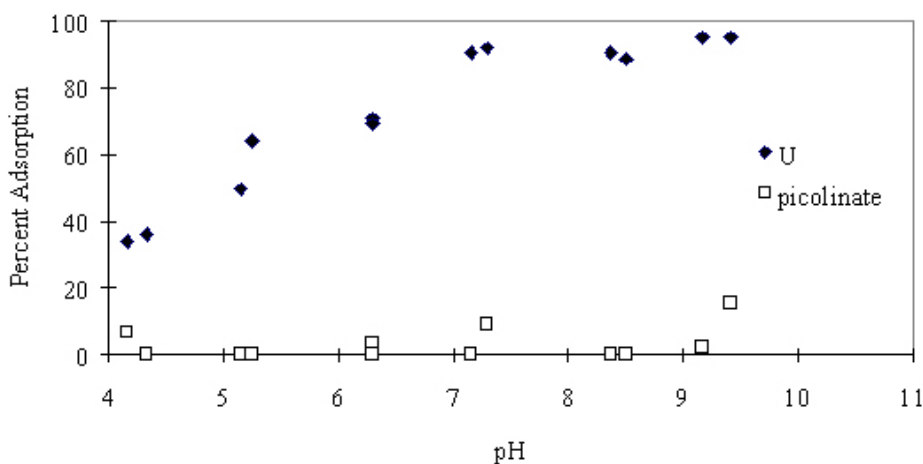
Figure 5.21. Percent Adsorption of UO_2^{2+} and Picolinate on Milford Soil as a Function of pH (0.5 g soil/30 ml, 0.003 molar Ca[ClO$_4$]$_2$ solution, with initial concentrations of UO_2^{2+} and picolinate of 10^{-5} M and 10^{-3} M, respectively)
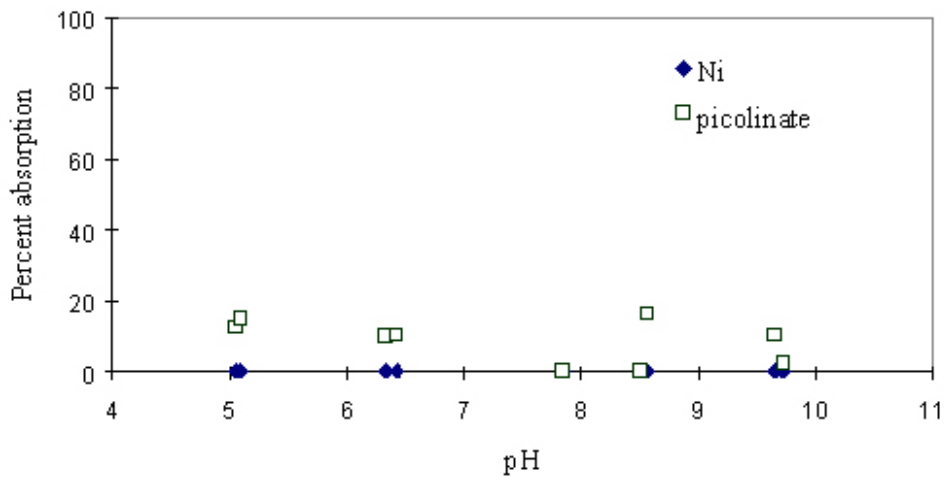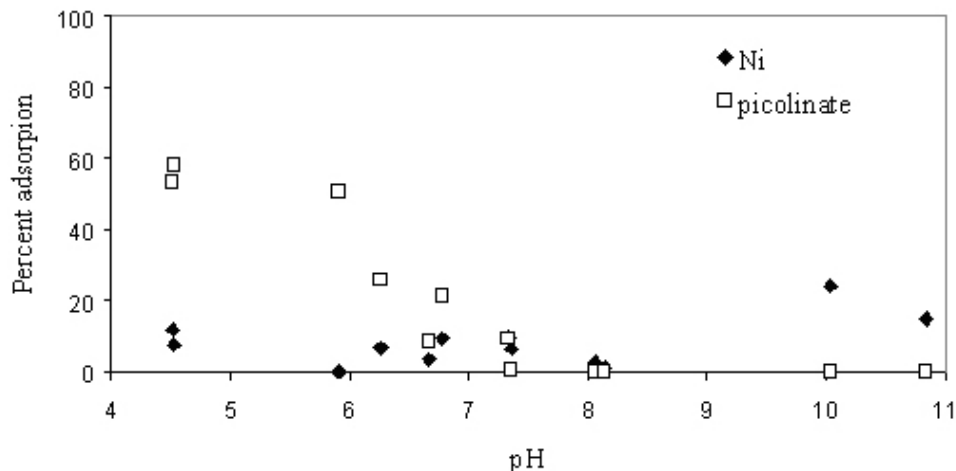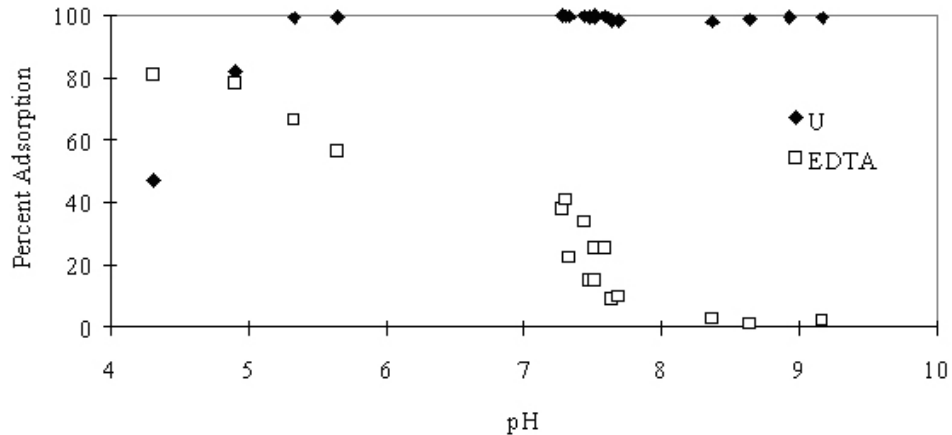
Figure 5.22. Percent Adsorption of UO_2^{2+} and EDTA on 1.2% Iron Oxide Coated Sand as a Function of pH (0.5 g soil/30 ml, 0.003 molar $Ca[ClO_4]_2$ solution, with initial concentrations of UO_2^{2+} and EDTA of 10^{-5} M and 10^{-5} M, respectively)

identical to that of Co^{2+} (Coughlin and Stone 1995). In the study of Girvin et al. (1993), the adsorption of EDTA was significantly less than when Co^{2+} was present. It was proposed that the EDTA species that were adsorbed in the absence of Co^{2+} were Al-EDTA^0 and Al-HEDTA^0 formed by dissolution of the δ-Al_2O_3. When Co^{2+} and EDTA were present in equal molar concentrations, the dominant EDTA species was Co-EDTA^{2-}. It was suggested that the Al-EDTA species (Al-EDTA$^-$ and Al-HEDTA^0) adsorb as outer sphere complexes and the affinity of the surface hydroxyls is greater for the Co-EDTA^{2-} species than for the Al-EDTA species. In our system, a very similar process appears to be occurring, but with HFO and Fe^{3+} instead of δ-Al_2O_3 and Al^{3+}. This explains why less adsorption of EDTA occurred in the U(VI) and EDTA system (Figure 5.22) than in the Ni^{2+} and EDTA system (Figure 5.7). These results and analysis suggest that U(VI) is not significantly complexed by EDTA under the conditions of this experiment.

UO_2^{2+} and EDTA adsorption results for three different soils (Milford, LK-1, and MNC-7) are illustrated in Figures 5.23, 5.24, and 5.25, respectively. The same experimental conditions used for the iron oxide coated sand experiment discussed above (Figure 5.22) were used for these three experiments. In all three cases, the adsorption of U(VI) is independent of EDTA, reflecting the lack of significant formation of UO_2^{2+} -EDTA complexes. Milford soil (Figure 5.23) shows the weakest adsorption for both U(VI) and EDTA, reflecting its sandy character with low iron oxide content (Table 3.3). The LK-1 results (Figure 5.24) indicate weak adsorption for EDTA similar to that of Milford soil. The adsorption of U(VI) onto LK-1 soil; however, is greater than for any of the other soils or the iron oxide coated sand. Apparently, U(VI) has a high affinity for the clay (ion-exchange sites) in this soil. LK-1 has the highest clay content of any of the soils at 46% (Table 3.3). The adsorption of both U(VI) and EDTA onto MNC-7 soil is very similar to that of the iron oxide coated sand. MNC-7 has the highest iron oxide content of any of the soils (Table 3.3) that explains the similarity in adsorption behavior between this soil and the iron oxide coated sand.

5.16
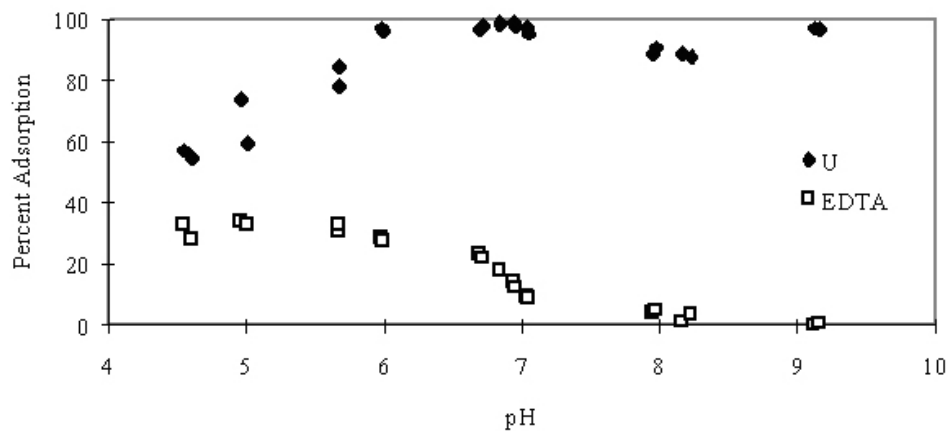
Figure 5.23. Percent Adsorption of UO_2^{2+} and EDTA on Milford Soil as a Function of pH (0.5 g soil/30 ml, 0.003 molar $Ca[ClO_4]_2$ solution, with initial concentrations of UO_2^{2+} and EDTA of 10^{-5} M and 10^{-5} M, respectively)
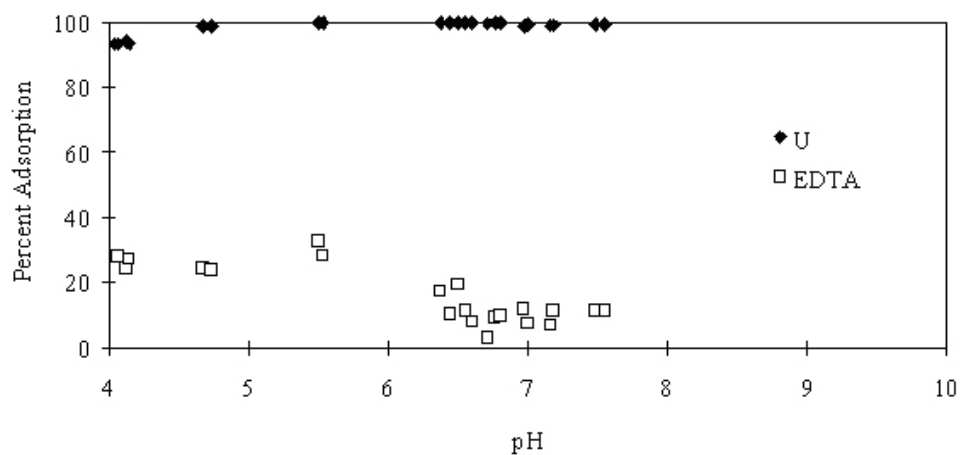
Figure 5.24. Percent Adsorption of UO_2^{2+} and EDTA on LK-1 Soil as a Function of pH (0.5 g soil/30 ml, 0.003 molar $Ca[ClO_4]_2$ solution, with initial concentrations of UO_2^{2+} and EDTA of 10^{-5} M and 10^{-5} M, respectively)

5.17
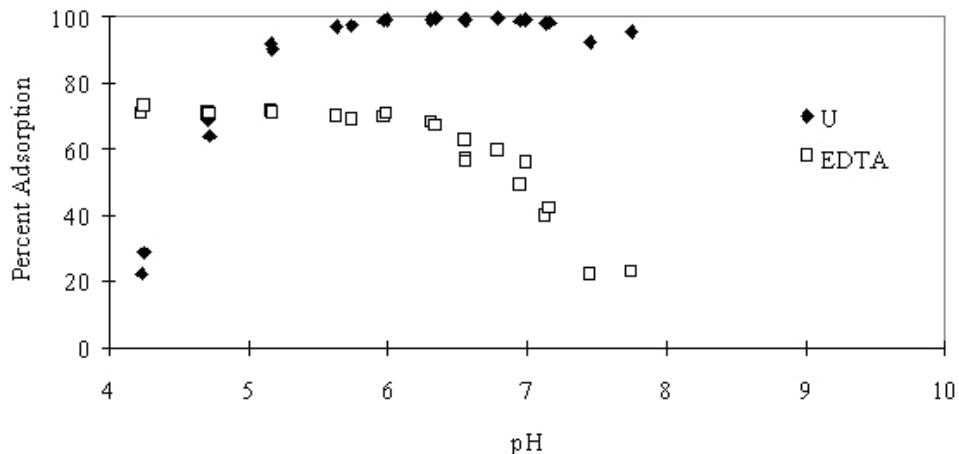
Figure 5.25. Percent Adsorption of UO$_2^{2+}$ and EDTA on MNC-7 Soil as a Function of pH (0.5 g soil/30 ml, 0.003 molar Ca[ClO$_4$]$_2$ solution, with initial concentrations of UO$_2^{2+}$ and EDTA of 10^{-5} M and 10^{-5} M, respectively)

5.1.8 Pu-Picolinate System

Adsorption of "oxidized" plutonium on Milford soil in the absence of any complexing agent is shown as a function of pH in Figure 5.26. The initial concentration of Pu in this experiment was 6.7×10^{-7} M. Although the Pu stock solution was initially in the form of PuO$_2^{2+}$, the oxidation state of the Pu at the end of the experiment is not certain (Bueppelmann et al. 1988). The adsorption of "oxidized" Pu on the Milford soil is less than that of the other actinides or actinide analogs used in this study. Sm^{3+}, Th^{4+}, NpO$_2^+$, and U(VI), all exhibit greater adsorption onto Milford soil than Pu. Because the oxidation state of the Pu in these experiments is uncertain further discussion regarding the reasons for this behavior would be speculative.

The results of another Pu adsorption experiment conducted under the same conditions with the exception that 10^{-5} M picolinate was added with the oxidized Pu to the Milford soil is shown in Figure 5.27. Again the "oxidized" Pu adsorption is low until pH values increase to above 8 and then approaches a maximum of 60% at pH values just below 10. At higher pH values adsorption of picolinate is expected to drop off to zero. The results shown here would suggest that picolinate adsorption remains relatively high at all pH values. The picolinate concentrations are not reliable because the beta spectra of the ^{14}C used to determine the picolinate concentrations contained interferences resulting from ^{241}Pu impurities in the ^{238}Pu stock solution. However, it is clear that the effect of the picolinate on the adsorption of Pu was insignificant, suggesting no significant amount of complexation.

Figure 5.28 illustrates results for an additional adsorption experiment conducted with "oxidized" Pu and picolinate. In this case, the Pu concentration was reduced to 10^{-8} M but the picolinate was maintained at 10^{-5} M. The degree of adsorption of the Pu is greater in this experiment. The higher degree of adsorption of Pu at lower concentrations is consistent with an adsorption media that contains a heterogeneous
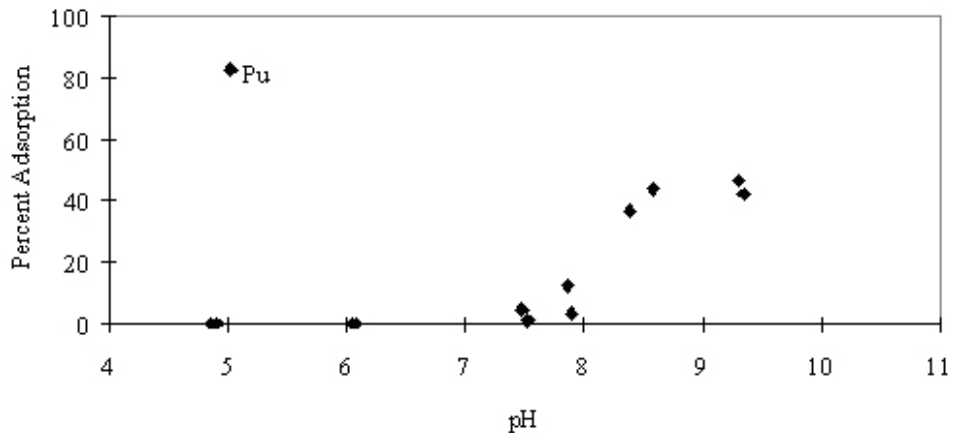
Figure 5.26. Percent Adsorption of Pu on Milford Soil as a Function of pH (0.5 g soil/ 30 ml, 0.003 molar Ca[ClO$_4$]$_2$ solution, with an initial Pu concentration of 6.7x10^{-7} M)
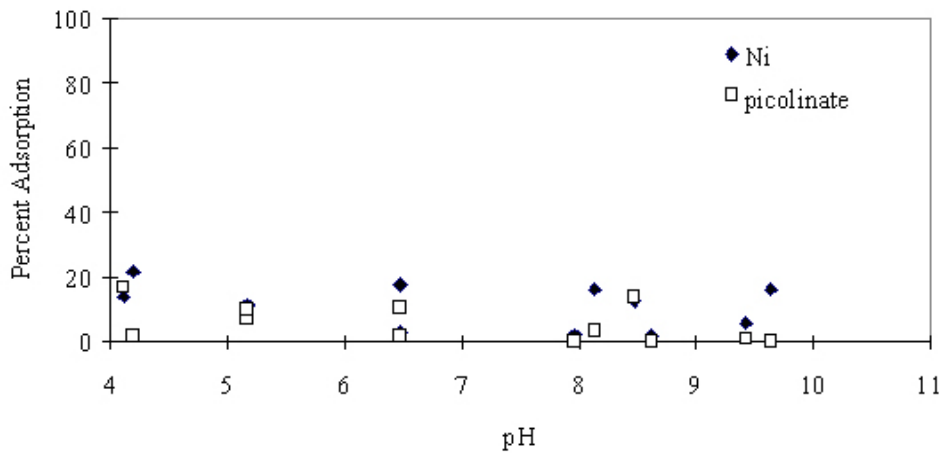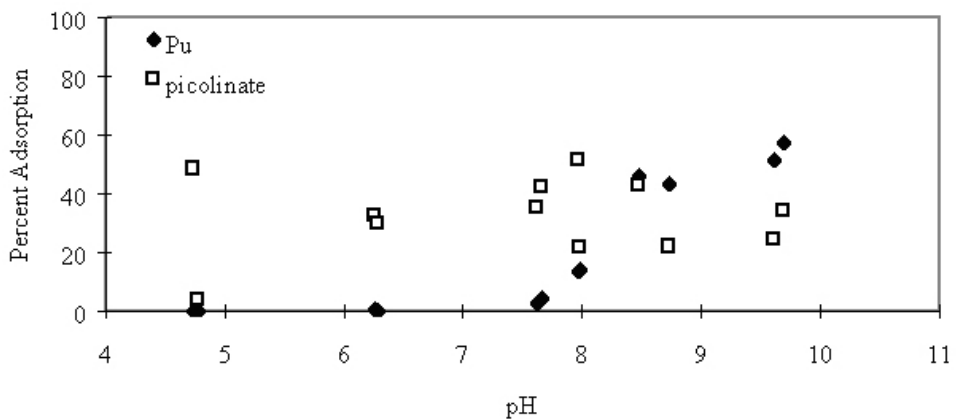

Figure 5.27. Percent Adsorption of Pu and Picolinate on Milford Soil as a Function of pH (0.5 g soil/30 ml, 0.003 molar Ca[ClO$_4$]$_2$ solution, with initial concentrations of Pu and picolinate of 6.7x10^{-7} M and 10^{-5} M, respectively)
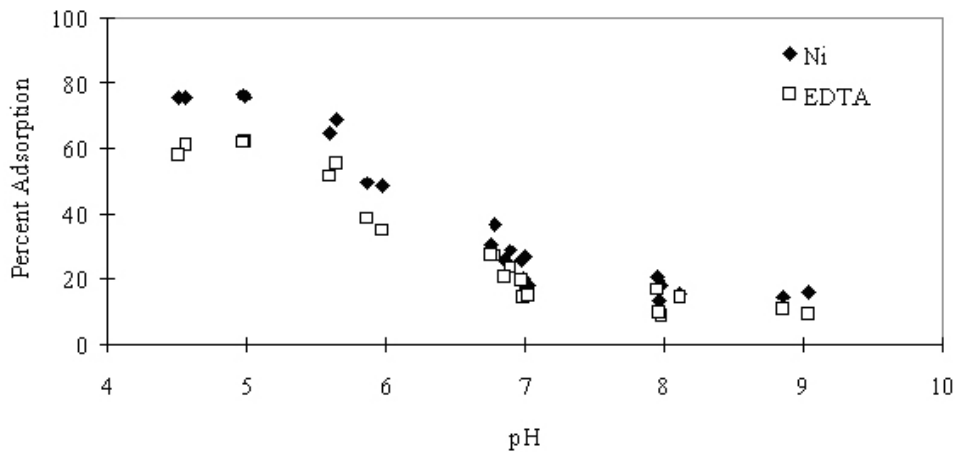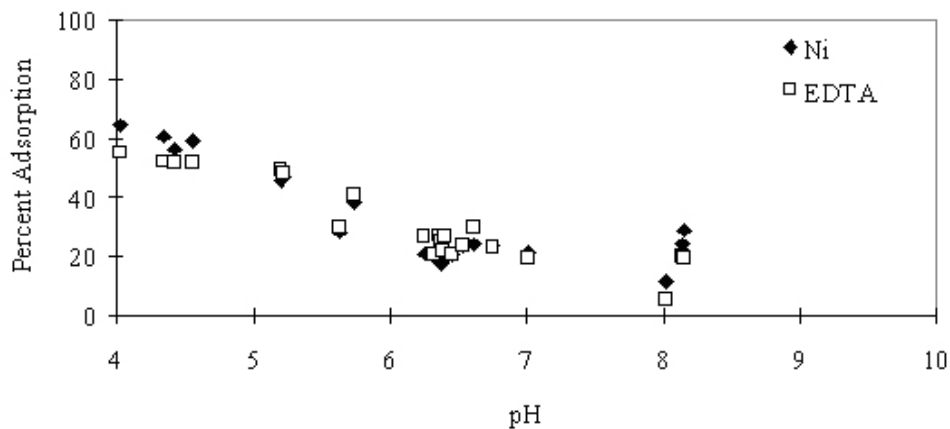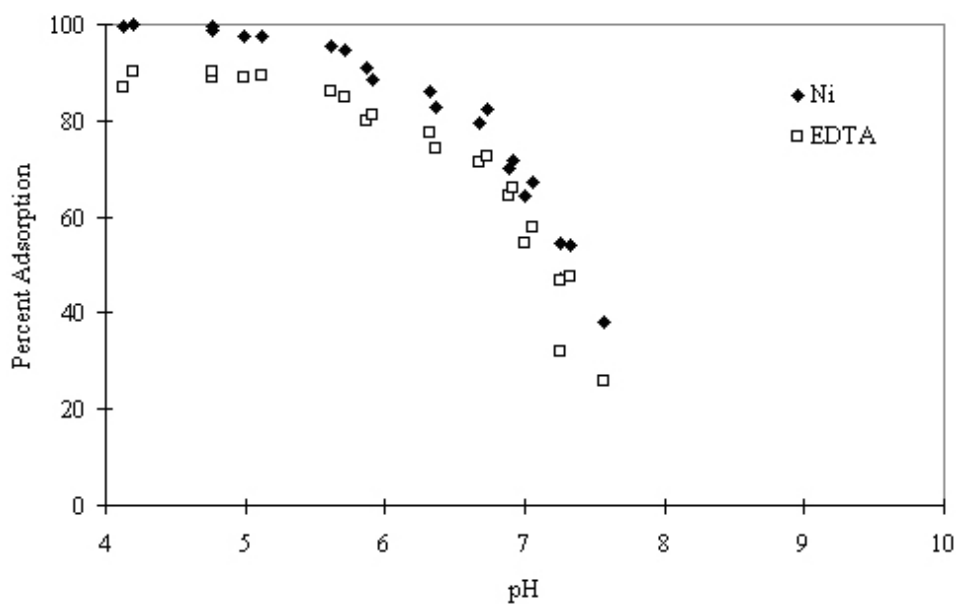
5.19
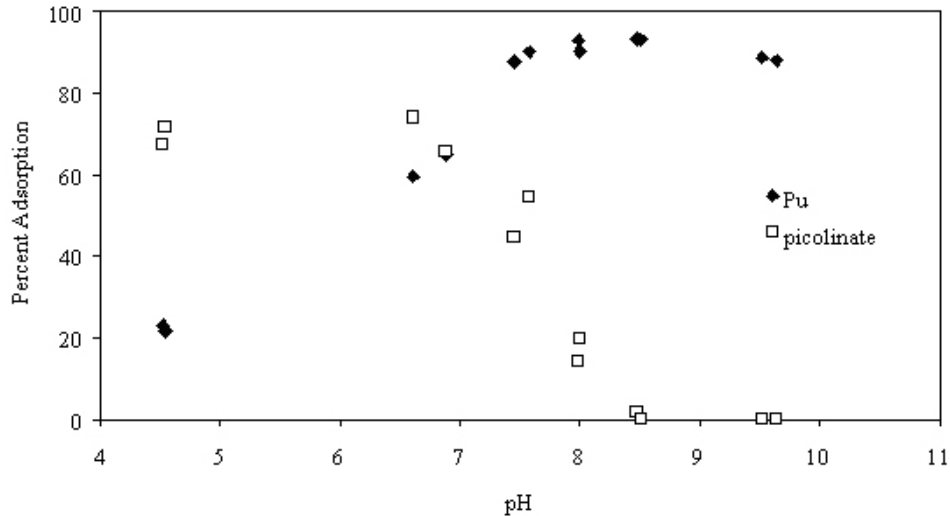
Figure 5.28. Percent Adsorption of Pu and Picolinate on Milford Soil as a Function of pH (0.5 g soil/30 ml, 0.003 molar Ca[ClO₄]₂ solution, with initial concentrations of Pu and picolinate of 10^{-8} M and 10^{-5} M, respectively)

distribution of adsorption sites. In other words, adsorption is taking place at a surface that contains sites with a range of binding energies. Initially, the adsorption will take place at sites with the highest energy and further surface complexation will occur at sites with progressively less energy. As a result of this process, adsorption will be strongest at the lowest concentration of adsorbate and the relative degree (i.e., percentage) of adsorption will decrease with increasing concentration of adsorbate. It seems safe to conclude that the "oxidized" Pu was predominately in valence states (V) and(VI) based on the relatively low adsorption tendencies at least for the tests at 6.7×10^{-7} M Pu starting concentrations. Reduced forms of Pu, valence states (III) and (IV), should have exhibited greater adsorption at the near neutral and alkaline pH values such as was observed for Sm(III) and Th(IV) discussed earlier.

The adsorption of picolinate in the "oxidized" Pu batch tests is consistent with previous results where complexation to metals was not significant and the ligand was adsorbing as a free anion.

The percent adsorption plots shown in Figures 5.1 through 5.28 can be formulated into K_d values readily because we also know the volume of solution used and mass of sediment in each test container. For convenience we have included Appendix B that lists the comparable Kd values in table form as a function of pH.

5.2 Flow-Through Column Experiments

As discussed in Section 3.3, flow through column tests allow one to study the adsorption of complexed metal-organic ligands at soil to solution ratios that are more realistic with actual conditions and under advective flow conditions where species can separate from each other during the various reactions. Further, flow through column tests allow one to study the desorption of adsorbed species more readily than batch adsorption tests. Thus near the end of the project, selected column tests were run to explore whether the results of the batch adsorption tests were yielding an accurate picture of the fate of organic ligand-radionuclide complexing agents in soil porewater germane to shallow land burial conditions. The column experiments are discussed in terms of the normalized concentration of the effluent (the observed

concentration in aliquots of effluent divided by the constant influent concentration that was pumped into the column at constant flow rate) plotted against the cumulative pore volumes of effluent collected out of the column. As discussed in Section 3.3, a pore volume is the amount of solution necessary to fill the void space [porosity] of the packed column. The breakthrough curve for each column experiment is a plot of the normalized effluent concentration $[C_{eff}/C_{inf}]$ plotted on the y axis versus the cumulative pore volumes collected plotted on the x axis. Because the column tests were run at a constant flow rate, the cumulative pore volumes are also linearly related to elapsed time. The number of pore volumes at which the breakthrough curve (normalized effluent concentration as plotted on the y axis) reaches a value of 0.5 is called the retardation factor. The retardation factor is related to the K_d as described in several classical transport text books (for example see Freeze and Cherry 1979). The following qualitative discussion describes the results of the six column tests that were run for this project and Figures 5.29 through 5.34 show the breakthrough plots.
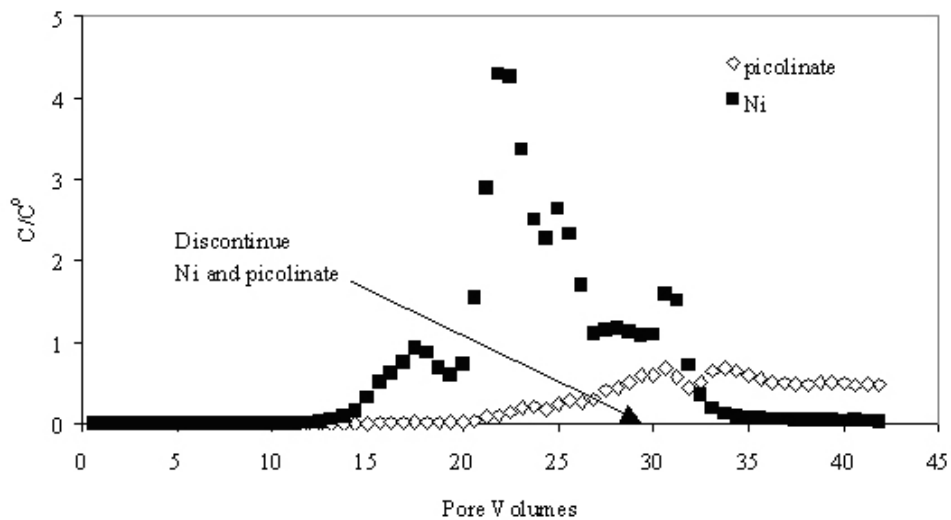
Figure 5.29. Flow Through Column Results for Ni^{2+} and Picolinate Through 1.2% Iron Oxide Coated Sand (influent solution 0.003 molar Ca[ClO$_4$]$_2$ with initial concentrations of Ni^{2+} and picolinate of 10^{-6} M and 10^{-4} M, respectively)

Ni^{2+} and picolinate transport through iron oxide coated sand at initial concentrations of 10^{-6} M and 10^{-4} M, respectively, are shown in Figure 5.29. The results indicate fairly complete adsorption of both Ni^{2+} and picolinate through the first 15 pore volumes of tracer-laden solution. After 15 pore volumes, the nickel begins to breakthrough the column until complete breakthrough is observed at about 17.5 pore volumes. During this time no picolinate is measured in the effluent. After 17.5 pore volumes, the Ni^{2+} in the effluent begins to decrease and then at about 20 pore volumes a sharp increase in Ni^{2+} is observed in the effluent. The Ni^{2+} concentration in the effluent exceeds the influent concentration by a factor of 4 at its peak at about 22 pore volumes. After 22 pore volumes the concentration of Ni^{2+} in the effluent falls off almost as precipitously (over pore volumes 24 to 34) as it increased. The injection of Ni-picolinate was stopped after 29 pore volumes and unspiked background electrolyte was injected for another 15 pore volumes. During the flushing period the Ni concentration in the effluent was somewhat erratic at first but soon dropped to near zero by the 33rd pore volume. Meanwhile the picolinate first broke through in the effluent at about the time the Ni started its dramatic rise (pore volume 20). However the rise in picolinate was slow and gradual. At the time that the tracers were stopped and flushing began, the picolinate break through had reached about 80%. Picolinate breakthrough dropped some after the flushing began but continued until the column was dismantled. The reason for this anomalous Ni behavior (finding elevated Ni concentrations of as much as 4 times greater than that in the influent) is not readily apparent. Measurements taken during the course of this experiment indicate that the effluent pH remained at about 6.7 through the first 20 pore volumes. At 20 pore volumes the pH increased suddenly to an average of about 7.4 (nearly the same as the influent) until the test was stopped at 42 pore volumes.

Comparison of the conditions of this column experiment with the batch Ni^{2+}-picolinate adsorption experiment conducted at a picolinate concentration of 10^{-4} M (see Figure 5.3 for batch results with similar picolinate but 10 times more Ni) indicates that only a small percentage of the Ni^{2+} and picolinate were adsorbed at pH 6.7 (approximately 5% for the nickel and 15% for the picolinate). The adsorption in the batch experiments appears to be relatively low compared to the complete adsorption observed in the column experiment up to approximately 15 pore volumes. This apparent discrepancy between the batch and the column results may be caused by the large difference in the liquid to solid ratios. For example, in the batch experiments the liquid to solid ratio was 60 L/kg. In the column experiment, 15 pore volumes equates to a liquid to solid ratio of only 3.6 L/kg. Also the batch data in Figure 5.3 at ten times higher Ni concentration likely underpredicts the percentage adsorption that would occur for a test with 10 times less Ni. Based on the column breakthrough data, the adsorption capacity of the 1.2% iron oxide coated sand for nickel in the presence of 10^{-4} M picolinate is 3.4 x 10^{-6} mol/kg before substantial breakthrough occurs.

A mass balance of the nickel and picolinate was conducted by accounting for the quantity of material in the effluent and what remained adsorbed on the column material. The material on the column was extracted twice using 1 M nitric acid at a soil to acid ratio of 1 to 5. For nickel, the mass balance was 102.2% made up of 96.4% in the effluent and 5.8% removed from the soil. For the picolinate 32.1% was accounted for in the effluent and 49.8% was extracted from the column for a total of 81.9%. It is uncertain if the 1 M nitric acid is an efficient extractant for removal of picolinate from soil. As a result,

the mass balance results for the picolinate are less certain. Thus with the excellent mass balance on Ni, we conclude that the unexpected high breakthrough between 20 and 25 pore volumes is not an artifact/error in our measurements.

We speculate that the Ni-picolinate complex and excess free picolinate is at first adsorbed onto the hydrous ferric oxide coatings and then the picolinate starts to interact with the ferric oxide. If the reaction was a simple exchange of metals attached to the picolinate ligand there would have to be strong tendency for the solid adsorbent to adsorb Fe(III)-picolinate complexes because we do not see a massive release of picolinate tracer along with the Ni. However, the picolinic ligand is present at 10 times the Ni concentration so that percentage changes in picolinic are muted. Further, free Ni adsorption to the ferric oxide coated sand shows that adsorption is quite sensitive to pH between values of 6.7 to 7.4 as shown in Figure 5.1 where the Ni percentage adsorbed changes from about 20 to 85% as pH increases from 6.7 to 7.4. The adsorption curve in Figure 5.1 would shift to the left (lower pH adsorption edge) for lower Ni concentrations and would shift to the right (higher pH adsorption edge) for larger Ni concentrations. Based on a Ni concentration of 4×10^{-6} M (four times the influent) we would expect at least 20 to 85% adsorption for the free Ni $[Ni^{+2}]$, if the picolinate was simply exchanging the Ni for Fe and allowing the free Ni ion to interact on its own. We thus can not explain the large percentage release of Ni between 20 and 25 pore volumes without evoking the partial dissolution of the ferric oxide substrate. This would effectively remove adsorption substrates for both the free cations (Ni^{2+} and Fe^{3+}), free picolinate, and the metal-ligand complexes. Unfortunately, we did not monitor dissolved Fe in the effluents to determine whether we caused net adsorption site disappearance. A much more quantitative analysis similar to the work of Davis et. al. (2000) for a flow through field test with transition metals and EDTA would be required to fully understand the results of this experiment. This column test does show that predictions that use simple constant K_d and constant source release constructs may not be exclusively conservative in predicting concentrations of contaminants in water downgradient from disposal sites.

Transport of Ni^{2+} and picolinate through Milford soil at initial concentrations of 10^{-6} M and 10^{-4} M, respectively, are shown in Figure 5.30. The results appear to be consistent with expectations based on the batch adsorption experiments. For example, the batch adsorption results in Figure 5-6 indicate that at pH 5.0 (the average pH measured in the column effluent), Ni^{2+} adsorption is relatively low. It can be expected that at the lower Ni^{2+} concentration used in the column experiment and higher solid to solution ratios, adsorption will be somewhat higher than that observed in the batch experiments (see Figure 5.6). For picolinate at concentrations below 10^{-3} M, adsorption at pH 5 is considerably higher than that of Ni^{2+} (see Figures 5.5 and 5.6). In Figure 5.30, it is apparent that the breakthrough of Ni^{2+} begins much sooner than that of picolinate. Ten pore volumes equates to only 1.6 L of leachate/kg soil before Ni^{2+} begins to breakthrough (a Ni^{2+} adsorption capacity of 1.6×10^{-4} mol/kg). It is interesting to note that the breakthrough of both Ni^{2+} and picolinate in this column test are very gradual and the C/C^o values are considerably less than 1.0. This type of behavior may also be indicative of adsorption site heterogeneity (binding sites with a range of binding energies). Also note that at 25 and 30 pore volumes of effluent there is a sudden decrease in C/C^o for Ni^{2+}. These decreases were due to temporary spikes in pH that occurred at this time (up to pH 7.0). These pH spikes resulted in a temporary increase in Ni^{2+} adsorption, but did not significantly affect the picolinate. We do not know what caused the two sudden changes in effluent pH.
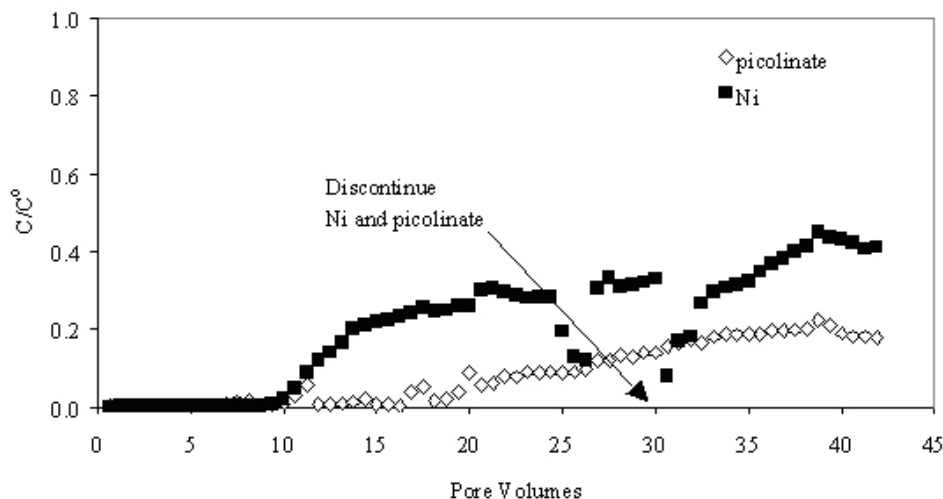
Figure 5.30. Flow Through Column Results for Ni^{2+} and Picolinate Through Milford Soil (influent solution 0.003 molar Ca[ClO4])$_2$ with initial concentrations of Ni^{2+} and picolinate of 10^{-6} M and 10^{-4} M, respectively)

For this test the metal-ligand laden solution was pumped for 30 pore volumes and then the solution without tracers was used to flush for an additional 13 pore volumes. The changing of solutions did not seem to change the breakthrough curves and is not considered related to the pH excursions. It would thus appear that the adsorption of the metal and ligand are reversible. If the adsorption was not reversible we would have expected the breakthrough curves to drop abruptly a few pore volumes after tracer was no longer being injected. The mass balance for the data in Figure 5.30 indicated that 29.3% of the nickel was accounted for in the effluent and 61.8% was extracted from the soil column for a total of 91.1% recovered. For the picolinate 11.7% was in the effluent and 23.1% was extracted from the soil column for a total of 34.8% recovered. Based on the shapes of the curves and the mass balances, we did not run the flushing long enough to elute all the reversibly held Ni and picolinate and that the picolinate, being adsorbed more strongly at the slightly acidic natural pH of the Milford soil, would require more flushing than would be needed for flushing the Ni.

The break through of another column experiment that was nearly the same as Figure 5.30 but with a picolinate concentration at 10^{-5} M is presented in Figure 5.31. No breakthrough of either Ni^{2+} or picolinate occurs for the first 30 pore volumes in this experiment. The average pH of the effluent in this experiment was 5.0, the natural pH of the Milford soil. No flushing was performed on this column because our intent was to concentrate on tests where relatively early breakthrough for one of the tracers was observed. The fact that the picolinate does not breakthrough is qualitatively consistent with the batch results in Figure 5.6 wherein 50 to 60% of picolinic acid is expected to adsorb. Given the much higher solid to solution ratio in the column test versus the batch tests breakthrough should be delayed. The lack of any breakthrough for the nickel in this experiment is surprising considering the fact that breakthrough
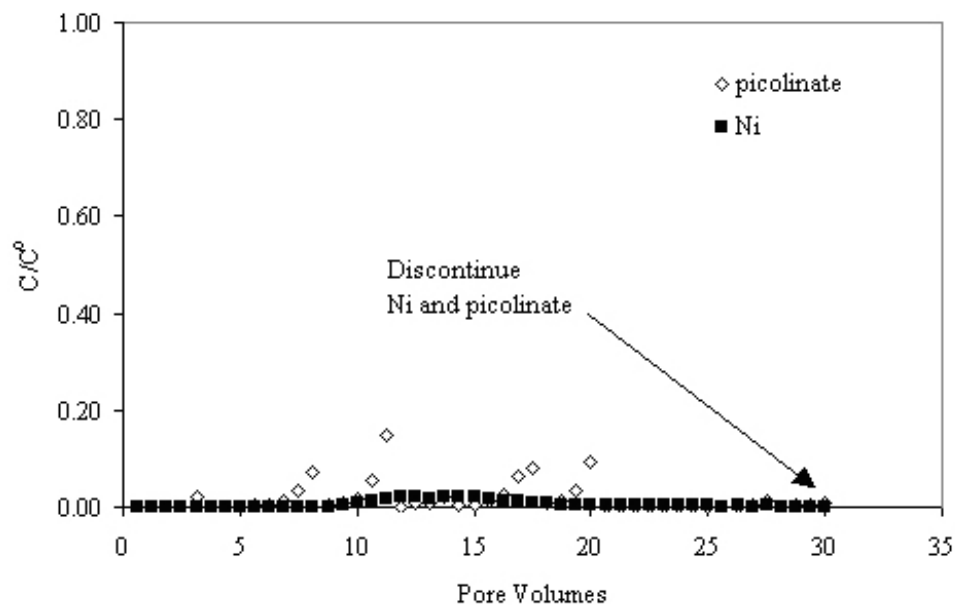
Figure 5.31. Flow Through Column Results for Ni^{2+} and Picolinate Through Milford Soil (influent solution 0.003 molar Ca[ClO4])$_2$ with initial concentrations of Ni^{2+} and picolinate of 10^{-6} M and 10^{-5} M, respectively)

did occur in the previous experiment [Figure 5.30] for the same soil, same pH, and same Ni^{2+} concentrations and the fact that very little adsorption of Ni^{2+} occurred at pH 5.0 both in the presence and absence of picolinate in the batch tests shown in Figures 5.5 and 5.6.

The mass balance for this experiment indicated that 0.6% of the nickel was in the effluent and 64.5% of the nickel could be extracted from the column material for a total of 65.1%. For the picolinate 1.7% was in the effluent and 1.0% extracted from the column material for a total recovery of 2.7%. The poor recovery compared to the other tests especially for the nickel suggests the results may be suspect. The results imply significant irreversible adsorption of both Ni and picolinate with contact with 1 M nitric acid, an observation that does not seem valid.

Figure 5.32 shows results for the flow-through experiment conducted for 10^{-5} M Ni^{2+} and 10^{-5} M EDTA through iron oxide coated sand. Essentially all the Ni^{2+} and approximately 90% of the EDTA are completely adsorbed onto the column during the first 32 pore volumes. At this point the concentrations of both Ni^{2+} and EDTA begin a gradual increase in concentration in the effluent. In this experiment the average effluent pH was nearly the same as the influent (7.5). Based on the quantity of iron oxide coated sand in the column, EDTA concentration in the influent, an EDTA adsorption maximum of 0.0049 moles/mole Fe at pH 4.5 (Szecsody et al. 1994) and an estimated fraction of available sites of 0.18 at pH 7.5 (Dzombak and Morel 1989), it was calculated that the adsorption capacity of this soil column for EDTA should be reached at 75 pore volumes, instead of the ~32 pore volumes observed.

5.25
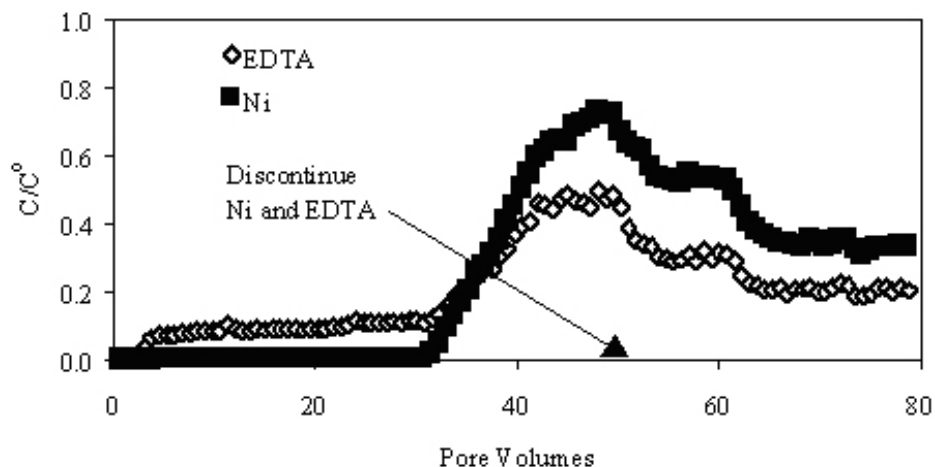
Figure 5.32. **Flow Through Column Results for Ni^{2+} and EDTA Through 1.2% Iron Oxide Coated Sand (influent solution 0.003 molar Ca[ClO$_4$]$_2$ with initial concentrations of Ni^{2+} and EDTA of 10^{-5} M and 10^{-5} M, respectively)**

The behavior observed in Figure 5.32, [the offset in the breakthrough percentage of Ni and EDTA tracers] can be explained as follows. Initially the Ni-EDTA complex is rapidly adsorbed to the iron oxides on the sand. After adsorption of the complex, dissociation of Ni^{2+} from some of the Ni-EDTA complex occurs, followed by ligand promoted dissolution (Szecsody et al. 1994; Stumm and Wieland 1990) of some of the iron oxide. This results in liberation of free Ni^{2+} and Fe(III)-EDTA complexes. At the pH of this experiment, the free Ni^{2+} is readily re-adsorbed to the iron oxides. Re-adsorption of the Fe(III)-EDTA complex is slow enough that a low (approximately 10% of the influent EDTA concentration), but significant amount of EDTA passes through the column until the adsorption capacity of the soil column for Fe(III)-EDTA is reached at approximately 32 pore volumes. After 32 pore volumes, the concentrations of Ni^{2+} and EDTA in the effluent begin to increase rapidly. It is suggested that after 32 pore volumes the adsorption capacity for all species [free Ni, Ni(II)-EDTA, Fe(III)-EDTA, and free EDTA] is approaching saturation and all species are beginning to pass through the column with decreased adsorption. After 32 pore volumes the rate of increase in effluent concentration of Ni^{2+} is faster than that of EDTA. This indicates that exhaustion of the adsorption capacity results in breakthrough behavior that is more complicated than the Ni-EDTA complexes simply passing through the column as one species with diminishing adsorption. The results suggest that in addition to intact Ni-EDTA complexes passing through the column, dissociation of Ni^{2+} from the adsorbed Ni-EDTA complexes is also occurring. Because the adsorption sites are nearly exhausted, adsorption of the free Ni^{2+} is inhibited, resulting in an increase in the Ni^{2+} concentration relative to EDTA in the effluent. Some of the EDTA remains adsorbed as Fe(III)-EDTA complexes.

After 49 pore volumes of Ni-ETDA laden solution was collected, the influent solution was changed to background electrolyte only and the column flushed for an additional 20 pore volumes. The effluent concentrations of both Ni and EDTA decreased slowly during the flushing but the offset (more Ni released than EDTA) continued. The mass balance results for this experiment are as follows: 43.1% of the nickel was in the effluent, 54.2% was extracted from the soil column for a total recovery of 97.3%. For EDTA, 35.3% was found in the effluent and 56.3% was extracted from the column for a total recovery of 91.5%. The results are quite good and suggest that with continued flushing, the total mass

injected would have shown up in effluent. That is, the adsorption reactions for the various tracers and their interactions with the iron oxide coated sands were reversible.

Figure 5.33 shows results for the flow-through experiment conducted for 10^{-5} M Ni^{2+} and EDTA through Milford soil that had been pre-equilibrated with caustic to simulate reaction with cement leachate. It is clear that the Ni-EDTA complexes are traveling through the column with very little adsorption. The breakthrough reached 100% after a few pore volumes. The average pH measured in the effluent was 9.8 because of our pre-treatment to remove the natural acidity as discussed in Section 3.3. The Ni-EDTA complex is strong and it remains intact during transport through the soil column.

The lack of adsorption is consistent with the batch results shown in Figure 5.8 that show very little adsorption of the Ni(II)-EDTA complex at pH values above 9. When injection of the Ni-EDTA laden solution was stopped and background electrolyte flushed through the column, the effluent concentrations of the tracers quickly dropped to zero as one would expect. There is a slight smearing in the trailing edge of this pulsed input compared to the shape of the leading edge. This is commonly found and is attributed to the slower diffusion of some tracer out of smaller pores during the desorption process. See van Genuchten (1981) and van Genuchten and Parker (1984) for discussion on analyzing breakthrough curves and the causes of asymmetry. The mass balance results for this experiment were 99.1% of the nickel was in the effluent and 0.3% was extractable from the soil column for a total of 99.4% recovered. For
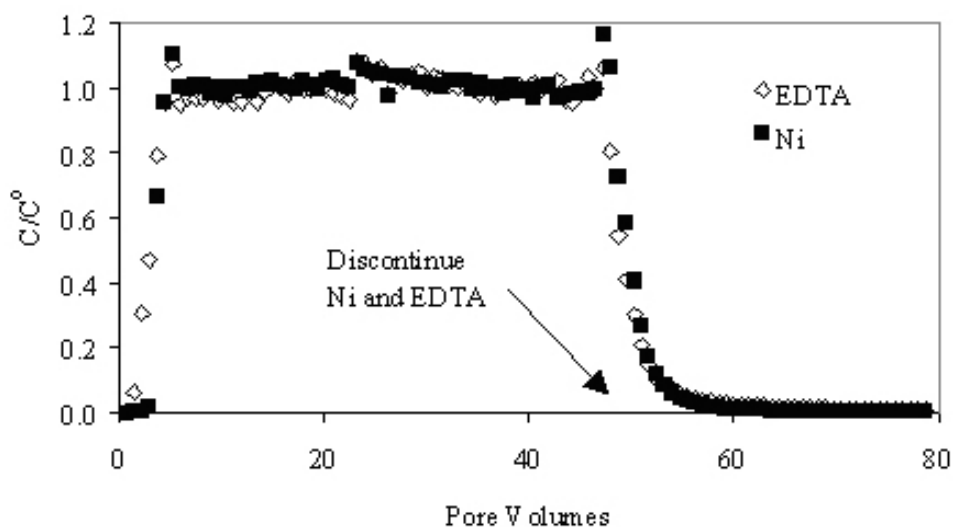
**Figure 5.33. Flow Through Column Results for Ni^{2+} and EDTA Through Milford Soil
(influent solution 0.003 molar $Ca[ClO_4]_2$ with initial concentrations of Ni^{2+}
and EDTA of 10^{-5} M and 10^{-5} M, respectively)**

EDTA, 98.1% was measured in the effluent and 1.7% was extracted from the soil column for a total of 99.8% recovered. Within experimental error essentially all of the tracer injected in the first 47 pore volumes was flushed out of the soil by the end of the experiment, suggesting that the small amount of adsorption that occurs in the very beginning of the experiment is completely reversible.

Results of a flow-through column experiment for Pu and picolinate through a column containing Milford soil that was pre-treated to remove natural acidity [to simulate cement leachate preconditioning] is shown in Figure 5.34. The initial concentrations of Pu and picolinate were 10^{-7} M and 10^{-4} M, respectively. The picolinate is being transported through the column almost completely uninhibited; whereas the Pu is completely adsorbed. The average effluent pH was 9.8, a pH value similar to cement leachate. These results are consistent with the results from the batch adsorption experiment shown in Figure 5.28 where the Pu and picolinate concentrations were each ten times lower. Both the column and the batch results suggest that oxidized Pu and picolinate do not form a strong complex and thus are acting independently in their adsorption reactions. At pH 9.8, Pu is highly adsorbing and picolinate does not adsorb at all. After 49 pore volumes of Pu and picolinate injection the solution was changed to background electrolyte alone and flow continued. The effluent concentrations of picolinate dropped rapidly to zero suggesting that any small amount of picolinate adsorbed in the soil was quickly and reversibly desorbed. However, no Pu was flushed out of the column even after an additional 31 pore volumes of flushing. Pu appears to be essentially irreversibly adsorbed to or precipitated in the Milford soil column or at least has a very high desorption K_d at the high pH value representative of cement leachate. The mass balance results for this experiment indicate that 0.0% of the Pu was found in the effluent, 97.1% of the Pu was extractable in the 1 M nitric acid from the soil for a total of 97.1% recovery. For the picolinate 99.1% was found in the effluent and 0.6% was extracted from the column for a total of 99.7%.

In summary, some of the column tests showed breakthrough that was qualitatively the same as the batch tests. In all the column tests but the one shown in Figure 5.31 the adsorption of the organic ligand-metal complex, or the free organic ligand and free metal (disassociated species) was reversible. That is, close to the total mass injected was recovered in the flushing stage or would have eventually flushed if enough untraced background solution had been pumped through the column. We do not understand why we had poor recovery in the column test shown in Figure 5.31 and this was the column not flushed at all.

The two tests that used the iron-oxide coated sand show complicated behavior that was interpreted as being caused by the ligand (both EDTA and picolinate) interacting with the ferric oxides. The Ni-organic ligand complex in both cases appears to exchange Ni for Fe to some extent such that free Ni^{+2} is produced and Fe(III)-organic complexes are formed that adsorb with different strengths to the soil than the Ni-organic complex. Further, we suspect that some of the organic ligand is dissolving the ferric oxide coatings (forming soluble ligand-Fe(III) complexes) and destroying sorption sites. The combination of all these reactions leads to rather complicated breakthrough curves that would require more detailed study. An excellent methodology for studying the transport of ETDA-transition metal complexes has recently been published [Davis et al. 2000]. A more quantitative analyses of our results would be possible using the Davis et al. 2000 approach.
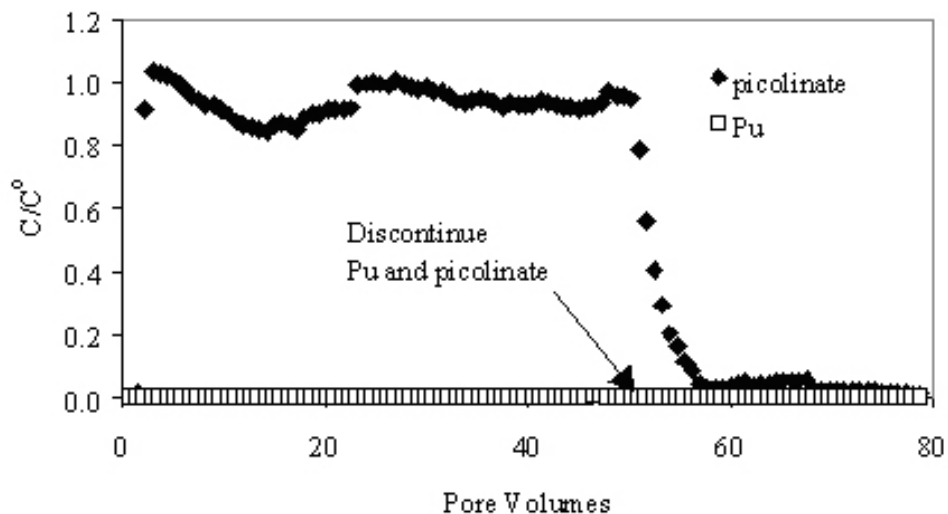
Figure 5.34. Flow Through Column Results for Pu and Picolinate Through Milford Soil (influent solution 0.003 molar Ca[ClO$_4$]$_2$ with initial concentrations of Pu and picolinate of 10^{-7} M and 10^{-4} M, respectively)

In two of the column tests the radionuclide-ligand appear to remain as a complex (see Figures 5.31 and 5.33), in three of the tests there is partial disassociation of the metal and ligand such that their break-through curves are different (see Figures 5.29, 5.30, and 5.32). For the final column test, the oxidized Pu and picolinic acid injected into Milford soil that had been pre-treated to remove natural acidity, the com-plex likely was never formed and the Pu and picolinate interact with the soil as free ions.

6.0 Summary and Recommendations

The available leach data for cement solidified spent resins from reactor piping decontamination suggests that maximum concentrations of organic ligands range from 2×10^{-3} to 10^{-4} M for picolinic acid and 3×10^{-4} to 10^{-5} M for EDTA. These ranges may in fact be elevated because the cement leachates have high pH values above 12. At pH 12, about 0.01 M "free" hydroxide is present in the leachates that will compete for anion exchange sites in the spent resins that contain the sorbed organic ligands and anionic ligand-metal complexes. Because anion exchange resins are regenerated using free hydroxide such as sodium hydroxide, the cement leachate may release higher concentrations of organic ligands and anionic complexes than the leachates of unsolidified spent resins disposed in high integrity containers. Only one datum was available for the concentration of EDTA from leached dewatered spent resins from the CAN-DEREM process. The concentration of total EDTA in the simulated groundwater leachate (pH = 7.5) was 2.4×10^{-4} M. This value is near the high end of the range found in leaching cement solidified resins from separate reactor decontaminations using older CAN-DEREM-like methods. The data base for concentrations of total organic ligands in leachates that could represent conditions in a disposal facility and surrounding sediment pore waters is not robust. For this project we had to conclude that the few data available represent the upper range of concentrations one might find. Obviously, the higher the concentration of organic ligands in leachate the more impact they might have on contaminant mobility because of mass action relationships in forming complexes.

Speciation calculations were conducted to determine the potential significance of organic chelating/complexing agents in facilitating transport of radionuclides from the cement solidified resin waste forms and dewatered resins and the subsequent solutions formed as leachate interacts with common soil and aquifer materials. This was accomplished using thermodynamic equilibrium calculations to determine the contribution of the organic chelating/complexing agents to the speciation scheme of the important radionuclides and stable metals in the leachates produced from spent resins. Initially the leachate solutions from cementitious waste forms have a high pH, which results from reactions with portland cement. The chemical evolution of these leachates can be expected to follow two pathways. If the leachates are contained within the waste site with an impermeable barrier, the high pH solutions could be neutralized by carbonic acid from the diffusion of CO_2 from the atmosphere or soil gas. Impermeable barriers are prone to failure and as a result will eventually leak. If the leachates escape into the soil column, it is expected that the pH will decrease due to the natural buffering capacity of the soil. To simulate these pH neutralization processes, speciation calculations were conducted as a function of pH. In these calculations it was assumed that the three principal soil components affecting pH and the subsequent speciation of important radionuclides and chelating agents are calcite, amorphous ferric hydroxide and gibbsite. The spent resin leachates were allowed to interact with finite amounts of these three representative phases to proxy for all dissolution/precipitation interactions that might occur in sediments. No adsorption reactions were included, however.

The chelate, radionuclide and metal concentrations selected for the speciation calculations were based on a review of decontamination waste leachate data. The most important decontamination processes from a waste disposal perspective are LOMI, CAN-DEREM and CITROX. A total of six cementitious leachates were selected for the modeling analysis to be representative of leachates derived from the LOMI, CAN-DEREM and CITROX spent resins solidified in cement. In general, the concentrations of the chelating agents and metals used in the speciation calculations were selected to be the highest measured in any of the INEEL leachates for a given cement waste form. For leachates in contact with cement (pH = 12.3), the most significant organic complexation occurred in the CAN-DECON and NS-1 leachates.

These two leachates were used as reasonable surrogates for the CAN-DEREM process for which no leach data are available for cement solidified material. EDTA or mixed OH-EDTA complexes dominated the speciation scheme of Mn^{2+}, Ni^{2+}, Sr^{2+}, and Zn^{2+}. Significant organic complexation also occurred for Am^{3+}, Co^{2+}, and Pu^{3+}. In the NS-1 leachates DTPA, EDTA or mixed OH-EDTA complexes dominated the speciation of Am^{3+}, Pu^{3+}, and Sr^{2+}. Significant organic complexation also occurred for Co^{2+}, Mn^{2+}, and Zn^{2+}.

Significant organic complexation also occurred in LOMI leachates in contact with cement, but only for leachates containing high concentrations of picolinate. In this case, picolinate complexes dominated the speciation scheme of Co^{2+} and Ni^{2+}. No comparable leachates are available for LOMI spent resins that are disposed without further treatment aside from dewatering. Assuming that there is no major difference in picolinate concentrations in leachates from cement solidified and dewatered spent resins, the calculations performed in Section 4 for the cement leachates will adequately describe the speciation of all LOMI process leachates.

The calculated speciation results indicate that in cement waste form leachates at high pH, DTPA and EDTA will influence the speciation of a wider range of radionuclides/metals to a greater extent than picolinate. In addition, oxalate at concentrations found in leachates will not significantly influence radionuclide/metal speciation. These findings indicate that the CITROX and LOMI decontamination processes may be preferred over the CAN-DEREM from a radionuclide mobility standpoint, because the two former processes do not use EDTA or DTPA.

As the pH of the leachate solution decreases, the effect of organic complexation increases. As pH decreases, the importance of hydrolysis of metals/radionuclides decreases, allowing more complexation with the leached organic ligands. For the LOMI leachates, the picolinate complexes dominated the speciation of Co^{2+}, Ni^{2+}, Zn^{2+} and was significant for Mn^{2+} and trivalent actinides, especially for the FitzPatrick leachate with its higher picolinate concentration. For the CAN-DECON leachate nearly all the metals and radionuclides are predicted to be complexed with EDTA until the pH drops below 6. Two exceptions are Pu^{4+} and Cs^+ which appear to remain unaffected by the organic ligands. In the CITROX leachates, oxalate and citrate complexes are predicted to dominate the speciation of trivalent actinides and nickel at common groundwater pH values (5-8.5).

Only one leach data set was available to address the leaching of un-solidified dewatered spent resins. This recent data set is for spent resins from the CAN-DEREM decontamination process. The leachate contained 2.4×10^{-4} M of total EDTA, which is near the high end of the range found in leachates from the cement solidified spent resins from the CAN-DECON and NS-1 processes. In addition, much higher concentrations of Ni^{2+}, Cr^{3+}, and Mn^{2+}, occurred in the leachates from the dewatered spent resins relative to the cement solidified waste leachates. These higher concentrations of transition metals in the leachates, significantly affects the speciation schemes of the system. The general speciation results for the non-solidified spent resin leachate that has not been in contact with the soil components (pH 7.49) are as follows. EDTA was found to dominate the speciation scheme of Am^{3+}, Co^{2+}, Fe^{3+}, Ni^{2+}, Pu^{3+}, and Cr^{3+}. EDTA accounted for fractional speciation of Mn^{2+} and Zn^{2+} (7% and 23%, respectively). Cs^+, Pu^{4+}, and Sr^{2+} were essentially uncomplexed by EDTA. It was apparent that an excess of metals relative to EDTA occurred in the leachate solution. As a result, complexation by EDTA preferentially occurred with the metals that had the largest equilibrium stability constants. This had the general effect of reducing the degree of complexation by EDTA for a number of radionuclides and metals. When the leachate solution was equilibrated with calcite, amorphous ferric hydroxide and gibbsite and the pH was adjust between 6 and 10, the major speciation changes that occurred were the result of $Cr(OH)_3$(am) precipitation above pH

7.5. As the $Cr(OH)_3(am)$ precipitated, EDTA was freed for complexation with other metals. The majority of the freed EDTA combined with the excess available Mn^{2+}.

It is important to recognize that these speciation calculations ignore the potential influence of soil adsorption reactions between the surface sites on soils and the free radionuclide/metals, free ligands and radionuclide/ligand complexes themselves.

The results of these speciation calculations can be condensed to the following conclusions. The organic chelating agents in decontamination waste leachates with the highest potential for mobilizing metals and radionuclides are EDTA and picolinate assuming that new decontamination schemes that use other chelates are not developed. The potential for EDTA to mobilize metals is highest for divalent transition metals, with a moderate potential for trivalent actinides. Picolinate appears to have significant potential to mobilize only Ni^{2+} and Co^{2+}.

In the batch adsorption studies we found that picolinate concentrations have to be 10^{-4} M or larger to significantly lower the adsorption tendencies of divalent transition metals such as Ni and Co. For other metals including Sm^{3+} [an analog for all trivalent actinides], Th^{4+} [an analog for all quadrivalent actinides], NpO_2^{+} [a likely analog for Pu(V)], UO_2^{2+}, and oxidized Pu, the picolinic acid concentration must reach concentrations greater than 10^{-3} M before any adsorption lowering impacts are expected for radionuclides and metals. Flow through column tests show that the type of soil and porewater pH are important variables that combine with organic ligand concentration to affect cationic metal/radionuclide adsorption. Even at picolinate concentrations of 10^{-4} M, soils with moderate hydrous oxide content and/or high cation exchange clay mineral content can retard the breakthrough of Ni for up to 10 pore volumes. We estimate that complete loss of adsorption tendencies would require picolinate concentrations in the neighborhood of 10^{-3} M.

EDTA forms stronger complexes with divalent transition metals and both batch and column tests with Ni have shown that metal adsorption can be blocked when EDTA solution concentrations are 10^{-5} M or higher. In a similar fashion EDTA complexes with oxycations such as NpO_2^{+}, UO_2^{2+}, and oxidized Pu are much weaker. Batch adsorption tests suggest that EDTA concentrations would have to be greater than 10^{-3} M to have adverse effects on (other than divalent transition metals) cationic metal/radionuclide adsorption onto most soils in contact with pore fluids at environmentally common pH's. Column tests also suggest that the adsorption of the ligands and ligand-metal/radionuclide complexes is reversible as evidenced from the flushing stages of the column tests.

Aside from the strong EDTA-divalent transition metal complex, most other picolinate and ETDA-cationic metal complexes appear to be labile (readily dissociated) during interactions with soils. As these organic ligand-cationic metal complexes migrate from the disposal facility, dilution and interaction with competing cations in the pore fluids and adsorption reactions will result in dissociation of all but the strongest or most kinetically recalcitrant complexes. It appears that the enhanced migration of cationic metals/radionuclides via organic ligand complexation may be limited to unique conditions. Conditions that promote enhanced migration over long distances include high concentrations of organic ligands, low concentrations of competing cations, alkaline pH values, organic ligands with slow biodegradation rates, and kinetically inert complexes. The column tests also showed evidence that picolinate and EDTA can react with iron hydrous oxides present as amorphous phases or coatings on sediments to exchange Fe(III) species for the divalent transition metals with the formation of Fe(III)-ligand aqueous species that can also adsorb to surface sorption sites. It also appears that these two organic ligands can partially dissolve ferric oxyhydroxides and destroy some of their sorption sites. The loss of sorption sites through

dissolution is a likely cause of the "snow plow" effect shown in Figure 5.29 where Ni concentrations exited the column at four times higher concentrations than were present in the influent.

At high pH values such as that created by cementitious wastes, mobilization of Ni^{2+} by EDTA becomes very significant. Under these conditions, adsorption of Ni^{2+} by soils and sediments is essentially zero. As a result, mixtures of metal/radionuclides and chelating agents (particularly EDTA) should not be co-disposed with high pH materials such as cement. This also indicates that cementitious waste forms are not a preferred disposal option for mixtures of transition metal/radionuclides and strongly binding chelating agents such as EDTA. For weaker binding organic complexants such as picolinate, citrate and oxalate, co-disposal of decontamination wastes and concrete should be acceptable.

The data present in Section 5 and Appendix B show that the K_d for metals/radionuclides, organic ligands, and their complexes are highly variable and a strong function of pH, ligand concentration and metal/ radionuclide concentration. These complicated relationships can be "systematized" using an adsorption construct called surface complexation modeling that is described below.

As we close out this project we offer the following recommendations. The available data base for leaching of spent resins from decontamination efforts is quite sparse. If possible, more data should be collected on the compositions of corrosion product/radionuclide laden fluids that are treated with the various ion exchange resins. The important data are the concentrations of the major metals, total organic ligand content, pH, and other common cations and inorganic anions. Knowledge of the radionuclide content is of lesser importance to perform thermodynamic speciation calculations and soil adsorption tests. This type of data also would be of interest to understand the ion exchange efficacy of the resins. It is possible that vendors would consider this information as proprietary as it could be used to understand the specifics of competitors methods.

Of direct interest is more leach tests on spent resins after dewatering and prior to packaging for disposal. As mentioned only one data set is available for one resin used to treat the spent fluids from one CAN-DEREM with AP reduction decontamination. More co-operation between researchers and vendors should be fostered to improve the database and general state of knowledge of the composition of spent resins and their leachates.

The other area that warrants more work is the quantitative determination of the adsorption properties of sediments and soils for picolinate-metal complexes using the "generalized surface complexation modeling approach" that is explained in Davis (2001), and Davis et al. (2000). Using this adsorption construct one would develop adsorption constants for particular soils that are akin to thermodynamic stability constants. Essentially the adsorption surface site is treated as if it were another ligand. Using batch adsorption tests, similar to those described in Section 5.1, wherein the concentrations of the metal and the organic ligand are varied systematically across a wide pH range, one can determine the adsorption stability constants. In addition one has to determine number of sorption sites per gram or per surface area for each soil. Specific surface areas are determined with traditional techniques such as tritium exchange and BET measurements (see Dzomback and Morell [1989] for details.

After such systematic studies have been performed on a few representative soils, all the parameters would be available to build a coupled chemical reaction transport model that can predict the migration of picolinate-metal/radionuclide wastes through aquifer sediments much like Davis et al. (2000) have performed for EDTA-transition metal complexes at a field site at Cape Cod, Maine.

7.0 References

Akers, D. W., J. W. McConnell, and N. Morcos. 1993b. *Characteristics of Low-Level Radioactive Decontamination Waste*. NUREG/CR-5672, EGG-2635, Vol. 3, U.S. Nuclear Regulatory Commission, Washington, D.C.

Akers, D. W., C. V. McIsaac, J. W. McConnell, N. Morcos, and R. M. Neilson, Jr. 1993a. *Radionuclide Releases from Cement-Solidified Decontamination Ion-Exchange Resins Leached in Simulated Groundwaters*. EGG-M-93056, EG&G Idaho, Inc., Idaho Falls, Idaho.

Akers, D. W., N. C. Kraft, and J. W. Mandler. 1994a. *Release of Radionuclides and Chelating Agents from Cement Solidified Decontamination Low-Level Radioactive Waste Collected from the Peach Bottom Atomic Power Station Unit 3*. NUREG/CR-6164, EGG-2722, U.S. Nuclear Regulatory Commission, Washington, D.C.

Akers, D. W., N. C. Kraft, and J. W. Mandler. 1994b. *Compression and Immersion Tests and Leaching of Radionuclides, Stable Metals, and Chelating Agents from Cement-Solidified Decontamination Waste Collected from Nuclear Power Stations*. NUREG/CR-6201, EGG-2736, U.S. Nuclear Regulatory Commission, Washington, D.C.

ANS. 1986. *Measurement of the Leachbility of Solidified Low-Level Radioactive Wastes by a Short-term Test Procedure*. ANSI/ANS 16.1, American Nuclear Society, La Grange Park, Illinois.

Bryce, A. L., W. A. Kornicker, and A. W. Elzerman. 1994. "Nickel Adsorption to Hydrous Ferric Oxide in the Presence of EDTA: Effects of Component Addition Sequence." *Environ. Sci. Technol*. 28:2353-2359.

Bueppelmann, K., J. I. Kim, and C. Lierse. 1988. "The Redox-Behavior of Plutonium in Saline Solutions Under Radiolysis Effects." *Radiochim. Acta* 44-45 (Pt. 1):65-70.

Coughlin, B. R., and A. T. Stone. 1995. "Nonreversible Adsorption of Divalent Metal Ions (Mn^{II}, Co^{II}, Ni^{II}, Cu^{II}, and Pb^{II}) onto Goethite: Effects of Acidification, Fe^{II} Addition, and Picolinic Acid Addition." *Environ. Sci. Technol*. 29:2445-2455.

Criscenti, L. J., and R. J. Serne. 1990. "Thermodynamic Modeling of Cement/Groundwater Interactions as a Tool for Long-Term Performance Assessment." In *Scientific Basis for Nuclear Waste Management XIII*. Editors V. M. Oversby and P. W. Brown, Materials Research Society, Pittsburg, Pennsylvania. Vol. 176:81-90.

Criscenti, L. J., R. J. Serne, K. M. Krupka, and M. I. Wood. 1996. *Predictive Calculations to Assess the Long-Term Effect of Cementitious Materials on the pH and Solubility of Uranium (VI) in a Shallow Land Disposal Environment*. PNNL-11182, Pacific Northwest National Laboratory, Richland, Washington.

Davis, J. A., D. B. Kent, J. A. Coston, K. M. Hess, and J. L. Joye. 2000. "Multispecies Reactive Tracer Test in an Aquifer with Spatially Variable Chemical Conditions." *Water Resources Research* 36:119-134.

Davis, J. A. 2001. *Surface Complexation Modeling of Uranium (IV) Adsorption on Natural Mineral Assemblages*. NUREG/CR-6708, U.S. Nuclear Regulatory Commission, Washington, D.C.

Dayal, R., R. F. Pietrzak, and J. H. Clinton. 1986. "Oxidation-Induced Geochemical Changes in Trench Leachates from Maxey Flats Low-level Radioactive Waste Disposal Site." *Nucl. Tech.* 72:184-193.

Dzombak, D. A., and F.M.M. Morel. 1989. *Surface Complexation Modeling*. John Wiley and Sons, New York.

Felmy, A. R., D. Rai, and M. J. Mason. 1991. "The Solubility of Hydrous Thorium(IV) Oxide in Chloride Media: Development of an Aqueous Ion-Interaction Model." *Radiochim. Acta* 55:177-185.

Freeze, R. A., and J. A. Cherry. 1979. *Groundwater*. Prentice-Hall, Inc., Englewood Cliffs, New Jersey.

Girvin, D. C., P. L. Gassman, and H. Bolton, Jr. 1993. "Adsorption of Aqueous Cobalt Ethylene-diaminetetraacetate by δ-Al_2O_3." *Soil Sci. Soc. Am. J.* 57:47-57.

Hsi, C. D., and D. Langmuir. 1985. "Adsorption of Uranyl onto Ferric Oxyhydroxides: Application of the Surface Complexation Site-Binding Model." *Geochem. Cosmochim. Acta* 49: 1931-1941.

Krupka, K. M., and R. J. Serne. 1998. *Effects on Radionuclide Concentrations by Cement/ Ground-Water Interaction in Support of Performance Assessment of Low-Level Radioactive Waste Disposal Facilities*. NUREG/CR-6377 (PNNL-11408), Pacific Northwest National Laboratory, Richland, Washington.

Martell, A. E., and R. M. Smith. 1989. *Critical Stability Constants, Vol. 5: First Supplement*. Plenum Press, New York.

McIsaac, E. V. 1993. "Leachability of Chelated Ion-Exchange Resins Solidified in Cement or Cement and Fly Ash." *Waste Management* 13:41-54.

McIsaac, C. V., D. W. Akers, J. W. McConnell, and N. Marcos. 1992. *Leach Studies of Cement-Solidified Ion Exchange Resins from Decontamination Processes at Operating Nuclear Power Stations*. EGG-M-92090, Idaho National Engineering Laboratory, Idaho Falls, Idaho.

McIsaac, E. V., D. W. Akers, and J. W. McConnell. 1991. *Effect of pH on the Release of Radionuclides and Chelating Agents from Cement-Solidified Decontamination Ion-Exchange Resins Collected from Operating Nuclear Power Stations*. NUREG/CR-5601, U.S. Nuclear Regulatory Commission, Washington, D.C.

McIsaac, C. V., and D. W. Akers. 1991. *Characteristics of Low-Level Radioactive Waste*. 1990 Annual Report, NUREG/CR-5672, Vol. 1, U.S. Nuclear Regulatory Commission, Washington, D.C.

Mclsaac, E. V., and J. W. Mandler. 1989. *The Leachability of Decontamination Ion-Exchange Resins Solidified in Cement at Operating Nuclear Power Plants*. NUREG/CR-5224, U.S. Nuclear Regulatory Commission, Washington, D.C.

Means, J. L., and C. A. Alexander. 1981. "The Environmental Biogeochemistry of Chelating Agents and Recommendations for the Disposal of Chelated Radioactive Wastes." *Nuclear and Chemical Waste Management* 2:183-196.

Means, J. L., D. A. Crerar, and J. 0. Duguid. 1978. "Migration of Radioactive Wastes: Radionuclide Mobilization by Complexing Agents." *Science* 200:1477-1482.

Morcos, N., J. W. McConnell, and D. W. Akers. 1992. *Characteristics of Low-Level Radioactive Waste*. NUREG/CR5672, EGG-2635, Vol. 2, U.S. Nuclear Regulatory Commission, Washington, D.C.

O'Donnell, E. 1983. "Insights Gained from NRC Research Investigations at the Maxey Flats LLW SLB Facility." In *Proceedings of the Fifth Annual Participants' Information Meeting DOE Low-Level Waste Management Program*, pp. 254-268. CONF-8308106, National Technical Information Service, Springfield, Virginia.

Papelis, C., K. F. Hayes, and J. 0. Leckie. 1988. *HYDRAQL: A Program for the Computation of Aqueous Batch Systems Including Surface-Complexation Modeling of Ion Adsorption at the Oxide/Solution Interface*. Technical Report No. 306, Environmental Engineering and Science, Department of Civil Engineering, Stanford University, Stanford, California.

Polzer, W. L., E. B. Fowler, and E. H. Essington. 1982. "Radioecology Studies at Maxey Flats, Kentucky: Radionuclides in Vegetal Samples." In *Radionuclide Distributions and Migration Mechanisms at Shallow Land Burial Sites*, pp. V-1-24. NUREG/CR-2383, U.S. Nuclear Regulatory Commission, Washington, D.C.

Schecher, W. E., and D. C. McAvoy. 1998. *MINEQL+ A Chemical Equilibrium Modeling System, Version 4.0 for Windows, User's Manual*. Environmental Research Software, Hallowell, Maine.

Serne, R. J., A. R. Felmy, K. J. Cantrell, K. M. Krupka, J. A. Campbell, H. Bolton, Jr., and J. K. Fredrickson. 1996. *Characterization of Radionuclides-Chelating Agent Complexes Found in Low-Level Radioactive Decontamination Waste*. NUREG/CR-6124, U.S. Nuclear Regulatory Commission, Washington, D.C.

Shaw, R. A., and C. J. Wood. 1985. "Chemical Decontamination: An Overview." *Nuclear News* 6:107-111.

Smee, J. L., D. Bradbury, and J. E. LeSurf. 1986. "Recent Experience with Dilute Chemical Decontamination." In *Proceedings of the Symposium on Advanced Nuclear Services*, pp. 1-18. Toronto Nuclear Association, Toronto, Ontario, Canada.

Speranzini, B. A., R. Voit, and M. Helms. 1990. "CAN-DECON Makes a Strong Comeback as CAN-DEREM." *Nuclear Engineering International* 9:52-55.

Stumm, W., and E. Wieland. 1990. "Dissolution of Oxide and Silicate Minerals: Rate Depend on Surface Speciation." In *Aquatic Chemical Kinetics*, ed. W. Stumm, pp. 367-400. Wiley-Interscience, New York.

Swan, T., M. G. Segal, W. J. Williams, and M. E. Pick. 1987. *LOMI Decontamination Reagents and Related Preoxidation Processes*. EPRI NP-5522M, Electric Power Research Institute, Palo Alto, California.

Szecsody, J. E., J. M. Zachara, and P. L. Bruckhart. 1994. "Adsorption-Dissolution Reactions Affecting the Distribution and Stability of $Co^{II}EDTA$ in Iron Oxide-Coated Sand." *Environ. Sci. Technol.* 28:1706-1716.

Van Genuchten, M. Th. 1981. *Non-Equilibrium Transport Parameters from Miscible Displacement Experiments*. Research Report 119, U.S. Salinity Laboratory, U.S. Department of Agriculture, Washington, D.C.

Van Genuchten, M. Th., and J.C. Parker. 1981. *Determining Transport Parameters from Laboratory and Field Tracer Experiments*. Bulletin 84-3, Virginia Agricultural Experiment Station, Blacksburg, Virginia.

Zachara, J. M, D. C. Girvin, R. L. Schmidt, and C. T. Resch. 1987. "Chromate Adsorption on Amorphous Iron Oxyhydroxide in the Presence of Major Groundwater Ions." *Environ. Sci. Technol.* 21: 589-594.

Appendix A

Thermodynamic Data

The thermodynamic data tabulated in Appendix A are arranged in 12 columns. The first column is the species identification number. The second column is the log of the formation constant of the species, at zero ionic strength and 25EC. Columns 3 through 10 contain a series of up to 4 component ID numbers and stoichiometric coefficients (respectively) of components that make up the species of interest. Column eleven contains the standard enthalpy of formation of the species at 25EC (kcal/mol). The last column may contain information regarding the name or chemical symbol of the species or the source of the data.

For this report the second column (log K) and columns 3-10 are of most interest as they define the formation stoichiometry and identify the logarithm of the stability constant for the reaction. For example, the first line defines the reaction that forms the radionuclide-ligand complex AmEDTA$^-$ (given ID number 600). The reaction is one mole of Am^{3+} (ID number 40) and one mole of EDTA^{4-} (ID number 128) forming one mole of complex.
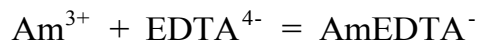
$$Am^{3+} \ + \ EDTA^{4-} \ = \ AmEDTA^{-}$$

$$\log k \ = \ \log\frac{[AmEDTA^{-}]}{[Am^{3+}][EDTA^{4-}]} \ = \ 20.64$$

As discussed in the text, the original sources for many of the thermodynamic constants in the database were not identified. In addition, when necessary the original database was supplemented with data that were not critically evaluated or in some cases estimates were used for complexes suspected of being important.

1	2	3	4	5	6	7	8	9	10	11	
573				List of TYPE II species; Revised from W2THRM.sav, 4/89(gap)							
600	20.64	40	1	128	1	0	0	0	0	0.0	AmEDTA(I-) KC
610	26.2	40	1	170	1	0	0	0	0	0.0	AmDTPA(2-)KC
611	28.18	40	1	170	1	50	1	0	0	0.0	AmHDTPA(1-) KC
620	9.72	40	1	117	1	0	0	0	0	0.0	AmCit KC
621	12.9	40	1	117	2	0	0	0	0	0.0	Am(Cit)2(3-) KC
622	12.61	40	1	117	1	50	1	0	0	0.0	AmHCit(l+) KC
630	7.02	40	1	118	1	0	0	0	0	0.0	AmOx(l+) KC
631	12.3	40	1	118	2	0	0	0	0	0.0	Am(Ox)2(1-) KC
640	4.49	40	1	126	1	0	0	0	0	0.0	AmPic(2+) KC
641	8.23	40	1	126	2	0	0	0	0	0.0	Am(Pic)2(1+) KC
642	11.10	40	1	126	3	0	0	0	0	0.0	Am(Pic)3 KC
650	7.7	40	1	101	1	0	0	0	0	0.0	AmCO3(1+) Cantrell, 1988
651	12.8	40	1	101	2	0	0	0	0	0.0	Arn(CO3)2(1-) Cantrell, 1988
660	3.65	40	1	102	1	0	0	0	0	0.0	AmSO4(1+) KC
670	-8.2	40	1	50	-1	0	0	0	0	0.0	AmOH(2+) Rai et al., 1983
671	-17.1	40	1	50	-2	0	0	0	0	0.0	Arn(OH)2(1+) Rai et al., 1983
672	-28.6	40	1	50	-3	0	0	0	0	0.0	Am(OH)3 Felmy et al., 1990
700	20.9	41	1	128	1	0	0	0	0	0.0	PuEDTA(O) KC
710	10.98	41	1	118	1	0	0	0	0	0.0	PuOx(2+) KC
711	20.27	41	1	118	2	0	0	0	0	0.0	Pu(Ox)2(0) KC
712	26.75	41	1	118	3	0	0	0	0	0.0	Pu(Ox)3(2-) KC
713	29.74	41	1	118	4	0	0	0	0	0.0	Pu(Ox)4(4-) KC
720	19.1	41	1	117	1	0	0	0	0	0.0	PuCit(+) KC
721	34.3	41	1	117	2	0	0	0	0	0.0	Pu(Cit)2(2-) KC
725	5.80	41	1	126	1	0	0	0	0	0.0	PuPic(3+) KC
730	-0.505	41	1	50	-1	0	0	0	0	0.0	PuOH(3+) Lemire and Tremaine, 1980
731	-2.32	41	1	50	-2	0	0	0	0	0.0	Pu(OH)2(2+) Lemire and Tremaine, 1980
732	-5.28	41	1	50	-3	0	0	0	0	0.0	Pu(OH)3(+) Lemire and Tremaine, 1980
733	-9.52	41	1	50	-4	0	0	0	0	0.0	Pu(OH)4(0) Lemire and Tremaine, 1980
740	19.14	41	1	101	1	0	0	0	0	0.0	PuCO3(2+) Falck, 1992
741	33.12	41	1	101	2	0	0	0	0	0.0	Pu(CO3)2(0) Falck, 1992
742	42.32	41	1	101	3	0	0	0	0	0.0	Pu(CO3)3(2-) Falck, 1992
743	46.65	41	1	101	4	0	0	0	0	0.0	Pu(CO3)4(4-) Falck, 1992
744	44.50	41	1	101	5	0	0	0	0	0.0	Pu(CO3)5(6-) Falck, 1992
750	0.01	41	1	50	-3	101	1	0	0	0.0	Pu(OH)3CO3(-) Falck, 1992
760	5.77	41	1	102	1	0	0	0	0	0.0	PuSO4(2+) Lemire and Tremaine, 1980
761	10.25	41	1	102	2	0	0	0	0	0.0	Pu(SO4)2(0) Read, 1991
770	0.14	41	1	103	1	0	0	0	0	0.0	PuCl(3+) Schwab and Felmy, 1982
1000	3.22	1	1	101	1	0	0	0	0	3.5460	CaCO3(aq),PB82
1010	11.43	1	1	50	1	101	1	0	0	-0.8710	CaHCO3, PB82
1020	2.31	1	1	102	1	0	0	0	0	1.6000	CaSO4 S/M,W2
1030	0.94	1	1	104	1	0	0	0	0	3.7980	??
1060	20.96	1	1	50	2	109	1	0	0	0.0000	VT84,Chris,#4
1070	6.46	1	1	109	1	0	0	0	0	0.0000	VT84,Chris,#l
1080	15.08	1	1	50	1	109	1	0	0	0.0000	VT84,Chris,#2
1100	11.00	1	1	128	1	0	0	0	0	0.0000	CaEDTA S/M
1101	16.0	1	1	128	1	50	1	0	0	0.0	CaHEDTA(-) Morel

A.2

1200	2.2	1	1	126	1	0	0	0	0	0.0	CaPIC(1+) Morel
1201	3.8	1	1	126	2	0	0	0	0	0.0	Ca(PIC)2 Morel
1210	4.7	1	1	117	1	0	0	0	0	0.0	CaCit(1-) Morel
1211	9.5	1	1	117	1	50	1	0	0	0.0	CaHCit Morel
1213	12.3	1	1	117	1	50	2	0	0	0.0	CaH2Cit(l+) Morel
1220	3.0	1	1	118	1	0	0	0	0	0.0	CaOx KC
1221	1.84	1	1	118	1	50	1	0	0	0.0	CaHOx(l+) KC
1230	12.88	1	1	170	1	0	0	0	0	0.0	CaDTPA(3-)Lindsay 1231
19.65	1	1	170	1	50	1	0	0	0	0.0	CaHDTPA(2-) Lindsay
1350	-12.85	1	1	50	-1	0	0	0	0	15.8380	CaOH+, B/M
1360	2.98	2	1	101	1	0	0	0	0	2.0200	MgCO3(aq),W2??
1370	11.51	2	1	50	1	101	1	0	0	-2.4270	MgHCO3,W2
1380	2.25	2	1	102	1	0	0	0	0	1.4000	MgSO4(aq),W2
1385	-1.00	2	1	103	1	0	0	0	0	0.0000	?? MgCl+, S/M
1390	1.82	2	1	104	1	0	0	0	0	4.6740	MgF+, phr
1420	6.59	2	1	109	1	0	0	0	0	0.0000	MgPO4-,VT84,phr
1425	21.07	2	1	109	1	50	2	0	0	0.0000	MgH2PO4+,VT84,phr
1430	15.22	2	1	50	1	109	1	0	0	0.0000	MgHPO4,VT84,phr
1435	8.95	2	1	128	1	0	0	0	0	0.0000	MgEDTA Davis
1436	15.1	2	1	128	1	50	1	0	0	0.0	MgHEDTA Morel
1500	2.6	2	1	126	1	0	0	0	0	0.0	MgPic(l+) Morel
1501	4.0	2	1	126	2	0	0	0	0	0.0	Mg(Pic)2 Morel
1510	4.7	2	1	117	1	0	0	0	0	0.0	Mgcit(1-) Morel
1511	9.2	2	1	117	1	50	1	0	0	0.0	MgHCit Morel
1520	3.42	2	1	118	1	0	0	0	0	0.0	MgOx KC
1521	4.38	2	1	118	2	0	0	0	0	0.0	Mg(Ox)2(2-) KC
1530	11.47	2	1	170	1	0	0	0	0	0.0	MgDTPA Lindsay
1531	18.98	2	1	170	1	50	1	0	0	0.0	MgHDTPA Lindsay
1730	-11.44	2	1	50	-1	0	0	0	0	15.4190	MgOH-, B/M
1750	11.50	3	1	50	1	101	1	0	0	0.0000	SrHCO3(aq), P/B
1760	2.76	3	1	101	1	0	0	0	0	0.0000	SrCO3(aq), P/B
1766	2.55	3	1	102	1	0	0	0	0	0.0000	SrSO4(aq), S/M
1770	-13.29	3	1	50	-1	0	0	0	0	0.0000	SrOH(aq), B/M
1780	1.8	3	1	126	1	0	0	0	0	0.0	SrPic(l+) Morel
1781	3.0	3	1	126	2	0	0	0	0	0.0	Sr(Pic)2 Morel
1790	4.1	3	1	117	1	0	0	0	0	0.0	SrCit(l-) Morel
1800	2.54	3	1	118	1	0	0	0	0	0.0	SrOx KC
1810	10.5	3	1	128	1	0	0	0	0	0.0	SrEDTA(2-) Morel
1811	14.9	3	1	128	1	50	0	0	0	0.0	SrHEDTA(-) Morel
1820	11.86	3	1	170	1	0	0	0	0	0.0	SrDTPA KC
1821	18.07	3	1	170	1	50	0	0	0	0.0	SrHDTPA KC
1960	0.85	4	1	102	1	0	0	0	0	2.2500	KSo4-. W2
1962	-0.70	4	1	103	1	0	0	0	0	0.0000	?? KC1(0),S/M??
1965	13.43	4	1	109	1	50	1	0	0	-3.5300	KHPO4-, VT84
1970	1.3	4	1	117	1	0	0	0	0	0.0	KCit(2-) Morel
1980	1.7	4	1	128	1	0	0	0	0	0.0	KEDTA(3-) Morel
2000	1.27	5	1	101	1	0	0	0	0	8.9110	NaCO3-, phr
2005	10.08	5	1	101	1	50	1	0	0	-3.6040	NaHCO3, phr
2010	0.70	5	1	102	1	0	0	0	0	1.1200	NaSO4-, W2,
2015	12.64	5	1	109	1	50	1	0	0	-3.5300	NaHPO4-, phr
2020	1.4	5	1	117	1	0	0	0	0	0.0	NaCit(2-) Morel
2030	2.5	5	1	128	1	0	0	0	0	0.0	NaEDTA(3-) Morel
2070	3.92	6	1	102	1	0	0	0	0	3.9100	FeSO4(+), W2
2080	5.42	6	1	102	2	0	0	0	0	4.6000	Fe(SO4)2-, W2
2090	1.48	6	1	103	1	0	0	0	0	5.6000	FeC12+

A.3

2100	2.13	6	1	103	2	0	0	0	0	0.0000	
2110	1.13	6	1	103	3	0	0	0	0	0.0000	
2120	6.20	6	1	104	1	0	0	0	0	2.7000	FeF2+ W2
2130	10.80	6	1	104	2	0	0	0	0	4.8000	
2140	14.00	6	1	104	3	0	0	0	0	5.4000	
2150	0.70	6	1	105	1	0	0	0	0	6.0000	FeBr2+ S/M
2160	2.10	6	1	106	1	0	0	0	0	0.0000	FeI2+
2170	17.77	6	1	50	1	109	1	0	0	2.2300	FeHPO4, W2
2180	24.98	6	1	50	2	109	1	0	0	-4.5200	FeH2PO4,W2
2190	23.50	6	1	50	1	112	1	0	0	0.0000	
2200	13.9	6	1	126	2	0	0	0	0	0.0	Fe(Pic)2(1+) Morel
2201	10.9	6	1	126	2	50	-1	0	0	0.0	FeOH(Pic) Morel
2300	13.5	6	1	117	1	0	0	0	0	0.0	FeCit Morel
2301	24.7	6	2	117	2	50	-2	0	0	0.0	Fe2(OH)2(Cit)2 Morel
2302	14.4	6	1	117	1	50	1	0	0	0.0	FeHCit(l+) KC
2303	10.2	6	1	117	1	50	-1	0	0	0.0	Fe(OH)Cit(l-) KC
2400	27.7	6	1	128	1	0	0	0	0	0.0	FeEDTA(-) Morel
2401	29.2	6	1	128	1	50	1	0	0	0.0	FeHEDTA Morel
2402	19.8	6	1	128	1	50	-1	0	0	0.0	Fe(OH)EDTA(-) Morel
2403	9.7	6	1	128	1	50	-2	0	0	0.0	Fe(OH)2EDTA(2-) Morel
2500	30.53	6	1	170	1	0	0	0	0	0.0	FeDTPA Lindsay
2501	34.53	6	1	170	1	50	0	0	0	0.0	FeHDTPA Lindsay
2502	19.43	6	1	170	1	50	-1	0	0	0.0	Fe(OH)DTPA Lindsay
2670	-2.19	6	1	50	-1	0	0	0	0	10.4000	FeOH2+,gap,7/81
2680	-5.67	6	1	50	-2	0	0	0	0	12.0000	Fe(OH)2+, gap
2690	-13.60	6	1	50	-3	0	0	0	0	28.0000	Fe(OH)3(0), gap
2700	-21.60	6	1	50	-4	0	0	0	0	44.0000	Fe(OH)4-, gap
2710	-2.95	6	2	50	-2	0	0	0	0	10.0000	?? Fe2(OH)2, gap
2715	-6.31	6	3	50	-4	0	0	0	0	14.3000	Fe3(OH)4, gap
2720	2.20	7	1	102	1	0	0	0	0	1.6000	
2725	1.10	7	1	101	1	50	1	0	0	0.0000	FeHCO3, SM5
2730	0.90	7	1	103	1	0	0	0	0	0.0000	?? FeCl+
2740	1.30	7	1	107	1	0	0	0	0	0.0000	??
2750	2.10	7	1	107	2	0	0	0	0	0.0000	??
2760	3.60	7	1	107	4	0	0	0	0	0.0000	??
2770	35.40	7	1	114	6	0	0	0	0	0.0000	??
2780	3.70	7	1	115	1	0	0	0	0	0.0000	??
2790	-9.50	7	1	50	-1	0	0	0	0	13.2000	FeOH+,B/M
2791	-20.57	7	1	50	-2	0	0	0	0	28.5600	Fe(OH)2(0),B/M
2792	-31.00	7	1	50	-3	0	0	0	0	30.3000	Fe(OH)3-,B/M
2793	-46.00	7	1	50	-4	0	0	0	0	0.0000	?? Fe(OH)4(2-)
3290	11.59	8	1	50	1	101	1	0	0	0.0000	MnHCO3(aq),PB82
3300	2.60	8	1	102	1	0	0	0	0	2.1000	??
3310	1.10	8	1	103	1	0	0	0	0	0.0000	??
3320	1.10	8	1	103	2	0	0	0	0	0.0000	??
3330	0.60	8	1	103	3	0	0	0	0	0.0000	??
3340	0.70	8	1	107	1	0	0	0	0	0.0000	??
3350	1.20	8	1	107	2	0	0	0	0	0.0000	??
3360	16.20	8	1	50	1	109	1	0	0	0.0000	??
3400	4.0	8	1	126	1	0	0	0	0	0.0	MnPic(l+) Morel
3401	7.1	8	1	126	2	0	0	0	0	0.0	Mn(Pic)2 Morel
3402	8.8	8	1	126	3	0	0	0	0	0.0	Mn(Pic)3(1-) Morel
3500	5.5	8	1	117	1	0	0	0	0	0.0	MnCit(l-) Morel
3501	9.4	8	1	117	1	50	1	0	0	0.0	MnHCit Morel
3600	3.9	8	1	118	1	0	0	0	0	0.0	MnOx KC
3601	5.25	8	1	118	2	0	0	0	0	0.0	Mn(Ox)2(2-) KC

A.4

3700	15.6	8	1	128	1	0	0	0	0	0.0	MnEDTA(2-) Morel
3701	19.1	8	1	128	1	50	1	0	0	0.0	MnHEDTA(-) Morel
3800	17.64	8	1	170	1	0	0	0	0	0.0	MnDTPA(3-) Lindsay
3801	22.70	8	1	170	1	50	1	0	0	0.0	MnHDTPA(2-) Lindsay
3900	-10.59	8	1	50	-1	0	0	0	0	0.0000	MnOH+,B/M
3901	-22.2	8	1	50	-2	0	0	0	0	0.0000	Mn(OH)2(aq),B/M
3910	-34.80	8	1	50	-3	0	0	0	0	0.0000	Mn(OH)3(aq),B/M
3911	-48.3	8	1	50	-4	0	0	0	0	0.0000	Mn(OH)4(aq),B/M
3912	-10.56	8	2	50	-1	0	0	0	0	0.0000	Mn2OH(aq),B/M
3913	-23.90	8	2	50	-3	0	0	0	0	0.0000	Mn2(OH)3(aq),B/M
3915	0.2	8	1	157	1	0	0	0	0	0.0000	MnNO3 S/M
3916	0.6	8	1	157	2	0	0	0	0	0.0000	Mn(NO3)2 S/M
3920	6.75	9	1	101	1	0	0	0	0	0.0000	B/M gap
3930	9.92	9	1	101	2	0	0	0	0	0.0000	B/M gap
3940	2.30	9	1	102	1	0	0	0	0	0.0000	??
3950	0.60	9	1	103	1	0	0	0	0	0.0000	??
3960	0.40	9	1	103	2	0	0	0	0	0.0000	??
3970	1.30	9	1	104	1	0	0	0	0	0.0000	??
3980	1.10	9	1	105	1	0	0	0	0	0.0000	??
3990	5.80	9	1	107	1	0	0	0	0	0.0000	??
4000	10.70	9	1	107	2	0	0	0	0	0.0000	??
4010	16.60	9	1	50	1	109	1	0	0	0.0000	??
4840	-8.00	9	1	50	-1	0	0	0	0	0.0000	B/M gap <
4841	-17.30	9	1	50	-2	0	0	0	0	0.0000	B/M gap <
4842	-27.80	9	1	50	-3	0	0	0	0	0.0000	B/M gap <
4843	-39.60	9	1	50	-4	0	0	0	0	0.0000	B/M gap
4850	-10.36	9	2	50	-2	0	0	0	0	0.0000	B/M gap
5000	2.7	10	1	102	1	0	0	0	0	1.6000	K-S/M,dH-??
5006	2.78	10	1	101	1	0	0	0	0	0.0000	S/M
5060	-12.80	10	1	50	-1	0	0	0	0	0.0000	??
5070	2.90	11	1	101	1	0	0	0	0	0.0000	Stipp
5071	6.4	11	1	101	2	0	0	0	0	0.0000	Stipp
5072	1.5	11	1	101	1	50	1	0	0	0.0000	Stipp
5080	2.30	11	1	102	1	0	0	0	0	0.0000	??
5090	1.98	11	1	103	1	0	0	0	0	0.3000	CdCl+, S/M
5100	2.60	11	1	103	2	0	0	0	0	0.9000	CdC12(0), S/M
5110	2.40	11	1	103	3	0	0	0	0	2.4000	CdC13-, S/M
5120	1.10	11	1	104	1	0	0	0	0	0.0000	??
5130	2.10	11	1	105	1	0	0	0	0	0.0000	??
5140	2.90	11	1	105	1	0	0	0	0	0.0000	??
5150	3.00	11	1	105	3	0	0	0	0	0.0000	??
5160	3.10	11	1	105	4	0	0	0	0	0.0000	??
5170	2.90	11	1	106	1	0	0	0	0	0.0000	??
5180	4.20	11	1	106	2	0	0	0	0	0.0000	??
5190	5.90	11	1	106	3	0	0	0	0	0.0000	??
5200	6.60	11	1	106	4	0	0	0	0	0.0000	??
5210	2.50	11	1	107	1	0	0	0	0	0.0000	??
5220	4.50	11	1	107	2	0	0	0	0	0.0000	?
5230	6.00	11	1	107	3	0	0	0	0	0.0000	??
5240	6.80	11	1	107	4	0	0	0	0	0.0000	?
5250	6.50	11	1	107	5	0	0	0	0	0.0000	?
5260	4.80	11	1	107	6	0	0	0	0	0.0000	??
5270	3.90	11	1	109	1	0	0	0	0	0.0000	??
5280	16.90	11	1	128	1	0	0	0	0	0.0000	CdEDTA Davis
5281	21.5	11	1	128	1	50	1	0	0	0.0	CdHEDTA Morel
5930	-10.08	11	1	50	-1	0	0	0	0	13.1000	CdOH+, B/M

A.5

5940	-20.35	11	1	50	-2	0	0	0	0	0.0000	?? Cd(OH)2(0)
5950	-33.30	11	1	50	-3	0	0	0	0	0.0000	?? Cd(OH)3-
5951	-47.35	11	1	50	-4	0	0	0	0	0.0000	?? Cd(OH)4(2-)
5952	-9.39	11	2	50	-1	0	0	0	0	10.9000	Cd2(OH)1(2+)
5955	5.30	12	1	101	1	0	0	0	0	0.0000	?? ZnCO3(0),W2
5956	9.63	12	1	101	2	0	0	0	0	0.0000	?? Zn(CO3)2(2-)
5957	12.43	12	1	50	1	101	1	0	0	0.0000	?? ZnHCO3+,W2
5960	2.38	12	1	102	1	0	0	0	0	1.5000	ZnSO4(0),W2
5965	3.28	12	1	102	2	0	0	0	0	0.0000	?? Zn(SO4)2(2-)
5970	0.43	12	1	103	1	0	0	0	0	0.0000	ZnCl+ Marcus
5980	0.61	12	1	103	2	0	0	0	0	0.0000	ZnC12 Marcus
5990	0.53	12	1	103	3	0	0	0	0	0.0000	ZnC13 Marcus
5995	0.20	12	1	103	4	0	0	0	0	0.0000	ZnC14 Marcus
5997	-7.48	12	1	50	-1	103	1	0	0	0.0000	?? ZnOHCl (aq),W2
6000	1.15	12	1	104	1	0	0	0	0	0.0000	?? ZnF+, W2
6010	0.10	12	1	105	1	0	0	0	0	0.0000	??
6020	2.20	12	1	107	1	0	0	0	0	0.0000	??
6030	4.50	12	1	107	2	0	0	0	0	0.0000	??
6040	7.00	12	1	107	3	0	0	0	0	0.0000	??
6050	9.00	12	1	107	4	0	0	0	0	0.0000	??
6060	15.70	12	1	50	1	109	1	0	0	0.0000	??
6100	5.7	12	1	126	1	0	0	0	0	0.0	ZnPic(l+) Morel
6101	10.3	12	1	126	2	0	0	0	0	0.0	Zn(Pic)2 Morel
6102	13.6	12	1	126	3	0	0	0	0	0.0	Zn(Pic)3(1-) Morel
6200	6.3	12	1	117	1	0	0	0	0	0.0	ZnCit(l-) Morel
6201	8.6	12	1	117	2	0	0	0	0	0.0	Zn(Cit)2(4-) Morel
6202	13.5	12	1	117	1	50	1	0	0	0.0	ZnHCit Morel
6203	12.9	12	1	117	1	50	2	0	0	0.0	ZnH2Cit(l+) Morel
6300	4.9	12	1	118	1	0	0	0	0	0.0	ZnOx KC
6301	7.6	12	1	118	2	0	0	0	0	0.0	Zn(Ox)2(2-) KC
6400	18.3	12	1	128	1	0	0	0	0	0.0	ZnEDTA(2-) Morel
6401	21.7	12	1	128	1	50	1	0	0	0.0	ZnHEDTA(-) Morel
6402	9.4	12	1	128	1	50	-1	0	0	0.0	Zn(OH)EDTA(3-) Morel
6500	20.42	12	1	170	1	0	0	0	0	0.0	ZnDTPA(3-) Lindsay
6501	26.68	12	1	170	1	50	1	0	0	0.0	ZnHDTPA(2-) Lindsay
6740	-8.96	12	1	50	-1	0	0	0	0	0.0000	?? ZnOH+, W2
6750	-16.90	12	1	50	-2	0	0	0	0	0.0000	??
6760	-28.40	12	1	50	-3	0	0	0	0	0.0000	??
6765	-41.20	12	1	50	-4	0	0	0	0	0.0000	??
6770	-9.00	12	2	50	-1	0	0	0	0	0.0000	?? Zn2OH(3+),B/M
6775	-57.80	12	2	50	-6	0	0	0	0	0.0000	?? B/M
6775	2.30	13	1	102	1	0	0	0	0	0.0000	??
6780	0.50	13	1	103	1	0	0	0	0	0.0000	??
6785	22.30	13	1	170	1	0	0	0	0	0.0	NiDTPA(3-) Lindsay
6786	28.63	13	1	170	1	50	1	0	0	0.0	NiHDTPA(2-) Lindsay
6790	1.10	13	1	104	1	0	0	0	0	0.0000	??
6800	0.60	13	1	105	1	0	0	0	0	0.0000	??
6810	2.70	13	1	107	1	0	0	0	0	0.0000	??
6820	4.80	13	1	107	2	0	0	0	0	0.0000	??
6830	6.50	13	1	107	3	0	0	0	0	0.0000	??
6840	7.70	13	1	107	4	0	0	0	0	0.0000	??
6841	7.2	13	1	126	1	0	0	0	0	0.0	NiPic(l+) Morel
6842	13.2	13	1	126	2	0	0	0	0	0.0	Ni(Pic)2 Morel
6843	17.9	13	1	126	3	0	0	0	0	0.0	Ni(Pic)3(1-) Morel
6844	6.7	13	1	117	1	0	0	0	0	0.0	NiCit(l-) Morel
6845	10.6	13	1	117	1	50	1	0	0	0.0	NiHCit Morel

A.6

6846	13.4	13	1	117	1	50	2	0	0	0.0	NiH2Cit(l+) Morel
6847	5.2	13	1	118	1	0	0	0	0	0.0	NiOx KC
6848	6.5	13	1	118	2	0	0	0	0	0.0	Ni(Ox)2(2-) KC
6850	-30.00	13	1	50	-3	0	0	0	0	0.0000	Ni(OH)3- B/M
6860	-19.00	13	1	50	-2	0	0	0	0	0.0000	Ni(OH)2(0) B/M
7590	-9.86	13	1	50	-1	0	0	0	0	0.0000	NiOH(+) B/M
7591	20.4	13	1	128	1	0	0	0	0	0.0	NiEDTA(2-) Morel
7592	24.0	13	1	128	1	50	1	0	0	0.0	NiHEDTA(-) Morel
7593	7.8	13	1	128	1	50	-1	0	0	0.0	Ni(OH)EDtA(3-) Morel
7595	30.70	14	2	99	2	0	0	0	0	0.0000	??
7600	2.40	14	1	102	1	0	0	0	0	0.0000	??
7610	3.50	14	1	102	2	0	0	0	0	0.0000	??
7620	7.27	14	1	103	1	0	0	0	0	0.0000	??
7630	14.00	14	1	103	2	0	0	0	0	0.0000	??
7640	14.88	14	1	103	3	0	0	0	0	0.0000	??
7650	15.60	14	1	103	4	0	0	0	0	0.0000	??
7660	1.60	14	1	104	1	0	0	0	0	0.0000	??
7670	9.60	14	1	105	1	0	0	0	0	0.0000	??
7680	18.10	14	1	105	2	0	0	0	0	0.0000	??
7690	20.50	14	1	105	3	0	0	0	0	0.0000	??
7700	21.60	14	1	105	4	0	0	0	0	0.0000	??
7710	13.40	14	1	106	1	0	0	0	0	0.0000	??
7720	24.60	14	1	106	2	0	0	0	0	0.0000	??
7730	28.40	14	1	106	3	0	0	0	0	0.0000	??
7740	30.30	14	1	106	4	0	0	0	0	0.0000	??
7750	8.70	14	1	107	1	0	0	0	0	0.0000	??
7760	17.50	14	1	107	2	0	0	0	0	0.0000	??
7770	18.50	14	1	107	3	0	0	0	0	0.0000	??
7780	19.30	14	1	107	4	0	0	0	0	0.0000	??
7790	68.00	14	1	50	2	108	2	0	0	0.0000	??
7800	54.20	14	1	108	2	0	0	0	0	0.0000	??
8040	-3.16	14	1	50	-1	0	0	0	0	0.0000	??
8050	-5.48	14	1	50	-2	0	0	0	0	0.0000	??
8052	-20.26	14	1	50	-3	0	0	0	0	0.0000	??
8054	4.75	14	1	50	-1	103	1	0	0	0.0000	??
8060	6.60	15	1	101	1	0	0	0	0	0.0	Bilinski 8/88
8070	10.06	15	1	101	2	0	0	0	0	0.0	Bilinski 8/88
8080	2.70	15	1	102	1	0	0	0	0	0.0000	??
8090	1.59	15	1	103	1	0	0	0	0	0.0000	PbC1 Smith/Martel
8100	1.80	15	1	103	2	0	0	0	0	0.0000	PbC12 Sm/Ma
8110	1.70	15	1	103	3	0	0	0	0	0.0000	PbC13 Sm/Ma
8120	1.40	15	1	103	1	0	0	0	0	0.0000	PbC14 Sm/Ma
8130	2.20	15	1	105	2	0	0	0	0	0.0000	??
8140	3.00	15	1	105	3	0	0	0	0	0.0000	??
8150	1.80	15	1	106	1	0	0	0	0	0.0000	??
8160	3.60	15	1	106	2	0	0	0	0	0.0000	??
8170	4.20	15	1	106	3	0	0	0	0	0.0000	??
8180	4.40	15	1	106	4	0	0	0	0	0.0000	??
8190	1.17	15	1	157	1	0	0	0	0	0.0000	S/M gap 8/88
8191	1.4	15	1	157	2	0	0	0	0	0.0000	S/M gap 8/88
8520	-7.71	15	1	50	-1	0	0	0	0	0.0000	B/M gap 8/88
8530	-17.12	15	1	50	-2	0	0	0	0	0.0000	B/M gap 8/88
8540	-28.06	15	1	50	-3	0	0	0	0	0.0000	B/M gap 8/88
8545	-6.36	15	2	50	-1	0	0	0	0	0.0000	B/M gap 8/88
8546	-23.88	15	3	50	-4	0	0	0	0	0.0000	B/M gap 8/88
8547	-20.88	15	4	50	-4	0	0	0	0	0.0000	B/M gap 8/88

A.7

8548	-43.61	15	6	50	-8	0	0	0	0	0.0000	B/M gap 8/88
8555	5.95	16	1	101	1	0	0	0	0	0.0000	Oxalate correl'n
8556	12.44	16	1	101	1	50	1	0	0	0.0000	Oxalate correl'n
8557	10.00	16	1	101	2	0	0	0	0	0.0000	Oxalate guess
8560	2.50	16	1	102	1	0	0	0	0	0.0000	??
8570	0.56	16	1	103	1	0	0	0	0	0.0000	S/M,gap 860812
8580	0.60	16	1	105	1	0	0	0	0	0.0000	??
8590	2.00	16	1	107	1	0	0	0	0	0.0000	??
8600	3.50	16	1	107	2	0	0	0	0	0.0000	??
8610	4.50	16	1	107	3	0	0	0	0	0.0000	??
8620	5.20	16	1	107	4	0	0	0	0	0.0000	??
8630	5.30	16	1	107	5	0	0	0	0	0.0000	??
8640	6.50	16	1	107	6	0	0	0	0	0.0000	??
8650	6.4	16	1	126	1	0	0	0	0	0.0	CoPic(l+) Morel
8651	11.3	16	1	126	2	0	0	0	0	0.0	Co(Pic)2 Morel
8652	15.8	16	1	126	3	0	0	0	0	0.0	Co(Pic)3(1-) Morel
8660	6.3	16	1	117	1	0	0	0	0	0.0	CoCit(l-) Morel
8661	10.3	16	1	117	1	50	1	0	0	0.0	CoHCit Morel
8662	12.9	16	1	117	1	50	2	0	0	0.0	CoH2Cit(l+) Morel
8670	4.7	16	1	118	1	0	0	0	0	0.0	CoOx KC
8671	7.0	16	1	118	2	0	0	0	0	0.0	Co(Ox)2(2-) KC
8680	18.1	16	1	128	1	0	0	0	0	0.0	CoEDTA(2-) Morel
8681	21.5	16	1	128	1	50	1	0	0	0.0	CoHEDTA(-) Morel
8690	21.28	16	1	170	1	0	0	0	0	0.0	CoDTPA(3-) Lindsay
8691	26.88	16	1	170	1	50	1	0	0	0.0	CoHDTPA(2-) Lindsay
8700	0.20	16	1	157	1	0	0	0	0	0.0000	S/M,gap
8702	0.66	16	1	157	2	0	0	0	0	0.0000	S/M,gap
9300	-9.65	16	1	50	-1	0	0	0	0	0.0000	B/M,gap
9302	-18.80	16	1	50	-2	0	0	0	0	0.0000	B/M,gap
9304	-31.50	16	1	50	-3	0	0	0	0	0.0000	B/M,gap
9306	-46.30	16	1	50	-4	0	0	0	0	0.0000	B/M,gap
9308	-11.20	16	2	50	-1	0	0	0	0	0.0000	B/M,gap
9310	-30.53	16	4	50	-4	0	0	0	0	0.0000	B/M,gap
9330	5.20	17	1	104	1	0	0	0	0	0.0000	??
9340	9.10	17	1	104	2	0	0	0	0	0.0000	??
9350	12.00	17	1	104	3	0	0	0	0	0.0000	??
9360	7.10	17	1	107	1	0	0	0	0	0.0000	??
9370	13.90	17	1	107	2	0	0	0	0	0.0000	??
9380	19.90	17	1	107	3	0	0	0	0	0.0000	??
9390	25.50	17	1	107	4	0	0	0	0	0.0000	??
9400	30.60	17	1	107	5	0	0	0	0	0.0000	??
9410	35.00	17	1	107	6	0	0	0	0	0.0000	??
9920	26.04	19	1	128	1	0	0	0	0	0.0	CrEDTA(-) KC
9921	28.25	19	1	128	1	50	1	0	0	0.0	CrHEDTA KC
9922	18.65	19	1	128	1	50	-1	0	0	0.0	Cr(OH)EDTA(2-) KC
9930	9.40	19	1	117	1	0	0	0	0	0.0	CrCit KC
9940	6.66	19	1	118	1	0	0	0	0	0.0	CrOx(+) KC
9941	12.27	19	1	118	2	0	0	0	0	0.0	Cr(Ox)2(-) KC
9942	16.76	19	1	118	3	0	0	0	0	0.0	Cr(Ox)3(3-) KC
9943	4.49	19	1	118	2	50	-1	0	0	0.0	CrOH(Ox)2(2-) KC
9944	-5.72	19	1	118	2	50	-2	0	0	0.0	Cr(OH)2(Ox)2(3-) KC
9950	11.72	19	1	126	2	0	0	0	0	0.0	Cr(Pic)2(+) KC
9450	1.30	18	1	102	1	0	0	0	0	0.0000	??
9460	3.30	18	1	103	1	0	0	0	0	0.000	Butler uncorr
9470	5.30	18	1	103	2	0	0	0	0	0.000	"
9480	5.30	18	1	103	3	0	0	0	0	0.000	"

9490	6.10	18	1	103	4	0	0	0	0	0.000	"
9500	4.30	18	1	105	1	0	0	0	0	0.0000	??
9510	7.30	18	1	105	2	0	0	0	0	0.0000	??
9520	7.70	18	1	105	3	0	0	0	0	0.0000	??
9530	8.10	18	1	105	4	0	0	0	0	0.0000	??
9540	14.00	18	1	106	1	0	0	0	0	0.0000	??
9550	13.90	18	1	106	2	0	0	0	0	0.0000	??
9560	3.20	18	1	107	1	0	0	0	0	0.0000	??
9570	7.20	18	1	107	2	0	0	0	0	0.0000	??
9580	14.00	18	1	50	1	108	1	0	0	0.0000	??
9590	19.00	18	1	50	2	108	2	0	0	0.0000	??
9600	17.30	18	1	108	1	0	0	0	0	0.0000	??
9880	-11.90	18	1	50	-1	0	0	0	0	0.0000	??
9881	-24.00	18	1	50	-2	0	0	0	0	0.0000	??
9890	4.90	19	1	102	1	0	0	0	0	0.0000	??
9900	5.20	19	1	104	1	0	0	0	0	0.0000	??
9910	9.10	19	1	104	2	0	0	0	0	0.0000	??
10000	-3.30	19	1	50	-1	0	0	0	0	0.0000	??
10010	-8.80	19	1	50	-2	0	0	0	0	0.0000	??
10020	-23.80	19	1	50	-4	0	0	0	0	0.0000	??
10022	-135.20	19	2	50	-14	99	-6	0	0	0.0000	??
10024	-68.40	19	1	50	-7	99	-3	0	0	0.0000	??
10026	-74.90	19	1	50	-8	99	-3	0	0	0.0000	??
10030	3.02	20	1	102	1	0	0	0	0	2.15	AlSo4n DKN,1984
10040	4.92	20	1	102	2	0	0	0	0	2.84	DKN
10050	6.98	20	1	104	1	0	0	0	0	1.06	AlFn DKN
10060	12.60	20	1	104	2	0	0	0	0	1.98	DKN
10070	16.65	20	1	104	3	0	0	0	0	2.16	DKN
10080	19.03	20	1	104	4	0	0	0	0	2.20	DKN
10090	20.91	20	1	104	5	0	0	0	0	1.84	DKN
10100	20.86	20	1	104	6	0	0	0	0	0.10	DKN
10200	18.9	20	1	128	1	0	0	0	0	0.0	AlEDTA(-) Morel
10201	21.6	20	1	128	1	50	1	0	0	0.0	AlHEDTA Morel
10202	12.6	20	1	128	1	50	-1	0	0	0.0	Al(OH)EDTA(2-) Morel
10203	2.0	20	1	128	1	50	-2	0	0	0.0	Al(OH)2EDTA(3-) Morel
10210	26.67	20	1	170	1	50	1	0	0	0.0	AlHDTPA(-) Lindsay
10211	13.87	20	1	170	1	50	-1	0	0	0.0	Al(OH)DTPA(3-) Lindsay
10220	9.96	20	1	117	1	0	0	0	0	0.0	AlCit KC
10221	12.93	20	1	117	1	50	1	0	0	0.0	AlHCit(+) KC
10230	7.77	20	1	118	1	0	0	0	0	0.0	AlOx(+) KC
10231	13.33	20	1	118	2	0	0	0	0	0.0	Al(Ox)2(-) KC
10232	16.92	20	1	118	3	0	0	0	0	0.0	Al(Ox)3(3-) KC
10340	-4.99	20	1	50	-1	0	0	0	0	11.90	AlOHn DKN
10345	-10.13	20	1	50	-2	0	0	0	0	22.00	DKN
10350	-23.30	20	1	50	-4	0	0	0	0	44.00	K Robie,H NBS
10355	-16.76	20	1	50	-3	0	0	0	0	33.00	DKN, 1984
10360	-0.10	21	1	103	1	0	0	0	0	0.0000	??
10370	0.00	21	1	104	1	0	0	0	0	0.0000	??
10420	0.60	22	1	102	1	0	0	0	0	0.0000	??
10480	-13.40	22	1	50	-1	0	0	0	0	0.0000	??
10490	1.90	23	1	102	1	0	0	0	0	0.0000	??
10500	3.00	23	1	102	2	0	0	0	0	0.0000	??
10510	2.00	23	1	102	3	0	0	0	0	0.0000	??
10520	1.60	23	1	103	1	0	0	0	0	0.0000	??
10530	5.60	23	1	104	1	0	0	0	0	0.0000	??
10540	9.70	23	1	104	2	0	0	0	0	0.0000	??

A.9

10550	12.70	23	1	104	3	0	0	0	0	0.0000	??
10770	-6.30	23	1	50	-1	0	0	0	0	0.0000	??
10901	-2.30	25	1	50	-1	0	0	0	0	0.0000	TiOOH(+),B/M
10902	-4.80	25	1	50	-2	0	0	0	0	0.0000	TiO(OH)2(0),B/M
10906	-1.68	25	8	50	-12	0	0	0	0	0.0000	Einaga8l
11010	26.36	25	1	50	1	109	1	0	0	0.0000	TiHPo4(aq),Einaga
11012	6.65	25	1	104	1	0	0	0	0	0.0	TiOF(+) Bond
11013	11.74	25	1	104	2	0	0	0	0	0.0	TiOF2(aq) Bond
11014	16.32	25	1	104	3	0	0	0	0	0.0	TiOF3(-) Bond
11015	20.38	25	1	104	4	0	0	0	0	0.0	TiOF4(2-) Bond
11020	9.70	26	1	104	2	0	0	0	0	0.0000	??
11030	10.20	26	1	104	3	0	0	0	0	0.0000	??
11040	1.10	26	1	105	1	0	0	0	0	0.0000	??
11050	1.70	26	1	105	2	0	0	0	0	0.0000	??
11060	1.40	26	1	105	3	0	0	0	0	0.0000	??
11110	-3.20	26	1	50	-1	0	0	0	0	0.0000	??
11480	3.70	29	1	102	1	0	0	0	0	0.0000	??
11490	0.80	29	1	103	1	0	0	0	0	0.0000	??
11500	4.10	29	1	104	1	0	0	0	0	0.0000	??
11510	7.50	29	1	104	2	0	0	0	0	0.0000	??
11520	0.70	29	1	105	1	0	0	0	0	0.0000	??
11530	19.30	29	1	109	1	0	0	0	0	0.0000	??
11840	-7.90	29	1	50	-1	0	0	0	0	0.0000	??
11850	26.90	30	1	107	2	0	0	0	0	0.0000	??
11870	5.80	31	1	102	1	0	0	0	0	0.0000	??
11880	9.40	31	1	102	2	0	0	0	0	0.0000	??
11890	1.40	31	1	103	1	0	0	0	0	0.0000	??
11900	8.80	31	1	104	1	0	0	0	0	0.0000	??
11910	15.70	31	1	104	2	0	0	0	0	0.0000	??
11920	20.80	31	1	104	3	0	0	0	0	0.0000	??
12090	-2.10	31	1	50	-1	0	0	0	0	0.0000	??
12100	-5.20	32	1	50	-1	0	0	0	0	0.0000	?? UO2OH(+),NEAj
12110	-11.90	32	1	50	-2	0	0	0	0	0.0000	?? after NEA
12112	-19.20	32	1	50	-3	0	0	0	0	0.0000	?? NEA
12114	-33.00	32	1	50	-4	0	0	0	0	0.0000	?? NEA
12120	-5.62	32	2	50	-2	0	0	0	0	0.0000	?? NEA
12122	-2.70	32	2	50	-1	0	0	0	0	0.0000	?? NEA
12123	-11.90	32	3	50	-4	0	0	0	0	0.0000	?? NEA
12125	-15.55	32	3	50	-5	0	0	0	0	0.0000	?? NEA
12127	-21.90	32	4	50	-7	0	0	0	0	0.0000	?? NEA
12128	-31.00	32	3	50	-7	0	0	0	0	0.000	NEA
12130	9.63	32	1	101	1	0	0	0	0	0.0000	?? CO3 cpxs NEA
12135	17.00	32	1	101	2	0	0	0	0	0.0000	?? NEA
12140	21.63	32	1	101	3	0	0	0	0	0.0000	?? NEA
12141	-1.18	32	2	101	1	50	-3	0	0	0.0000	?? vj
12145	5.08	32	1	104	1	0	0	0	0	0.0000	?? vj
12150	8.84	32	1	104	2	0	0	0	0	0.0000	?? vj
12155	11.27	32	1	104	3	0	0	0	0	0.0000	?? vj
12160	12.43	32	1	104	4	0	0	0	0	0.0000	?? vj
12165	0.21	32	1	103	1	0	0	0	0	0.0000	?? S/M
12170	2.95	32	1	102	1	0	0	0	0	0.0000	?? S/M
12175	4.00	32	1	102	2	0	0	0	0	0.0000	?? S/M
12180	23.20	32	1	109	1	50	2	0	0	0.0000	?? vj thesis
12185	22.90	32	1	109	1	50	3	0	0	0.0000	?? vj thesis
12200	45.24	32	1	109	2	50	4	0	0	0.0000	?? vj thesis
12205	46.00	32	1	109	2	50	5	0	0	0.0000	?? vj thesis

12210	20.53	32	1	112	1	50	1	0	0	0.0000	?? ??
12211	6.36	32	1	118	1	0	0	0	0	0.0000	?? S/M I=0.1
12212	10.59	32	1	118	2	0	0	0	0	0.0000	?? S/M I=0.1
12212	11.00	32	1	118	3	0	0	0	0	0.0000	?? S/M I=1.0
12225	-0.65	36	1	50	-1	0	0	0	0	0.0000	??
12230	-2.26	36	1	50	-2	0	0	0	0	0.0000	??
12235	-4.89	36	1	50	-3	0	0	0	0	0.0000	??
12240	-8.55	36	1	50	-4	0	0	0	0	0.0000	??
12245	-13.16	36	1	50	-5	0	0	0	0	0.0000	??
12250	-5.75	36	2	50	-5	0	0	0	0	0.0000	??
12255	3.69	36	1	102	1	0	0	0	0	0.0000	??
12260	6.05	36	1	102	2	0	0	0	0	0.0000	??
12265	-0.86	36	1	103	1	0	0	0	0	0.0000	??
12270	8.60	36	1	104	1	0	0	0	0	0.0000	??
12275	14.40	36	1	104	2	0	0	0	0	0.0000	??
12280	19.10	36	1	104	3	0	0	0	0	0.0000	??
12285	23.60	36	1	104	4	0	0	0	0	0.0000	??
12290	25.22	36	1	104	5	0	0	0	0	0.0000	??
12295	27.68	36	1	104	6	0	0	0	0	0.0000	??
12300	24.34	36	1	109	1	50	1	0	0	0.0000	??
12305	46.70	36	1	109	2	50	2	0	0	0.0000	??
12310	67.67	36	1	109	3	50	3	0	0	0.0000	??
12315	88.05	36	1	109	4	50	4	0	0	0.0000	??
12530	10.32	50	1	101	1	0	0	0	0	-3.5610	HCO3-, pb82
12540	16.67	50	2	101	1	0	0	0	0	-5.7380	H2CO3, pb82
12550	1.99	50	1	102	1	0	0	0	0	4.9100	HSO4-, W2
12555	0.20	50	1	103	1	0	0	0	0	0.0000	HCl, Henly
12560	3.17	50	1	104	1	0	0	0	0	3.4600	HF, W2
12565	3.75	50	1	104	2	0	0	0	0	4.5500	HF2-, W2
12570	9.24	50	1	107	1	0	0	0	0	0.0	NH4OH, Butler
12580	12.92	50	1	108	1	0	0	0	0	-12.1000	HS-, S/M
12590	19.91	50	2	108	1	0	0	0	0	-5.3000	H2S, S/M
12600	12.35	50	1	109	1	0	0	0	0	-3.5300	phr
12610	19.55	50	2	109	1	0	0	0	0	-4.5200	phr
12620	21.70	50	3	109	1	0	0	0	0	-3.6200	phr
12650	9.32	50	1	114	1	0	0	0	0	0.0000	??
12651	6.40	50	1	117	1	0	0	0	0	0.0	HCit(2-) Morel
12652	11.16	50	2	117	1	0	0	0	0	0.0	H2Cit(1-) Morel
12653	14.29	50	3	117	1	0	0	0	0	0.0	H3Cit Morel
12655	1.25	50	2	118	1	0	0	0	0	0.0000	?? S/M
12656	4.27	50	1	118	1	0	0	0	0	0.0000	?? S/M
12658	5.39	50	1	126	1	0	0	0	0	0.0	HPiC Morel
12659	6.40	50	2	126	1	0	0	0	0	0.0	H2Pic(l+) Morel
12660	11.00	50	1	128	1	0	0	0	0	0.0	HEDTA(3-) S/M
12661	17.3	50	2	128	1	0	0	0	0	0.0	H2EDTA(2-) SIM/
12661	19.6	50	3	128	1	0	0	0	0	0.0	H3EDTA(1-) S/M
12661	21.8	50	4	128	1	0	0	0	0	0.0	H4EDTA S/M
12670	11.48	50	1	170	1	0	0	0	0	0.0	HDTPA(4-) Lindsay
12671	20.89	50	2	170	1	0	0	0	0	0.0	H2DTPA(3-) Lindsay
12672	25.83	50	3	170	1	0	0	0	0	0.0	H3DTPA(2-) Lindsay
12673	28.92	50	4	170	1	0	0	0	0	0.0	H4DTPA(-) Lindsay
12674	30.96	50	5	170	1	0	0	0	0	0.0	H5DTPA Lindsay
12700	9.24	50	1	148	1	0	0	0	0	-3.2300	H3BO3, B/M
12701	9.11	50	1	148	2	0	0	0	0	-1.8600	B2O(OH)5(-), B/M
12702	20.68	50	1	148	3	0	0	0	0	-10.2900	B3O3(OH)4(-),B/M
12703	20.66	50	1	148	4	0	0	0	0	-19.9200	B4O5(OH)4(2-)

A.11

12705	8.83	50	1	148	1	104	1	0	0	-1.3800	BFx(OH)3-x(-),W2
12706	16.87	50	2	148	1	104	2	0	0	-1.6000	W2
12707	22.91	50	3	148	1	104	3	0	0	-4.8100	W2
12708	29.52	50	4	148	1	104	4	0	0	-5.0200	W2
12710	13.09	50	1	112	1	0	0	0	0	-4.6400	H3SiO4, gap, 9/82
12720	22.92	50	2	112	1	0	0	0	0	-10.7580	H4SiO4, gap
12722	53.10	50	6	112	1	104	6	0	0	-27.0180	SiF6, W2
13520	4.30	50	1	152	1	0	0	0	0	0.0000	??
13530	3.70	50	1	153	1	0	0	0	0	0.0000	??
13540	11.50	50	1	154	1	0	0	0	0	0.0	HAsO42-,B/M
13541	18.46	50	2	154	1	0	0	0	0	0.0	H2AsO4-,B/M
13542	20.70	50	3	154	1	0	0	0	0	0.0	H3AsO4, B/M
13551	28.42	162	1	50	4	0	0	0	0	0.0000	??
13553	25.15	162	1	50	3	0	0	0	0	0.0000	??
13555	21.33	162	1	50	2	0	0	0	0	0.0000	??
13557	13.27	162	1	50	1	0	0	0	0	0.0000	??
13561	-5.67	163	1	50	-1	0	0	0	0	0.0000	??
13565	-2.26	164	1	50	-1	0	0	0	0	0.0000	??
13567	-5.85	164	1	50	-2	0	0	0	0	0.0000	??
13569	-10.98	164	1	50	-3	0	0	0	0	0.0000	??
13570	8.50	50	1	156	1	0	0	0	0	0.0000	??
13580	11.20	50	2	156	1	0	0	0	0	0.0000	??
13595	-13.99	50	-1	0	0	0	0	0	0	13.3380	OH-, Robie
8		following are type III									
15000	13.01	6	1	7	-1	99	1	0	0	-9.7000	Fe(3)/Fe(2), Robie
15010	31.60	17	1	16	-1	99	1	0	0	0.0000	Co(3)/Co(2)
15020	-5.10	27	1	26	-1	99	2	0	0	0.0000	Sn(IV)/Sn(II)
15030	2.70	9	1	33	-1	99	1	0	0	0.0000	Cu(2)/Cu(l)
15040	20.72	102	1	108	-1	50	8	99	8	-48.0520	SO4/S2-, Robie
15050	9.22	32	1	50	4	99	2	36	-1	0.0000	
15060	45.36	162	1	163	-1	50	6	99	1	0.0000	
15070	51.07	162	1	164	-1	50	99	2	0	0.0000	
0		TYPE IV: No solids or gases autoclassified TYPE IV									
0		TYPE V: No solids or gases autoclassified. TYPE V									
217		TYPE VI: All solids & gases autoclassified TYPE VI									
20000	8.48	1	1	101	1	0	0	0	0	2.2970	Calcite, pb82
20002	8.34	1	1	101	1	0	0	0	0	2.5900	Aragonite, pb82
20010	4.32	1	1	102	1	0	0	0	0	0.2700	Gypsum, Robie sign H?
20012	4.12	1	1	102	1	0	0	0	0	4.3000	Anhydrite, Robie
20020	10.96	1	1	104	2	0	0	0	0	-4.7100	Fluorite, Robie
20028	18.87	1	1	109	1	50	1	0	0	0.0000	Brushite, Garrels
20029	19.24	1	1	109	1	50	1	0	0	0.0000	Monetite, VT84
20030	57.54	1	5	50	-1	109	3	0	0	0.0000	OH-apa, VT84, Bell
20035	59.74	1	5	104	1	109	3	0	0	0.0000	F-apa, VT84
20040	48.20	1	4	50	1	109	3	0	0	0.0000	
20050	19.30	1	1	50	1	109	1	0	0	0.0000	
20070	8.70	1	1	112	1	0	0	0	0	0.0000	
20100	7.40	1	1	152	1	0	0	0	0	0.0000	
20110	22.90	1	3	154	2	0	0	0	0	0.0000	
20120	5.50	1	3	154	2	0	0	0	0	0.0000	
20130	-22.68	1	1	50	-2	0	0	0	0	34.9920	Portlandite, Robie
20140	8.20	2	1	101	1	0	0	0	0	7.3400	Magnesite, Rbie
20142	5.17	2	1	101	1	0	0	0	0	-13.5700	Nesquehonite, Rbie
20143	-9.59	2	2	101	1	50	-2	0	0	-3.7300	Artinite, Rbie
20144	9.72	2	5	101	4	50	-2	0	0	19.3400	Hydromagnes, Robie
20145	17.02	2	1	1	1	101	2	0	0	8.2900	Dolomite, PHR

A.12

20146	-41.62	2	3	1	1	101	4	0	0	29.2400	Huntite, Rbie
20148	2.14	2	1	102	1	0	0	0	0	-2.8200	Epsomite, W2
20150	8.00	2	1	104	2	0	0	0	0	0.0000	
20160	28.40	2	3	109	2	0	0	0	0	0.0000	
20180	24.40	2	3	154	2	0	0	0	0	0.0000	
20190	4.90	2	1	156	1	0	0	0	0	0.0000	
20200	-16.76	2	1	50	-2	0	0	0	0	14.3300	Brucite, Robie
20210	9.27	3	1	101	1	0	0	0	0	0.0	SrCO3(c), P/B
20220	6.50	3	1	102	1	0	0	0	0	0.5	SrSO4(c) S/M
20230	8.60	3	1	104	2	0	0	0	0	0.0	
20240	2.40	3	1	112	1	0	0	0	0	0.0	
20260	22.80	3	3	154	2	0	0	0	0	0.0	
20270	6.10	3	1	156	1	0	0	0	0	0.0	
20280	25.80	6	1	109	1	0	0	0	0	0.0	
20290	21.70	6	1	154	1	0	0	0	0	0.0	Scorodite, Rmstidt
20300	31.60	6	2	156	3	0	0	0	0	0.0	
20305	8.77	6	3	50	-8	99	1	0	0	41.3700	Magnetite, Robie
20310	-2.71	6	1	50	-3	0	0	0	0	0.0	Fe(OH)3am, gap
20312	1.68	6	1	50	-3	0	0	0	0	14.5400	Goethite, Robie
20313	3.84	6	2	50	-6	0	0	0	0	31.0350	Hematite, Robie
20314	11.20	6	3	50	-6	5	1	102	1	36.1800	Na-jarosite, W2
20316	14.80	6	3	50	-6	4	1	102	1	31.2800	K-jarosite, W2
20318	12.10	6	3	50	-5	102	1	0	0	55.1500	H-jarosite, W2
20320	10.50	7	1	101	1	0	0	0	0	6.9900	FeCO3(c), Robie
20330	16.83	7	1	108	1	0	0	0	0	-10.2600	ppt FeS, B67
20331	17.56	7	1	108	1	0	0	0	0	-11.3700	Mackinawite, B67
20332	18.96	7	1	108	1	0	0	0	0	-10.7220	Pyrrhotite, B67
20338	44.32	7	1	108	2	99	-2	0	0	-35.4800	Pyrite, Robie
20335	69.57	7	3	108	4	99	-2	0	0	-44.7840	Greigite, B67
20340	33.30	7	3	109	2	0	0	0	0	0.0	
20350	16.40	7	1	112	1	0	0	0	0	0.0	
20360	-12.10	7	1	50	-2	0	0	0	0	0.	Fe(OH)2, B/M
20365	-13.82	7	1	99	2	0	0	0	0	21.295	Fe metal, Robie
20370	9.30	8	1	101	1	0	0	0	0	0.0	S/M MnCO3(c)
20380	14.80	8	1	108	1	0	0	0	0	0.0	
20400	10.70	8	1	112	1	0	0	0	0	0.0	
20410	29.60	8	3	154	2	0	0	0	0	0.0	
20420	7.30	8	1	156	1	0	0	0	0	0.0	
20430	-15.20	8	1	50	-2	0	0	0	0	0.0	B/M, Mn(OH)2(ppt)
20440	5.92	9	2	50	-2	101	1	0	0	0.0	malachite, gap see lotus
20441	18.32	9	3	50	-2	101	2	0	0	0.0	azurite, gap see lotus
20450	38.30	9	1	108	1	0	0	0	0	0.0	
20460	37.70	9	3	109	2	0	0	0	0	0.0	
20480	39.80	9	3	154	2	0	0	0	0	0.0	
20490	7.70	9	1	156	1	0	0	0	0	0.0	
20500	-7.62	9	1	50	-2	0	0	0	0	0.0	CuO(c) B/M gap
20501	-10.31	9	1	50	-2	0	0	0	0	0.0	Cu(OH)2(am) Gulens
20505	11.48	9	1	99	2	0	0	0	0	-15.48	Cu(2+)>Cu, Robie
20510	10.00	10	1	101	1	0	0	0	0	0.0	
20520	9.95	10	1	102	1	0	0	0	0	-6.281	Barite, Robie sign H?
20530	6.10	10	1	104	2	0	0	0	0	0.0	
20550	54.80	10	3	154	2	0	0	0	0	0.0	
20560	6.60	10	1	156	1	0	0	0	0	0.0	
20570	12.00	11	1	101	1	0	0	0	0	0.0	Stipp
20580	27.80	11	1	108	1	0	0	0	0	0.0	
20600	37.40	11	3	154	2	0	0	0	0	0.0	

20610	8.30	11	1	156	1	0	0	0	0	0.0	
20620	-13.65	11	1	50	-2	0	0	0	0	0.0	beta-Cd(OH)2 B/M?
20630	10.80	12	1	101	1	0	0	0	0	0.0	
20640	23.00	12	1	108	1	0	0	0	0	0.0	
20650	36.70	12	3	109	2	0	0	0	0	0.0	
20660	18.50	12	1	112	1	0	0	0	0	0.0	
20680	27.90	12	3	154	2	0	0	0	0	0.0	
20690	7.70	12	1	156	1	0	0	0	0	0.0	
20700	-11.14	12	1	50	-2	0	0	0	0	0.0	Zn(OH)2, B/M
20705	-15.11	12	2	50	-3	103	1	0	0	0.0	Zn2(OH)3Cl B/M
20710	8.20	13	1	101	1	0	0	0	0	0.0	
20720	22.90	13	1	108	1	0	0	0	0	0.0	
20730	30.20	13	3	154	2	0	0	0	0	0.0	
20740	5.30	13	1	156	1	0	0	0	0	0.0	
20750	-10-80	13	1	50	-2	0	0	0	0	0.0000	Ni(OH)2 B/M
20760	53.70	14	1	108	1	0	0	0	0	0.0	
20770	-1.87	14	1	50	-2	0	0	0	0	0.0	
20780	13.35	15	1	101	1	0	0	0	0	0.0000	PbCO3, Bilinski
20790	19.34	15	3	50	-2	101	2	0	0	0.0000	Pb3(OH)2(CO3)2
20800	7.70	15	1	102	1	0	0	0	0	0.0	
20810	7.60	15	1	104	2	0	0	0	0	0.0	
20820	27.90	15	1	108	1	0	0	0	0	0.0	
20830	12.60	15	1	50	1	109	1	0	0	0.0	
20840	43.00	15	3	109	2	0	0	0	0	0.0	
20850	60.90	15	5	50	-1	109	3	0	0	0.0	
20860	3.50	15	2	50	-2	112	1	0	0	0.0	
20880	13.00	15	1	152	1	0	0	0	0	0.0	
20890	36.30	15	3	154	2	0	0	0	0	0.0	
20900	11.50	15	1	156	1	0	0	0	0	0.0	
20910	-12.72	15	1	50	-2	0	0	0	0	0.0000	PbO(red) B/M
20920	10.12	16	1	101	1	0	0	0	0	4.6000	Naumov
20921	9.98	16	1	101	1	0	0	0	0	4.6000	S/M
20930	24.30	16	1	108	1	0	0	0	0	0.0	
20940	32.80	16	3	154	2	0	0	0	0	0.0	
20950	7.10	16	1	156	1	0	0	0	0	0.0	
20960	-12.28	16	1	50	-2	0	0	0	0	21.5500	inactpink,B/M
20962	-13.78	16	1	50	-2	0	0	0	0	0.0	act blue,B/M
20970	3.70	17	1	50	-3	0	0	0	0	0.0	
20980	10.90	18	2	101	1	0	0	0	0	0.0	
20990	4.90	18	2	102	1	0	0	0	0	0.0	
21000	9.90	18	1	103	1	0	0	0	0	0.0	
21010	12.30	18	1	105	1	0	0	0	0	0.0	
21020	15.90	18	1	106	1	0	0	0	0	0.0	
21030	51.40	18	2	108	1	0	0	0	0	0.0	
21040	16.00	18	3	109	1	0	0	0	0	0.0	
21080	11.40	18	2	152	1	0	0	0	0	0.0	
21090	11.20	18	2	153	1	0	0	0	0	0.0	
21100	19.30	18	3	154	1	0	0	0	0	0.0	
21110	14.90	18	2	156	1	0	0	0	0	0.0	
21120	-6.30	18	1	50	-1	0	0	0	0	0.0	
21130	20.90	19	1	154	1	0	0	0	0	0.0	
21140	-9.60	19	1	50	-3	0	0	0	0	0.0	
21150	22.50	20	1	109	1	0	0	0	0	0.0	
21142	5.17	20	1	4	1	102	1	0	0	-7.2200	alum, W2
21170	16.60	20	1	154	1	0	0	0	0	0.0	
21180	-8.11	20	1	50	-3	0	0	0	0	22.8	Gibbs, DKN1984

A.14

21181	-9.35	20	1	50	-3	0	0	0	0	22.8	Hem, Gibbs, DKN
21182	-10.80	20	1	50	-3	0	0	0	0	22.8	Amorph, DKN
21190	11.23	20	2	50	-3	109	1	0	0	0.0	Augelite, Vie
21192	30.45	20	3	50	-3	109	2	0	0	0.0	Wavellite, Vie
21200	21.45	20	3	50	-5	109	2	1	1	0.0	Crandall, Vie
21202	19.03	20	1	109	1	0	0	0	0	0.0	Variscite, Vie
21220	0.74	25	1	50	-2	0	0	0	0	0.0	am-Ti02 B/M edttd
21221	2.14	25	1	50	-2	0	0	0	0	0.0	rutile, Capi
21222	1.89	25	1	50	-2	0	0	0	0	0.0	anatase, Capi
21225	-16.10	25	1	50	-4	1	1	0	0	0.0	a-perovskite, Capi
21226	-15.91	25	1	50	-4	1	1	0	0	0.0	b-perovskite, Capi
21227	-15.79	25	1	50	-2	1	1	112	1	0.0	sphene, Capi
21228	-7.80	25	1	50	-4	7	1	0	0	0.0	ilmenite, Capi
21230	19.33	25	1	50	1	109	1	0	0	0.0	TiHPO4, Einaga
21240	0.40	26	1	50	-2	0	0	0	0	0.0	
21250	1.00	27	1	50	-4	0	0	0	0	0.0	
21320	11.10	29	2	108	3	0	0	0	0	0.0	
21330	22.10	29	1	109	1	0	0	0	0	0.0	
21340	25.30	29	2	156	3	0	0	0	0	0.0	
21350	-21.00	29	1	50	-3	0	0	0	0	0.0	
21360	31.60	30	1	50	-1	0	0	0	0	0.0	
21370	20.50	31	1	156	2	0	0	0	0	0.0	
21380	-44.40	31	1	50	-4	0	0	0	0	0.0	
21385	-5.55	32	1	50	-2	0	0	0	0	0.0000	schoep??, vjthesis
21388	-5.40	32	1	50	-2	0	0	0	0	12.0450	schoep, Langmuir
21392	13.86	32	1	99	2	0	0	0	0	0.0	uraninite
21393	53.15	32	2	1	1	155	2	0	0	0.0	tyuyammite
21395	14.11	32	1	101	1	0	0	0	0	1.4400	UO2CO3, vj thesis
21396	24.38	32	1	101	3	5	4	0	0	0.0000	Na4UO2(CO3)3 OW83
21397	28.36	32	2	1	1	112	2	0	0	0.0	uranophane
21398	56.55	32	2	4	2	155	2	0	0	0.0	
21399	48.61	32	2	1	1	109	2	0	0	0.0	
21400	51.32	32	2	4	2	109	2	0	0	0.0	
21401	50.16	32	2	5	2	109	2	0	0	0.0	
21402	48.09	32	2	50	2	109	2	0	0	0.0	
21403	70.31	32	2	50	2	107	2	109	2	0.0	
21404	47.58	32	2	2	1	109	2	0	0	0.0	
21405	46.00	32	2	7	1	109	2	0	0	0.0	
21406	33.77	32	2	9	1	109	2	0	0	0.0	
21407	33.11	32	2	15	1	109	2	0	0	0.0	
21408	48.31	32	2	3	1	109	2	0	0	0.0	
21409	67.14	32	2	10	1	109	2	0	0	0.0	
21410	25.00	32	1	50	1	109	1	0	0	0.0	vj thesis
21411	50.96	32	3	109	2	0	0	0	0	0.0	vj thesis
21413	-4.82	36	1	50	-4	0	0	0	0	0.0	
21414	4.63	36	1	50	-4	0	0	0	0	0.0	
21415	-21.05	36	3	50	-16	99	-4	0	0	0.0	
21418	54.12	36	1	1	1	109	2	0	0	0.0	
21420	51.50	36	1	50	2	109	2	0	0	0.0	
21422	18.50	36	1	104	4	0	0	0	0	0.0	
21424	27.58	36	1	104	4	0	0	0	0	0.0	
21470	-42.00	8	1	50	-4	99	-2	0	0	0.0	
21480	-61.70	8	3	50	-8	99	1	0	0	0.0	
21490	-25.70	8	1	50	-3	99	-1	0	0	0.0	
21500	-49.20	15	1	50	-4	99	-2	0	0	0.0	
21520	28.70	14	1	99	2	0	0	0	0	0.0	

21417	51.50	36	1	50	2	109	2	0	0	0.0	
21530	15.03	108	1	99	-2	0	0	0	0	7.8870	S(2-)>S(0),Robie
21550	82.15	162	2	50	8	99	2	0	0	0.0	
21570	58.33	162	2	50	6	0	0	0	0	0.0	
23900	26.92	50	2	112	1	0	0	0	0	-17.3080	Quartz, gap
23901	25.66	50	2	112	1	0	0	0	0	-14.2260	Amorph, gap
23902	26.65	50	2	112	1	0	0	0	0	-16.9400	Chalcedony, gap
23904	26.37	50	2	112	1	0	0	0	0	-16.4130	Cristobalite, gap
24000	16.29	20	2	1	3	112	3	50	-6	70.5560	Grossular, HH78
24001	24.62	20	3	1	2	112	3	50	-7	75.2180	Clinozoisite
24200	38.58	5	1	20	1	112	2	0	0	-0.2090	Analcime, HH78
24201	77.42	1	1	20	2	112	4	0	0	2.5670	Laumontite, HH78
24202	73.01	1	1	20	2	112	4	0	0	15.2680	Wairakite, HH78
24299	64.56	20	1	5	1	112	3	50	2	-15.0490	
24300	65.68	20	1	5	1	112	3	50	2	-17.6820	Albite, HH78
24301	68.72	20	1	4	1	112	3	50	2	-24.3500	K-Spar, HH78
24305	18.66	20	1	1	1	112	2	50	-4	49.7310	Anorthite, HH78
24310	467.24	20	14	1	1	112	22	0	0	0.0000	Ca-montmo, Vie
24311	870.5	20	22	1	3	112	60	2	11	0.0000	Ca,Mg-SAz-1, M&S
24400	38.21	20	2	50	-2	112	2	0	0	13.862	Kaolin2 Vie
24401	40.23	20	2	50	-2	112	2	0	0	11.3550	KaolinlHRK
24402	34.29	20	2	50	-2	112	2	0	0	11.3550	Halloysite, HRK
24410	54.23	4	1	20	3	112	3	50	-4	24.5140	Muscovite, HH78
24450	106.50	2	4	50	4	112	6	0	0	-18.1630	Sepiolite, HH78
24460	24.76	2	1	1	1	112	2	0	0	25.94	Diopside, HH78
24470	14.28	2	3	50	-2	112	2	0	0	27.42	Chrysotile, HH78
24999	83.12	50	-4	99	-4	0	0	0	0	-136.6300	Oxygen gas, Robie
25000	18.14	50	2	101	1	0	0	0	0	-0.9620	CO2 gas, PB82

Conventions:
logK and delta H for aqueous complexes retain sign formation reaction
logK and delta H for solids: reverse sign found for dissolution reaction!!!

References and Sources of Data:

Bil   Bilinski and Schindler, GCA 46,921-928
Bond   Bond/Hefter IUPAC # 27 1980
B67   Berner, 1967 NOT checked to see that Ka for H2S is consistent
         Enthalpies estimated, see W2THRM binder
B/M   BAES, C.F., AND MESMER, R.E.(1976) HYDROLYSIS OF
         CATIONS, WILEY-INTERSCIENCE, NEW YORK
         CAUTION!!! symbol "<" means B/M say "less than"
Capi   if Ti cmpd, then Capi's estimates;
         if phosphates, then Viellard Am Min 64 626 (1979)
Chris   Christensen/Izatt Handbook of metal ligand heats, 1983 for CaPhos cpxs, two agree with phr
Einaga   Einaga/Komatsu J. Inorg Nucl Chem 43 2449 1981
gap   G.A. Parks evaluated and selected from several sources, see W2THRM binder
Henly   Henly et al., Fluid Mineral Equilibria, 1984
HRK   Hemingway, B.S., Robie, R.A., AND Kittrick, J.A.,
         REVISED VALUES FOR THE GIBBS FREE ENERGY OF FORMATION
         OF [AL(OH)4-](AQ), DIASPORE, BOEHMITE, AND BAYERITE AT
         298.15 K AND 1 BAR, THE THERMODYNAMIC PROPERTIES OF

          KAOLINITE, ...ETC., G.C.A., v42, P 1533-1543, 1978 HRK kaolin agrees with
HH78   Helgeson, H.A., Delaney, J.M., Nesbitt, H.W., and Bird, D.K. SUMMARY AND CRITIQUE OF THE
THERMODYNAMIC PROPERTIES OF ROCK-FORMING MINERALS, AM. J. SCI., v278A, ppl-229, 1978
Marcus Marcus and Maydan 1962/63, cf Sillen 62Mn/63/Me, chosen because agrees
          well with extrap from high t by Ruaya/Seward GCA 1986
          If enthalpy given, frm Ruaya/Seward
NEA   Grenthe, I., J. Fuger, R. J. M. Konings, R. J. Lemire, A. B. Muller, C. Nguyen-Trung, and H. Wanner. 1992.
          Chemical Thermodynamics Series, Volume 1: Chemical Thermodynamics of Uranium. eds. Wanner, H. and I.
          Forest, North-Holland, Elsevier Science Publishing Company, Inc., New York, New York.
OW83   Tentative. Obrien and Williams, 1983, Min.Mag quoting Blake for Ks but using vj's stability const
          for UO2(CO3)3 cpx, see OW reprint for calcs.

PB82   Plummer and Busenberg, 1982, GCA
P/B   For Sr: Busenberg et al. GCA 48,2021,1984
PHR   PARKHURST, D.L., THORSTENSON, D.C., AND PLUMMER, L.N.
          (1980) PHREEQE - A COMPUTER PROGRAM FOR GEOCHEMICAL
          CALCULATIONS, USGS, WATER RESOURCES INVESTIGATIONS, 80-96
Robie   ROBIE, R.A., HEMINGWAY, B.S., AND FISHER, J.R. (1978)
          THERMODYNAMIC PROPERTIES OF MINERALS AND RELATED SUB
          SUBSTANCES AT 298.15 K AND 1 BAR PRESSURE AND AT
          HIGHER TEMPERATURES, USGS BULL. 1452
S/M   SMITH AND MARTELL (   )
W2   Ball/Jenne/Nordstrom, 1979, WATEQ2
          AND BALL/NORDSTROM/ (1980),
          ADDITIONAL AND REVISED THERMOCHEMICAL DATA AND COMPUTER
          CODE FOR WATEQ2- A COMPUTERIZED CHEMICAL MODEL FOR
          TRACE AND MAJOR ELEMENT SPECIATION AND MINERAL
          EQUILIBRIA OF NATURAL WATERS, U.S.G.S. WATER SUPPLY
          INVESTIGATIONS 78-116 (AN OPEN FILE REPORT, 109PP)
Vie   directly from Viellard (see Capi) editted for MNQL with my Ka values from this compilation
vj   Vijay Tripathi, Dissertation
VT84   Vieillard and Tardy (1984) in Nriagu and Moore, PHOSPHATE MINERALS pl7lff.

??   Source not identified in original database.

References for data added by authors

Cantrell, K. J. 1988. Actinide(III) Carbonate Complexation. *Polyhedron*, 7(7), 573-574.

Falck, W. E. 1992. *CHEM/VAL Project: Critical Evaluation of the CHEM/VAL Thermodynamic Database for the
Aqueous Species, Gases, and Solids Containing Chromium, Mercury, Selenium, and Thallium*. Report prepared for the
U.S. Environmental Protection Agency the Pacific Northwest Laboratory, Richland, Washington.

Felmy, A. R., Rai, D., and R. W. Fulton. 1990. The Solubility of AmOHCO3 and the Aqueous Thermodynamics of
the System Na+ - Am3+ - HCO3- - CO32- - OH- - H2O. *Radiochim. Acta*, 50, 193-204.

KC   Various sources including S/M and analog estimates.

Lemire, R. J. and P. R. Tremaine. 1980. Uranium and Plutonium Equilibria in Aqueous Solutions to 200 C. *J. of Chem. Eng. Data*, 25, 361-370.

Lindsay, W. L. 1979. Chemical Equilibria in Soils.

Morel, F. M. M. 1983. Principals of Aquatic Chemistry.

Read, D. (ed.). 1991. *CHEM/VAL Project. Report on Stages 3 and 4, Testing of Coupled Chemical Transport Models*. Commission of the European Communities, Topical Report No. EUR13675EN, Luxembourg.

Rai, D., R. G. Strickert, D. A. Moore, and J. L. Ryan. 1983. Am(III) Hydrolysis Constants and Solubility of Am(III) Hydroxide. *Radiochim. Acta*, 33, 201-206.

Schwab, A. and A. Felmy. 1982. Review and Reevaluation of Pu Thermodynamic Data, PNL-SA-10731 (Draft Manuscript), Pacific Northwest Laboratory, Richland, Washington.

Appendix B

Kd Values [mL/g] as a Function of pH for Batch Adsorption Experiments

IOCS is iron coated sand. See Table 3.4 for other soil descriptions.

Metal Conc.	Kd (metal)	Ligand Conc.	Kd (ligand)	Adsorbent	pH
10e-5 Ni	0.0	0.0	-	1.2% IOCS	4.40
10e-5 Ni	8.5	0.0	-	1.2% IOCS	5.78
10e-5 Ni	35.8	0.0	-	1.2% IOCS	6.58
10e-5 Ni	379.3	0.0	-	1.2% IOCS	7.13
10e-5 Ni	2531.5	0.0	-	1.2% IOCS	8.13
10e-5 Ni	6975.6	0.0	-	1.2% IOCS	10.12
10e-5 Ni	1.7	10e-3 Pic	10.1	1.2% IOCS	3.90
10e-5 Ni	4.1	10e-3 Pic	8.3	1.2% IOCS	3.92
10e-5 Ni	0.0	10e-3 Pic	9.3	1.2% IOCS	5.05
10e-5 Ni	0.0	10e-3 Pic	11.0	1.2% IOCS	5.10
10e-5 Ni	0.0	10e-3 Pic	7.3	1.2% IOCS	6.33
10e-5 Ni	0.0	10e-3 Pic	7.4	1.2% IOCS	6.43
10e-5 Ni	0.0	10e-3 Pic	0.0	1.2% IOCS	7.85
10e-5 Ni	0.0	10e-3 Pic	0.0	1.2% IOCS	7.85
10e-5 Ni	0.0	10e-3 Pic	0.0	1.2% IOCS	8.51
10e-5 Ni	0.0	10e-3 Pic	13.2	1.2% IOCS	8.57
10e-5 Ni	0.0	10e-3 Pic	7.5	1.2% IOCS	9.65
	0.0	10e-3 Pic	1.5	1.2% IOCS	9.73
10e-5 Ni	11.8	10e-4 Pic	53.3	1.2% IOCS	4.52
10e-5 Ni	7.5	10e-4 Pic	58	1.2% IOCS	4.53
10e-5 Ni	0	10e-4 Pic	50.6	1.2% IOCS	5.91
10e-5 Ni	6.7	10e-4 Pic	25.9	1.2% IOCS	6.26
10e-5 Ni	3.5	10e-4 Pic	8.4	1.2% IOCS	6.67
10e-5 Ni	9.3	10e-4 Pic	21.1	1.2% IOCS	6.78
10e-5 Ni	9.5	10e-4 Pic	9.3	1.2% IOCS	7.33
10e-5 Ni	6.5	10e-4 Pic	0.5	1.2% IOCS	7.36
10e-5 Ni	2.6	10e-4 Pic	0	1.2% IOCS	8.06
10e-5 Ni	1.2	10e-4 Pic	0	1.2% IOCS	8.14
10e-5 Ni	24.2	10e-4 Pic	0	1.2% IOCS	10.04
10e-5 Ni	14.9	10e-4 Pic	0	1.2% IOCS	10.84
10e-5 Ni	6.9	10e-5 Pic	206.0	1.2% IOCS	4.39
10e-5 Ni	14.6	10e-5 Pic	29.0	1.2% IOCS	6.26
10e-5 Ni	37.3	10e-5 Pic	15.2	1.2% IOCS	6.70
10e-5 Ni	57.3	10e-5 Pic	17.6	1.2% IOCS	7.06
10e-5 Ni	151.7	10e-5 Pic	15.5	1.2% IOCS	8.20
10e-5 Ni	2539.3	10e-5 Pic	25.7	1.2% IOCS	10.12
10e-5 Ni	92039.1	10e-3 Pic	1186.7	Milford Soil	4.24
10e-5 Ni	2415456.7	10e-3 Pic	943.5	Milford Soil	4.26

Metal Conc.	Kd (metal)	Ligand Conc.	Kd (ligand)	Adsorbent	pH
10e-5 Ni	20359.5	10e-3 Pic	989.8	Milford Soil	4.84
10e-5 Ni	20559.7	10e-3 Pic	830.0	Milford Soil	4.91
10e-5 Ni	2506.0	10e-3 Pic	542.1	Milford Soil	6.24
10e-5 Ni	3836.5	10e-3 Pic	562.5	Milford Soil	6.34
10e-5 Ni	82.1	10e-3 Pic	62.3	Milford Soil	6.38
10e-5 Ni	506.4	10e-3 Pic	273.4	Milford Soil	6.39
10e-5 Ni	30.5	10e-3 Pic	20.6	Milford Soil	6.96
10e-5 Ni	31.1	10e-3 Pic	22.9	Milford Soil	6.97
10e-5 Ni	22.6	10e-3 Pic	18.6	Milford Soil	6.98
10e-5 Ni	18.4	10e-3 Pic	15.6	Milford Soil	6.98
10e-5 Ni	17.1	10e-3 Pic	11.7	Milford Soil	7.46
10e-5 Ni	18.8	10e-3 Pic	10.8	Milford Soil	7.51
10e-5 Ni	13.9	10e-3 Pic	10.6	Milford Soil	7.56
10e-5 Ni	9.9	10e-3 Pic	3.9	Milford Soil	7.67
10e-5 Ni	12.6	10e-3 Pic	6.9	Milford Soil	7.77
10e-5 Ni	12.2	10e-3 Pic	3.2	Milford Soil	7.86
10e-5 Ni	10.4	10e-3 Pic	3.9	Milford Soil	7.95
10e-5 Ni	7.3	10e-3 Pic	0.0	Milford Soil	7.98
10e-5 Ni	16.2	10e-3 Pic	3.2	Milford Soil	8.13
10e-5 Ni	9.6	10e-5 Pic	11.9	Milford Soil	4.11
10e-5 Ni	17.7	10e-5 Pic	1.1	Milford Soil	4.19
10e-5 Ni	7.5	10e-5 Pic	4.4	Milford Soil	5.16
10e-5 Ni	7.9	10e-5 Pic	6.8	Milford Soil	5.17
10e-5 Ni	13.7	10e-5 Pic	7.5	Milford Soil	6.47
10e-5 Ni	1.8	10e-5 Pic	1.2	Milford Soil	6.47
10e-5 Ni	1.3	10e-5 Pic	0.0	Milford Soil	7.97
10e-5 Ni	12.1	10e-5 Pic	2.1	Milford Soil	8.14
10e-5 Ni	9.2	10e-5 Pic	10.2	Milford Soil	8.48
10e-5 Ni	1.0	10e-5 Pic	0.0	Milford Soil	8.62
10e-5 Ni	3.9	10e-5 Pic	0.5	Milford Soil	9.43
10e-5 Ni	12.7	10e-5 Pic	0.0	Milford Soil	9.64
10e-5 Ni	92039.1	10e-5 EDTA	1186.7	1.2% IOCS	4.24
10e-5 Ni	2415456.7	10e-5 EDTA	943.5	1.2% IOCS	4.26
10e-5 Ni	20359.5	10e-5 EDTA	989.8	1.2% IOCS	4.84
10e-5 Ni	20559.7	10e-5 EDTA	830.0	1.2% IOCS	4.91
10e-5 Ni	2506.0	10e-5 EDTA	542.1	1.2% IOCS	6.24
10e-5 Ni	3836.5	10e-5 EDTA	562.5	1.2% IOCS	6.34
10e-5 Ni	82.1	10e-5 EDTA	62.3	1.2% IOCS	6.38
10e-5 Ni	506.4	10e-5 EDTA	273.4	1.2% IOCS	6.39
10e-5 Ni	30.5	10e-5 EDTA	20.6	1.2% IOCS	6.96
10e-5 Ni	31.1	10e-5 EDTA	22.9	1.2% IOCS	6.97
10e-5 Ni	22.6	10e-5 EDTA	18.6	1.2% IOCS	6.98
10e-5 Ni	18.4	10e-5 EDTA	15.6	1.2% IOCS	6.98
10e-5 Ni	17.1	10e-5 EDTA	11.7	1.2% IOCS	7.46
10e-5 Ni	18.8	10e-5 EDTA	10.8	1.2% IOCS	7.51
10e-5 Ni	13.9	10e-5 EDTA	10.6	1.2% IOCS	7.56

B.2

Metal Conc.	Kd (metal)	Ligand Conc.	Kd (ligand)	Adsorbent	pH
10e-5 Ni	9.9	10e-5 EDTA	3.9	1.2% IOCS	7.67
10e-5 Ni	12.6	10e-5 EDTA	6.9	1.2% IOCS	7.77
10e-5 Ni	12.2	10e-5 EDTA	3.2	1.2% IOCS	7.86
10e-5 Ni	10.4	10e-5 EDTA	3.9	1.2% IOCS	7.95
10e-5 Ni	7.3	10e-5 EDTA	0.0	1.2% IOCS	7.98
10e-5 Ni	16.2	10e-5 EDTA	3.2	1.2% IOCS	8.13
10e-5 Ni	190.6	10e-5 EDTA	85.5	Milford Soil	4.51
10e-5 Ni	191.3	10e-5 EDTA	96.5	Milford Soil	4.56
10e-5 Ni	195.9	10e-5 EDTA	98.1	Milford Soil	4.97
10e-5 Ni	191.4	10e-5 EDTA	99.8	Milford Soil	4.98
10e-5 Ni	110.3	10e-5 EDTA	64.5	Milford Soil	5.59
10e-5 Ni	131.8	10e-5 EDTA	74.0	Milford Soil	5.64
10e-5 Ni	60.1	10e-5 EDTA	38.6	Milford Soil	5.86
10e-5 Ni	57.1	10e-5 EDTA	32.5	Milford Soil	5.97
10e-5 Ni	27.7	10e-5 EDTA	23.6	Milford Soil	6.75
10e-5 Ni	35.4	10e-5 EDTA	22.4	Milford Soil	6.78
10e-5 Ni	21.5	10e-5 EDTA	15.9	Milford Soil	6.85
10e-5 Ni	24.4	10e-5 EDTA	18.5	Milford Soil	6.89
10e-5 Ni	21.7	10e-5 EDTA	15.2	Milford Soil	6.97
10e-5 Ni	15.4	10e-5 EDTA	10.2	Milford Soil	6.98
10e-5 Ni	22.2	10e-5 EDTA	11.0	Milford Soil	7.00
10e-5 Ni	13.7	10e-5 EDTA	10.7	Milford Soil	7.02
10e-5 Ni	15.9	10e-5 EDTA	12.4	Milford Soil	7.95
10e-5 Ni	9.5	10e-5 EDTA	6.8	Milford Soil	7.96
10e-5 Ni	13.7	10e-5 EDTA	6.0	Milford Soil	7.98
10e-5 Ni	11.0	10e-5 EDTA	10.3	Milford Soil	8.11
10e-5 Ni	10.5	10e-5 EDTA	7.5	Milford Soil	8.85
10e-5 Ni	11.8	10e-5 EDTA	6.2	Milford Soil	9.03
10e-5 Ni	28.5	10e-5 EDTA	19.4	LK-1	4.03
10e-5 Ni	24.9	10e-5 EDTA	17.6	LK-1	4.34
10e-5 Ni	20.5	10e-5 EDTA	17.2	LK-1	4.42
10e-5 Ni	23.1	10e-5 EDTA	17.0	LK-1	4.56
10e-5 Ni	13.2	10e-5 EDTA	15.5	LK-1	5.20
10e-5 Ni	14.0	10e-5 EDTA	14.9	LK-1	5.22
10e-5 Ni	6.3	10e-5 EDTA	6.8	LK-1	5.63
10e-5 Ni	9.8	10e-5 EDTA	10.9	LK-1	5.74
10e-5 Ni	4.3	10e-5 EDTA	5.8	LK-1	6.25
10e-5 Ni	3.9	10e-5 EDTA	4.1	LK-1	6.32
10e-5 Ni	5.5	10e-5 EDTA	5.9	LK-1	6.36
10e-5 Ni	3.3	10e-5 EDTA	5.4	LK-1	6.37
10e-5 Ni	3.8	10e-5 EDTA	4.6	LK-1	6.39
10e-5 Ni	4.1	10e-5 EDTA	6.0	LK-1	6.40
10e-5 Ni	4.2	10e-5 EDTA	4.2	LK-1	6.45
10e-5 Ni	5.1	10e-5 EDTA	5.1	LK-1	6.53
10e-5 Ni	5.1	10e-5 EDTA	6.8	LK-1	6.61
10e-5 Ni	4.8	10e-5 EDTA	4.8	LK-1	6.75

B.3

Metal Conc.	Kd (metal)	Ligand Conc.	Kd (ligand)	Adsorbent	pH
10e-5 Ni	4.3	10e-5 EDTA	3.8	LK-1	7.01
10e-5 Ni	2.1	10e-5 EDTA	0.9	LK-1	8.02
10e-5 Ni	5.2	10e-5 EDTA	4.1	LK-1	8.14
10e-5 Ni	6.6	10e-5 EDTA	4.0	LK-1	8.15
10e-5 Ni	16915.2	10e-5 EDTA	423.8	MNC-7	4.13
10e-5 Ni	31158.4	10e-5 EDTA	574.9	MNC-7	4.20
10e-5 Ni	5308.0	10e-5 EDTA	514.4	MNC-7	4.76
10e-5 Ni	11088.7	10e-5 EDTA	575.1	MNC-7	4.76
10e-5 Ni	2649.3	10e-5 EDTA	493.1	MNC-7	4.99
10e-5 Ni	2481.1	10e-5 EDTA	516.4	MNC-7	5.12
10e-5 Ni	1399.4	10e-5 EDTA	386.9	MNC-7	5.62
10e-5 Ni	1142.7	10e-5 EDTA	371.7	MNC-7	5.71
10e-5 Ni	613.0	10e-5 EDTA	248.3	MNC-7	5.87
10e-5 Ni	491.2	10e-5 EDTA	268.4	MNC-7	5.91
10e-5 Ni	398.1	10e-5 EDTA	223.8	MNC-7	6.32
10e-5 Ni	294.6	10e-5 EDTA	175.2	MNC-7	6.36
10e-5 Ni	242.9	10e-5 EDTA	154.3	MNC-7	6.67
10e-5 Ni	284.9	10e-5 EDTA	160.1	MNC-7	6.73
10e-5 Ni	147.2	10e-5 EDTA	112.5	MNC-7	6.89
10e-5 Ni	154.2	10e-5 EDTA	117.9	MNC-7	6.92
10e-5 Ni	107.3	10e-5 EDTA	70.8	MNC-7	7.00
10e-5 Ni	132.5	10e-5 EDTA	89.0	MNC-7	7.06
10e-5 Ni	74.4	10e-5 EDTA	53.8	MNC-7	7.25
10e-5 Ni	53.3	10e-5 EDTA	28.4	MNC-7	7.26
10e-5 Ni	67.9	10e-5 EDTA	52.6	MNC-7	7.33
10e-5 Ni	40.1	10e-5 EDTA	23.0	MNC-7	7.56
10e-5 Sm	36.1	10e-5 Pic	974.8	1.2% IOCS	4.37
10e-5 Sm	35.5	10e-5 Pic	975.4	1.2% IOCS	4.38
10e-5 Sm	78.1	10e-5 Pic	451.2	1.2% IOCS	5.37
10e-5 Sm	105.6	10e-5 Pic	440.4	1.2% IOCS	5.53
10e-5 Sm	902.0	10e-5 Pic	139.3	1.2% IOCS	6.04
10e-5 Sm	968.1	10e-5 Pic	195.2	1.2% IOCS	6.06
10e-5 Sm	6923.0	10e-5 Pic	10.6	1.2% IOCS	7.89
10e-5 Sm	221151.0	10e-5 Pic	8.7	1.2% IOCS	8.01
10e-5 Sm	5121.4	10e-5 Pic	6.5	1.2% IOCS	8.45
10e-5 Sm	2895.9	10e-5 Pic	4.5	1.2% IOCS	8.57
10e-5 Sm	213428.5	10e-5 Pic	1.4	1.2% IOCS	9.48
10e-5 Sm	3535.4	10e-5 Pic	3.8	1.2% IOCS	9.67
10e-8 Sm	0.0	10e-5 Pic	58.3	Milford Soil	4.26
10e-8 Sm	4.9	10e-5 Pic	55.5	Milford Soil	4.20
10e-8 Sm	103.6	10e-5 Pic	65.3	Milford Soil	5.71
10e-8 Sm	296.4	10e-5 Pic	54.0	Milford Soil	5.85
10e-8 Sm	1993.0	10e-5 Pic	13.5	Milford Soil	7.24
10e-8 Sm	1411.4	10e-5 Pic	20.9	Milford Soil	7.27
10e-8 Sm	120.0	10e-5 Pic	0.0	Milford Soil	7.90
10e-8 Sm	115.3	10e-5 Pic	0.0	Milford Soil	7.92

B.4

Metal Conc.	Kd (metal)	Ligand Conc.	Kd (ligand)	Adsorbent	pH
10e-8 Sm	487.8	10e-5 Pic	0.0	Milford Soil	8.34
10e-8 Sm	1020.1	10e-5 Pic	0.0	Milford Soil	8.40
10e-8 Sm	2740.6	10e-5 Pic	0.0	Milford Soil	9.60
10e-8 Sm	5396.6	10e-5 Pic	0.0	Milford Soil	9.68
10e-5 Sm	166.4	10e-5 Pic	92.9	Milford Soil	4.84
10e-5 Sm	143.9	10e-5 Pic	113.7	Milford Soil	4.85
10e-5 Sm	194.9	10e-5 Pic	294.5	Milford Soil	5.73
10e-5 Sm	155.0	10e-5 Pic	505.0	Milford Soil	6.01
10e-5 Sm	51.7	10e-5 Pic	5583.0	Milford Soil	6.78
10e-5 Sm	41.9	10e-5 Pic	4291.6	Milford Soil	6.89
10e-5 Sm	5.4	10e-5 Pic	272368.7	Milford Soil	8.04
10e-5 Sm	0.0	10e-5 Pic	283270.0	Milford Soil	8.13
10e-5 Sm	1.2	10e-5 Pic	383.9	Milford Soil	8.74
10e-5 Sm	6.8	10e-5 Pic	362.3	Milford Soil	8.77
10e-5 Sm	1.9	10e-5 Pic	950.2	Milford Soil	9.85
10e-5 Sm	0.0	10e-5 Pic	1501.6	Milford Soil	9.91
10e-5 Th	22.3	10e-5 Pic	213.5	1.2% IOCS	4.25
10e-5 Th	32.1	10e-5 Pic	239.9	1.2% IOCS	4.27
10e-5 Th	74.6	10e-5 Pic	296.3	1.2% IOCS	5.12
10e-5 Th	86.1	10e-5 Pic	300.0	1.2% IOCS	5.14
10e-5 Th	85.0	10e-5 Pic	141.1	1.2% IOCS	6.18
10e-5 Th	88.7	10e-5 Pic	119.6	1.2% IOCS	6.24
10e-5 Th	770.8	10e-5 Pic	30.1	1.2% IOCS	7.92
10e-5 Th	611.6	10e-5 Pic	32.1	1.2% IOCS	8.06
10e-5 Th	1981.8	10e-5 Pic	21.7	1.2% IOCS	8.51
10e-5 Th	1373.3	10e-5 Pic	22.4	1.2% IOCS	8.65
10e-5 Th	3544.0	10e-5 Pic	22.2	1.2% IOCS	9.66
10e-5 Th	3844.5	10e-5 Pic	18.0	1.2% IOCS	9.71
10e-5 Th	201.0	10e-5 Pic	196.1	Milford Soil	4.63
10e-5 Th	202.3	10e-5 Pic	276.7	Milford Soil	4.70
10e-5 Th	146.4	10e-5 Pic	184.0	Milford Soil	5.70
10e-5 Th	128.7	10e-5 Pic	164.7	Milford Soil	5.75
10e-5 Th	1381.5	10e-5 Pic	136.9	Milford Soil	7.40
10e-5 Th	1449.2	10e-5 Pic	144.8	Milford Soil	7.46
10e-5 Th	1278.2	10e-5 Pic	40.7	Milford Soil	8.29
10e-5 Th	1671.5	10e-5 Pic	42.3	Milford Soil	8.40
10e-5 Th	633.2	10e-5 Pic	38.6	Milford Soil	8.84
10e-5 Th	1070.3	10e-5 Pic	35.2	Milford Soil	8.89
10e-5 Th	2601.5	10e-5 Pic	34.7	Milford Soil	10.09
10e-5 Th	3787.5	10e-5 Pic	38.6	Milford Soil	10.13
6.7x10e-7 Np	2.4	0.0	-	1.2% IOCS	4.12
6.7x10e-7 Np	1.1	0.0	-	1.2% IOCS	4.13
6.7x10e-7 Np	5.7	0.0	-	1.2% IOCS	5.10
6.7x10e-7 Np	6.4	0.0	-	1.2% IOCS	5.16
6.7x10e-7 Np	37.6	0.0	-	1.2% IOCS	6.14
6.7x10e-7 Np	43.3	0.0	-	1.2% IOCS	6.16

Metal Conc.	Kd (metal)	Ligand Conc.	Kd (ligand)	Adsorbent	pH
6.7x10e-7 Np	500.2	0.0	-	1.2% IOCS	7.85
6.7x10e-7 Np	1327.0	0.0	-	1.2% IOCS	7.93
6.7x10e-7 Np	969.8	0.0	-	1.2% IOCS	8.28
6.7x10e-7 Np	2551.7	0.0	-	1.2% IOCS	8.40
6.7x10e-7 Np	9348.3	0.0	-	1.2% IOCS	9.22
6.7x10e-7 Np	1963.8	0.0	-	1.2% IOCS	9.28
6.7x10e-7 Np	2.8	10e-5 Pic	1072.6	1.2% IOCS	4.09
6.7x10e-7 Np	3.0	10e-5 Pic	885.0	1.2% IOCS	4.15
6.7x10e-7 Np	10.5	10e-5 Pic	619.6	1.2% IOCS	4.94
6.7x10e-7 Np	9.8	10e-5 Pic	612.5	1.2% IOCS	5.30
6.7x10e-7 Np	13.6	10e-5 Pic	72.6	1.2% IOCS	6.16
6.7x10e-7 Np	36.7	10e-5 Pic	120.1	1.2% IOCS	6.16
6.7x10e-7 Np	658.4	10e-5 Pic	12.7	1.2% IOCS	7.67
6.7x10e-7 Np	696.0	10e-5 Pic	16.4	1.2% IOCS	7.89
6.7x10e-7 Np	2226.6	10e-5 Pic	5.3	1.2% IOCS	8.30
6.7x10e-7 Np	1775.2	10e-5 Pic	0.0	1.2% IOCS	8.32
6.7x10e-7 Np	9069.2	10e-5 Pic	3.9	1.2% IOCS	9.14
6.7x10e-7 Np	4874.8	10e-5 Pic	5.2	1.2% IOCS	9.26
6.7x10e-7 Np	1.8	0.0	-	Milford Soil	4.60
6.7x10e-7 Np	0.0	0.0	-	Milford Soil	4.61
6.7x10e-7 Np	2.6	0.0	-	Milford Soil	5.33
6.7x10e-7 Np	7.1	0.0	-	Milford Soil	5.67
6.7x10e-7 Np	21.1	0.0	-	Milford Soil	6.21
6.7x10e-7 Np	17.5	0.0	-	Milford Soil	6.31
6.7x10e-7 Np	122.2	0.0	-	Milford Soil	7.55
6.7x10e-7 Np	122.5	0.0	-	Milford Soil	7.62
6.7x10e-7 Np	248.3	0.0	-	Milford Soil	7.65
6.7x10e-7 Np	301.1	0.0	-	Milford Soil	7.79
6.7x10e-7 Np	748.0	0.0	-	Milford Soil	9.75
6.7x10e-7 Np	740.8	0.0	-	Milford Soil	9.76
6.7x10e-7 Np	0.1	10e-5 Pic	149	Milford Soil	4.63
6.7x10e-7 Np	0	10e-5 Pic	141.2	Milford Soil	4.73
6.7x10e-7 Np	5.8	10e-5 Pic	168.9	Milford Soil	5.61
6.7x10e-7 Np	9.4	10e-5 Pic	132.8	Milford Soil	5.84
6.7x10e-7 Np	15.4	10e-5 Pic	77.7	Milford Soil	6.3
6.7x10e-7 Np	16.7	10e-5 Pic	56.8	Milford Soil	6.35
6.7x10e-7 Np	107	10e-5 Pic	10.2	Milford Soil	7.45
6.7x10e-7 Np	121.3	10e-5 Pic	5.9	Milford Soil	7.48
6.7x10e-7 Np	209.3	10e-5 Pic	1.7	Milford Soil	7.98
6.7x10e-7 Np	217.1	10e-5 Pic	2.6	Milford Soil	8.05
6.7x10e-7 Np	567.5	10e-5 Pic	1.4	Milford Soil	9.76
6.7x10e-7 Np	559.4	10e-5 Pic	6	Milford Soil	9.85
10e-5 U	28.5	10e-3 Pic	7.4	1.2% IOCS	4.32
10e-5 U	37.8	10e-3 Pic	6.4	1.2% IOCS	4.35
10e-5 U	218.2	10e-3 Pic	9.4	1.2% IOCS	5.29
10e-5 U	242.2	10e-3 Pic	14.8	1.2% IOCS	5.30

Metal Conc.	Kd (metal)	Ligand Conc.	Kd (ligand)	Adsorbent	pH
10e-5 U	825.4	10e-3 Pic	0.0	1.2% IOCS	6.34
10e-5 U	609.5	10e-3 Pic	0.0	1.2% IOCS	6.37
10e-5 U	1385.6	10e-3 Pic	1.0	1.2% IOCS	6.82
10e-5 U	3323.5	10e-3 Pic	0.0	1.2% IOCS	6.83
10e-5 U	4527.1	10e-3 Pic	0.0	1.2% IOCS	7.30
10e-5 U	5379.7	10e-3 Pic	0.0	1.2% IOCS	7.38
10e-5 U	3772.2	10e-3 Pic	0.0	1.2% IOCS	7.68
10e-5 U	2468.8	10e-3 Pic	0.0	1.2% IOCS	7.92
10e-5 U	33.9	10e-3 Pic	4.6	Milford Soil	4.16
10e-5 U	40.1	10e-3 Pic	0.0	Milford Soil	4.33
10e-5 U	64.4	10e-3 Pic	0.0	Milford Soil	5.15
10e-5 U	112.4	10e-3 Pic	0.0	Milford Soil	5.24
10e-5 U	160.8	10e-3 Pic	2.5	Milford Soil	6.29
10e-5 U	148.0	10e-3 Pic	0.0	Milford Soil	6.30
10e-5 U	598.4	10e-3 Pic	0.0	Milford Soil	7.15
10e-5 U	750.8	10e-3 Pic	6.4	Milford Soil	7.29
10e-5 U	625.9	10e-3 Pic	0.0	Milford Soil	8.37
10e-5 U	501.4	10e-3 Pic	0.0	Milford Soil	8.50
10e-5 U	1263.3	10e-3 Pic	1.4	Milford Soil	9.17
10e-5 U	1245.5	10e-3 Pic	11.7	Milford Soil	9.42
10e-5 U	0.0	10e-5 EDTA	614.0	1.2% IOCS	3.14
10e-5 U	0.0	10e-5 EDTA	539.1	1.2% IOCS	3.18
10e-5 U	0.0	10e-5 EDTA	528.2	1.2% IOCS	3.24
10e-5 U	0.0	10e-5 EDTA	514.7	1.2% IOCS	3.34
10e-5 U	53.2	10e-5 EDTA	253.3	1.2% IOCS	4.31
10e-5 U	251.1	10e-5 EDTA	196.4	1.2% IOCS	4.9
10e-5 U	6398.6	10e-5 EDTA	115.1	1.2% IOCS	5.33
10e-5 U	12129.3	10e-5 EDTA	74.1	1.2% IOCS	5.65
10e-5 U	71301.6	10e-5 EDTA	34.8	1.2% IOCS	7.28
10e-5 U	19678.3	10e-5 EDTA	42.5	1.2% IOCS	7.3
10e-5 U	15244.1	10e-5 EDTA	16.5	1.2% IOCS	7.33
10e-5 U	19310.4	10e-5 EDTA	28.6	1.2% IOCS	7.44
10e-5 U	8499.4	10e-5 EDTA	10.8	1.2% IOCS	7.48
10e-5 U	11692.5	10e-5 EDTA	10.2	1.2% IOCS	7.51
10e-5 U	25849.9	10e-5 EDTA	20.2	1.2% IOCS	7.52
10e-5 U	17543.1	10e-5 EDTA	19.4	1.2% IOCS	7.58
10e-5 U	3479.6	10e-5 EDTA	6.2	1.2% IOCS	7.64
10e-5 U	3289.8	10e-5 EDTA	6.7	1.2% IOCS	7.69
10e-5 U	2725.8	10e-5 EDTA	1.6	1.2% IOCS	8.37
10e-5 U	4417.4	10e-5 EDTA	0.6	1.2% IOCS	8.64
10e-5 U	9605.6	10e-5 EDTA	0.0	1.2% IOCS	8.93
10e-5 U	6626.2	10e-5 EDTA	1.2	1.2% IOCS	9.17
10e-5 U	81.2	10e-5 EDTA	29.6	Milford Soil	4.55
10e-5 U	76.1	10e-5 EDTA	24.5	Milford Soil	4.61
10e-5 U	165.4	10e-5 EDTA	30.2	Milford Soil	4.96
10e-5 U	88.2	10e-5 EDTA	29.7	Milford Soil	5.01

B.7

Metal Conc.	Kd (metal)	Ligand Conc.	Kd (ligand)	Adsorbent	pH
10e-5 U	213.9	10e-5 EDTA	26.4	Milford Soil	5.67
10e-5 U	328.4	10e-5 EDTA	29.3	Milford Soil	5.67
10e-5 U	2026.2	10e-5 EDTA	24.3	Milford Soil	5.98
10e-5 U	1454.5	10e-5 EDTA	22.8	Milford Soil	5.99
10e-5 U	1837.9	10e-5 EDTA	18.8	Milford Soil	6.69
10e-5 U	3064.0	10e-5 EDTA	17.2	Milford Soil	6.72
10e-5 U	3927.5	10e-5 EDTA	13.4	Milford Soil	6.84
10e-5 U	4544.8	10e-5 EDTA	13.4	Milford Soil	6.84
10e-5 U	5148.6	10e-5 EDTA	10.0	Milford Soil	6.94
10e-5 U	2978.3	10e-5 EDTA	8.7	Milford Soil	6.95
10e-5 U	2179.2	10e-5 EDTA	6.3	Milford Soil	7.04
10e-5 U	1265.9	10e-5 EDTA	5.8	Milford Soil	7.05
10e-5 U	481.2	10e-5 EDTA	2.5	Milford Soil	7.95
10e-5 U	599.2	10e-5 EDTA	3.1	Milford Soil	7.97
10e-5 U	488.5	10e-5 EDTA	0.7	Milford Soil	8.16
10e-5 U	436.9	10e-5 EDTA	2.3	Milford Soil	8.23
10e-5 U	2026.1	10e-5 EDTA	0.0	Milford Soil	9.12
10e-5 U	1835.2	10e-5 EDTA	0.3	Milford Soil	9.16
10e-5 U	821.2	10e-5 EDTA	22.6	LK-1	4.04
10e-5 U	844.3	10e-5 EDTA	23.3	LK-1	4.06
10e-5 U	992.9	10e-5 EDTA	19.8	LK-1	4.12
10e-5 U	900.0	10e-5 EDTA	24.0	LK-1	4.14
10e-5 U	4644.6	10e-5 EDTA	20.3	LK-1	4.67
10e-5 U	5162.2	10e-5 EDTA	19.7	LK-1	4.73
10e-5 U	52827.3	10e-5 EDTA	29.3	LK-1	5.50
10e-5 U	23433.7	10e-5 EDTA	24.7	LK-1	5.53
10e-5 U	32382.4	10e-5 EDTA	13.9	LK-1	6.37
10e-5 U	55035.1	10e-5 EDTA	7.3	LK-1	6.44
10e-5 U	32976.5	10e-5 EDTA	15.1	LK-1	6.50
10e-5 U	61528.2	10e-5 EDTA	8.3	LK-1	6.55
10e-5 U	26013.7	10e-5 EDTA	5.3	LK-1	6.60
10e-5 U	9077.8	10e-5 EDTA	1.2	LK-1	6.71
10e-5 U	68238.0	10e-5 EDTA	17.9	LK-1	6.76
10e-5 U	29014.4	10e-5 EDTA	6.7	LK-1	6.80
10e-5 U	4613.1	10e-5 EDTA	8.3	LK-1	6.97
10e-5 U	2524.5	10e-5 EDTA	1.6	LK-1	7.00
10e-5 U	5995.8	10e-5 EDTA	4.5	LK-1	7.16
10e-5 U	6946.1	10e-5 EDTA	7.9	LK-1	7.18
10e-5 U	8157.7	10e-5 EDTA	8.0	LK-1	7.48
10e-5 U	9593.1	10e-5 EDTA	7.9	LK-1	7.55
10e-5 U	18.2	10e-5 EDTA	153.0	MNC-70	4.23
10e-5 U	20.1	10e-5 EDTA	136.9	MNC-70	4.25
10e-5 U	144.2	10e-5 EDTA	159.6	MNC-70	4.71
10e-5 U	109.7	10e-5 EDTA	150.2	MNC-70	4.72
10e-5 U	717.3	10e-5 EDTA	159.2	MNC-70	5.16
10e-5 U	595.5	10e-5 EDTA	154.5	MNC-70	5.17

Metal Conc.	Kd (metal)	Ligand Conc.	Kd (ligand)	Adsorbent	pH
10e-5 U	2204.7	10e-5 EDTA	151.4	MNC-70	5.63
10e-5 U	2340.3	10e-5 EDTA	141.0	MNC-70	5.74
10e-5 U	5246.4	10e-5 EDTA	144.0	MNC-70	5.97
10e-5 U	6978.3	10e-5 EDTA	153.5	MNC-70	5.99
10e-5 U	8925.4	10e-5 EDTA	136.2	MNC-70	6.31
10e-5 U	12808.9	10e-5 EDTA	131.7	MNC-70	6.34
10e-5 U	8372.9	10e-5 EDTA	109.9	MNC-70	6.55
10e-5 U	7715.3	10e-5 EDTA	81.9	MNC-70	6.56
10e-5 U	9311.1	10e-5 EDTA	89.7	MNC-70	6.56
10e-5 U	13769.7	10e-5 EDTA	96.9	MNC-70	6.79
10e-5 U	5203.1	10e-5 EDTA	62.6	MNC-70	6.95
10e-5 U	7963.8	10e-5 EDTA	81.2	MNC-70	6.99
10e-5 U	3529.4	10e-5 EDTA	42.8	MNC-70	7.13
10e-5 U	3852.6	10e-5 EDTA	47.4	MNC-70	7.16
10e-5 U	775.1	10e-5 EDTA	18.0	MNC-70	7.45
10e-5 U	1390.7	10e-5 EDTA	19.1	MNC-70	7.75
6.7x10e-7 Pu	0	0.0	-	Milford Soil	4.86
6.7x10e-7 Pu	0	0.0	-	Milford Soil	4.91
6.7x10e-7 Pu	0	0.0	-	Milford Soil	6.05
6.7x10e-7 Pu	0	0.0	-	Milford Soil	6.08
6.7x10e-7 Pu	3	0.0	-	Milford Soil	7.47
6.7x10e-7 Pu	0.7	0.0	-	Milford Soil	7.52
6.7x10e-7 Pu	8.7	0.0	-	Milford Soil	7.86
6.7x10e-7 Pu	2.1	0.0	-	Milford Soil	7.89
6.7x10e-7 Pu	36.1	0.0	-	Milford Soil	8.39
6.7x10e-7 Pu	49.2	0.0	-	Milford Soil	8.58
6.7x10e-7 Pu	53.3	0.0	-	Milford Soil	9.30
6.7x10e-7 Pu	45.5	0.0	-	Milford Soil	9.34
6.7x10e-7 Pu	0	-	-	Milford Soil	4.78
6.7x10e-7 Pu	0	-	-	Milford Soil	4.74
6.7x10e-7 Pu	0.2	-	-	Milford Soil	6.27
6.7x10e-7 Pu	0	-	-	Milford Soil	6.28
6.7x10e-7 Pu	1.5	-	-	Milford Soil	7.63
6.7x10e-7 Pu	2.6	-	-	Milford Soil	7.67
6.7x10e-7 Pu	9.7	-	-	Milford Soil	7.97
6.7x10e-7 Pu	9.9	-	-	Milford Soil	7.98
6.7x10e-7 Pu	52.9	-	-	Milford Soil	8.47
6.7x10e-7 Pu	46.7	-	-	Milford Soil	8.74
6.7x10e-7 Pu	64.9	-	-	Milford Soil	9.61
6.7x10e-7 Pu	84	-	-	Milford Soil	9.69
1.0x10e-8 Pu	18.5	10e-5 Pic	126.8	Milford Soil	4.52
1.0x10e-8 Pu	16.8	10e-5 Pic	153.2	Milford Soil	4.54
1.0x10e-8 Pu	87.5	10e-5 Pic	169.2	Milford Soil	6.61
1.0x10e-8 Pu	109.7	10e-5 Pic	114.4	Milford Soil	6.88
1.0x10e-8 Pu	512.2	10e-5 Pic	57.4	Milford Soil	7.45
1.0x10e-8 Pu	547.5	10e-5 Pic	71.3	Milford Soil	7.58

Metal Conc.	Kd (metal)	Ligand Conc.	Kd (ligand)	Adsorbent	pH
1.0x10e-8 Pu	600.1	10e-5 Pic	7.4	Milford Soil	7.99
1.0x10e-8 Pu	569.0	10e-5 Pic	14.9	Milford Soil	8.00
1.0x10e-8 Pu	515.7	10e-5 Pic	0.7	Milford Soil	8.48
1.0x10e-8 Pu	829.1	10e-5 Pic	0.0	Milford Soil	8.51
1.0x10e-8 Pu	490.1	10e-5 Pic	0.0	Milford Soil	9.52
1.0x10e-8 Pu	852.9	10e-5 Pic	0.0	Milford Soil	9.64